United States
Environmental Protection
Agency

Office of Research and
Development
Washington DC 20460

EPA/600/R-99/110
January 2000

EPA

Analytic Element Modeling of Coastal Aquifers

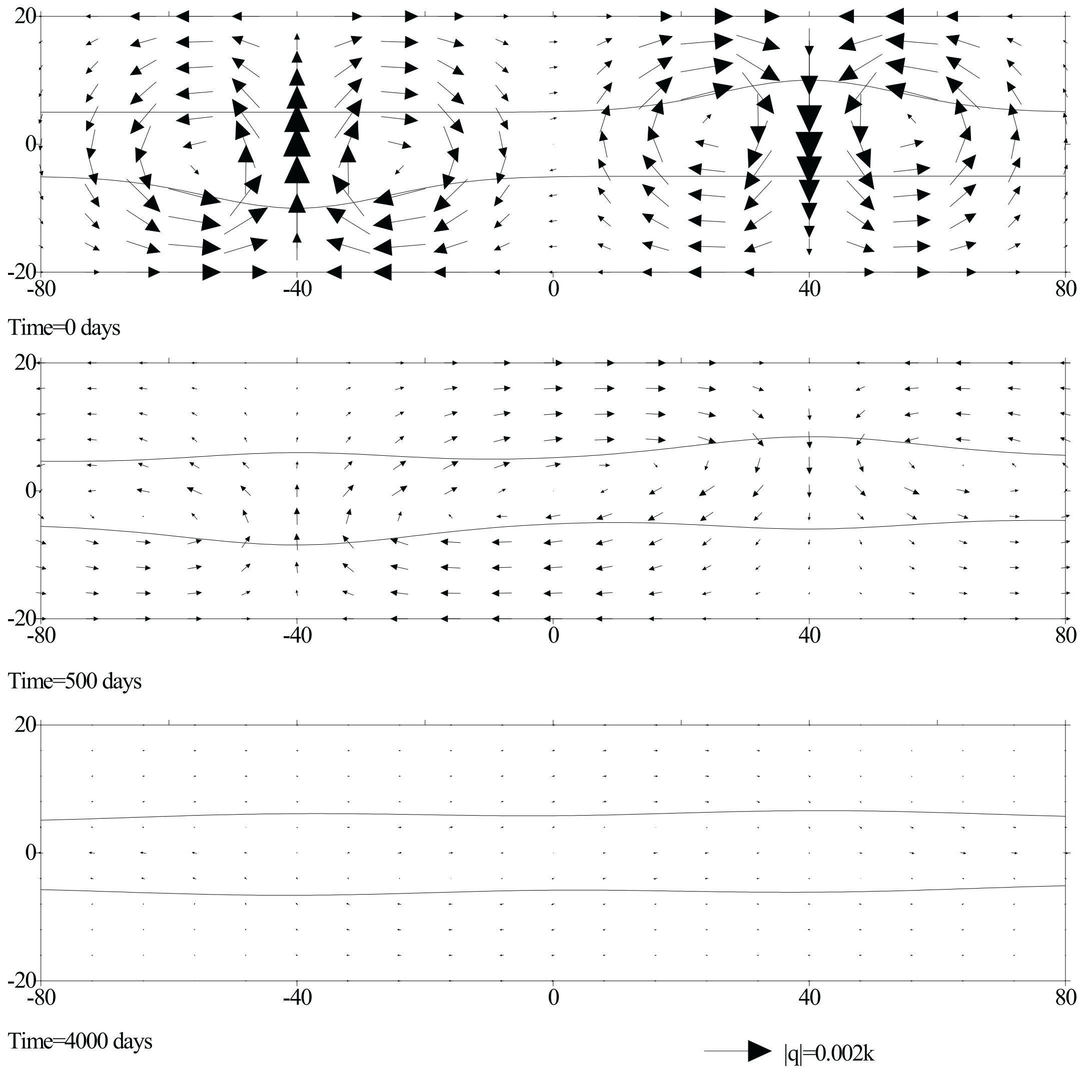

EPA/600/R-99/110
January 2000

Analytic Element Modeling of Coastal Aquifers

by

Mark Bakker
University of Minnesota, Minneapolis

Stephen R. Kraemer
U.S. Environmental Protection Agency
Ada, Oklahoma

Willem J. de Lange
Institute for Inland Water Management and Waste Water Treatment (RIZA)
Lelystad, The Netherlands

Otto D.L. Strack
University of Minnesota, Minneapolis

CR-823718

Project Officer

Stephen R. Kraemer
Subsurface Protection and Remediation Division
National Risk Management Research Laboratory
Ada, OK 74820

National Risk Management Research Laboratory
Office of Research and Development
U.S. Environmental Protection Agency
Cincinnati, OH 45268

Notice

The U.S. Environmental Protection Agency through its Office of Research and Development partially funded and collaborated in the research described here under Cooperative Agreement No. CR-823718 to the University of Minnesota, Dr. Otto Strack, Principal Investigator. It has been subjected to the Agency's peer and administrative review and has been approved for publication as an EPA document. Mention of trade names or commercial products does not constitute endorsement or recommendation for use.

All research projects making conclusions or recommendations based on environmentally related measurements and funded by the Environmental Protection Agency are required to participate in the Agency Quality Assurance Plan. This project did not involve physical measurements and, as such, did not require a QA plan.

Abstract

Four topics were studied concerning the modeling of ground-water flow in coastal aquifers with analytic elements: (1) practical experience was obtained by constructing a ground-water model of the shallow aquifers below the Delmarva Peninsula USA using the commercial program MVAEM; (2) a significant increase in performance was obtained by implementing the theory for variable density flow in a computer program that ran on a supercomputer using vectorization; (3) a new representation for the density variation was developed that can simulate the change from brackish to fresh water more accurately; and (4) it was shown that for a specific example of a bell-shaped transition zone a Dupuit model gives accurate results unless the bell-shape is too narrow compared to the thickness of the aquifer.

Foreword

The U.S. Environmental Protection Agency is charged by Congress with protecting the Nation's land, air and water resources. Under a mandate of national environmental laws, the Agency strives to formulate and implement actions leading to a compatible balance between human activities and the ability of natural systems to support and nurture life. To meet these mandates, EPA's research program is providing data and technical support for solving environmental problems today and building a science knowledge base necessary to manage our ecological resources wisely, understand how pollutants affect our health, and prevent or reduce environmental risks in the future.

The National Risk Management Research Laboratory is the Agency's center for investigation of technological and management approaches for reducing risks from threats to human health and the environment. The focus of the Laboratory's research program is on methods for the prevention and control of pollution to air, land, water, and subsurface resources; protection of water quality in public water systems; remediation of contaminated sites and ground water; and prevention and control of indoor air pollution. The goal of this research effort is to catalyze development and implementation of innovative, cost-effective environmental technologies; develop scientific and engineering information needed by EPA to support regulatory and policy decisions, and provide technical support and information transfer to ensure effective implementation of environmental regulations and strategies.

Salt water intrusion is a potential threat to drinking water supplies in the coastal areas of the USA due to over-pumping. In addition to the pumping, groundwater flow in coastal aquifers is affected by the difference in density between fresh and salt water. Computer models provide a tool for predicting the movement of salt water under past, present, and future pumping conditions. However, the simulation of three-dimensional variable density flow is computationally expensive. This project investigates innovations in algorithm formulation and computing architecture for problem solving involving variable density groundwater flow, with the aquifers beneath the Delmarva Peninsula, USA, providing context.

Clinton W. Hall, Director
Subsurface Protection and Remediation Division
National Risk Management Research Laboratory

Contents

Acknowledgements

Funding for this project came through the EPA High Performance Computing and Communication program, which is managed by Ms. Joan Novak, EPA Atmospheric Modeling Division, Research Triangle Park, North Carolina. Computer time on the CrayC916 was obtained through a grant from the Minnesota Supercomputer Institute to the University of Minnesota. Dr. Erik Anderson and Dr. David Steward contributed to the project while at the Department of Civil Engineering of the University of Minnesota, Minneapolis. The technical content of the report benefited from reviews by Dr. Henk Haitjema, Indiana University, Bloomington, Dr. Willem Zaadnoordijk, IWACO and Delft University of Technology, The Netherlands, and Dr. Gualbert Oude Essink, Utrecht University, The Netherlands. Ms. Joan Elliott provided the editorial review.

Contact information (as of January 2000):

Dr. Mark Bakker, University of Nebraska, Dept. of Civil Engineering, 6001 Dodge Street, Omaha, NE 68182, mbakker@unomaha.edu

Dr. Stephen Kraemer, USEPA, 960 College Station Road, Athens, GA 30605, kraemer.stephen@epa.gov

Dr. Wim de Lange, RIZA, P.O. Box 17,8200 AA Lelystad, The Netherlands, W.dLange@riza.rws.minvenw.nl

Dr. Otto Strack, University of Minnesota, 122 Civil Engineering, 500 Pillsbury Drive S.E., Minneapolis, MN 55455, strac001@tc.umn.edu

Introduction

Motivation

Salt water intrusion is a potential threat to drinking water supplies in the coastal areas of the USA. Cities along the coast are increasing their pumping of groundwater to support a rising population. The increased pumping may result in an increase of chlorides in the well water due to the upconing of brackish groundwater. Even a small concentration of chlorides will give the water a salty taste; water tastes salty to most people if the concentration of chlorides is 0.25 g/l or greater. Sea water, on the other hand, contains about 18 grams of chlorides per liter. The maximum guideline concentration set by the World Health Organization is 0.25 grams of chlorides per liter. The potential upconing of brackish groundwater may be studied by the simulation of groundwater flow with a numerical model.

Groundwater flow in coastal aquifers is affected by the difference in density between fresh and salt water. The fresh water is separated from the salt water through a brackish transition zone, in which the salinity (and thus the density) of the water varies from that of salt water to that of fresh water. If the transition zone is relatively thin, the transition from fresh to salt water may be modeled as an abrupt one: the fresh water is separated from the salt water by an interface. If this is not the case, the effect of the variation in density on the flow in the transition zone must be taken into account. The modeling of the flow generated by variations in density, the variable density flow, is the subject of this report. Specifically, it is investigated whether groundwater flow in coastal aquifers can be modeled under the Dupuit approximation in combination with analytic elements.

Background

Numerous numerical models are available to simulate variable density flow for both two–dimensional flow in the vertical plane and three–dimensional flow. The flow field may be modeled with the finite–element method or the finite–difference method while the solute transport equation may also be solved by the random walk method or the method of characteristics. Two–dimensional models include SUTRA (Voss, 1984), and MOCDENSE (Sanford and Konikow, 1985), the variable density version of MOC (Konikow and Bredehoeft, 1978). Three–dimensional models include HST3D (Kipp, 1986) and SWICHA (Lester, 1991). Maas and Emke (1988) developed a procedure to simulate variable density flow with numerical models for single density flow. Olsthoorn (1996) presented a method to use MODFLOW (McDonald and Harbaugh, 1984) for variable density flow. The three–dimensional version of MOC, called MOC3D (1996), has been modified to include density driven flow by Oude Essink (1998).

The construction of numerical models of three–dimensional variable density flow is limited by the availability of density data and by the speed of digital computers (Oude Essink and Boekelman, 1996). The Dupuit approximation may be adopted to reduce the computation time and for the usual reason of simplicity (Strack, 1995). The resistance to flow in the vertical direction is neglected in Dupuit models, and vertical flow is governed by continuity of flow only; this leads to a hydrostatic pressure distribution in the vertical direction. The Dupuit approximation is reasonable for flow in aquifers of great horizontal extend, also referred to as aquifers with shallow flow or regional flow. It is possible to construct regional groundwater flow models of coastal aquifers by adopting the Dupuit approximation. The Dupuit theory for variable density flow may be combined with any method to model Dupuit flow in a single density model. In this report the flow field is modeled with analytic elements (Strack, 1989; Haitjema, 1995). Analytic element models have been constructed successfully to simulate the fresh water head in the coastal aquifers of The Netherlands (e.g., Minnema and van der Meij, 1997). A model of a coastal aquifer beneath the Delmarva Peninsula is described in this report.

The Dupuit theory for variable density flow

The Dupuit theory for variable density flow, as formulated by Strack (1995), assumes that the density distribution in the aquifer is known at some time. In practice, the density is known only at a number of isolated points. Strack (1995) proposes to represent the density distribution with a three–dimensional interpolator function that interpolates between the points of known density; he suggests to use the multiquadric radial basis interpolator (Hardy, 1971) for this purpose. It is noted that the multiquadric interpolator is a form of Kriging; the interpolator is identical to Kriging with a linear variogram if the shape factor in the interpolator is set equal to zero.

The density distribution (and thus the flow field) will change over time as the salt moves with the groundwater flow. The flow is incompressible in Strack's model and the flow field thus represents the flow at a given time. The evolution of the density distribution in the aquifer may be simulated by numerical integration through time. During each time step, the velocity field is fixed and the salt is moved with the groundwater flow. At the end of a time step the velocity field corresponding to the new density distribution is computed and the process is repeated. This procedure is also known as successive steady–state solutions; transient solutions are obtained with successive steady–state solutions throughout this report. Second order processes that affect the salinity distribution, such as diffusion, are neglected. It may be expected that such a procedure gives reasonable results for relatively short times (on the order of 25 years, as is of interest for most engineering problems).

Strack's theory has been implemented, prior to this study, in the proprietary computer program Multi–layer Variable density Analytic Element Model (MVAEM). The computation time involved in the construction of large regional models of the fresh water head with MVAEM is significant. Multi–layer models that include thousands of points where the salinity is specified take on the order of hours to compute a solution on a high end PC (in 1996). A large portion of the computation time is used to compute the effect of the variation in density on the flow. The computation times of the transient simulations involve a repeated computation of the solution at different times plus a large number of evaluations of the velocity in the aquifer and is of the order of days or more, as compared to the hours it takes to obtain one steady–state solution. These computation times diminish the practicality of the modeling approach.

The use of a Dupuit model to simulate variable density flow raises a number of additional issues. Transient simulations require an accurate representation of the velocity field (not just of heads) and the numerical integration requires an analysis of stability and convergence. Furthermore, it must be investigated how accurate a Dupuit model is to simulate the change of a salt distribution over time, especially in the case of upconing of salt or brackish water. Dupuit models are generally used for regional (shallow) flow and may become inaccurate when the shallow flow assumption is not appropriate, for example near a partially penetrating well where the flow field changes rapidly over a distance of several times the aquifer thickness. And finally, the assessment of the upconing of salt water below a pumping well needs analysis of the physical stability of the transition zone itself.

Objective

The objective of this report is to investigate the performance of the Dupuit theory for variable density flow combined with analytic elements to model groundwater flow in coastal aquifers. It is impossible to answer all the questions raised in the foregoing in one project. This project concerns four areas of study:

1. The analytic element modeling of groundwater flow in the first confined aquifer beneath the Delmarva Peninsula.

2. The reduction of computation time by the use of a supercomputer.

3. The accurate representation of the density distribution.

4. The implications of adopting the Dupuit approximation for variable density flow.

Report structure

The report is structured as follows. In Chapter 1, a model is presented of the fresh water head in the first confined aquifer on the Delmarva Peninsula using the program MVAEM. The salt distribution (and thus the density distribution) was modeled separately prior to the groundwater flow simulations; use was made of a three–dimensional visualization package.

The Dupuit theory for variable density flow is derived following the paper by Strack (1995) in Chapter 2. The density distribution is represented by a three–dimensional multiquadric interpolator, as is done in the program MVAEM, which was used for the modeling study. The second half of this chapter (starting with the section "Head and potential") is highly mathematical and intended for the reader who is interested in implementing the theory in a computer program. Reading this section is not required for understanding the subsequent chapters.

It is investigated in Chapter 3 whether the use of a supercomputer will reduce the impractically long computation times to such a level that interactive modeling becomes possible. The Dupuit theory for variable density flow was implemented in the analytic element code Variable Density Single Layer Wells Line–sinks (VDSLWL), which is based on the public domain program SLWL (Strack, 1989). VDSLWL was written to run on a vector machine, the CrayC916 at the Minnesota Supercomputer Institute. A brief description of the density module is provided and some implementation issues are addressed.

The performance of the multiquadric interpolator to represent the density distribution is investigated in Chapter 4. The multiquadric interpolator includes a shape factor that controls the smoothness of the interpolator. In practice, this shape factor is often set close to zero to obtain a reasonable representation of the density distribution. This leads to an acceptable approximation of the fresh water head, but the resulting velocity field appears to be physically unrealistic. A new representation for the density distribution is proposed to overcome this problem. This representation is better controlled but also less flexible. A new exact solution for variable density flow in a vertical cross–section is presented and compared to the Dupuit solution. The derivation of the expressions for the specific discharge vector corresponding to the new representation of the density distribution is lengthy and is presented separately in Chapter 5. Finally, results are summarized and conclusions drawn in Chapter 6.

CHAPTER 1

An Analytic Element Model of the Upper Chesapeake Aquifer, Delmarva Peninsula (USA)

Introduction

Salt water intrusion is a potential threat to drinking water supplies relying on groundwater in coastal aquifers of the USA. The World Health Organization has set a guideline concentration of chlorides at 250 mg/l; water tastes salty to most people when the concentration of chlorides is greater than this value. The city of Ocean City, Maryland, on the mid Atlantic coastal plain, has experienced a rise in the chlorides in one of its wells from 70 mg/l in 1975 to 215 mg/l in 1988. The well field is probably experiencing upconing of brackish water from the underlying aquifer due to increased pumping (Achmad and Wilson, 1993). The increased pumping is needed to supply water to the growing population in the region.

The analytic element method for modeling groundwater flow has been extended to represent the influence of a variation in density of the water (due to a variation in salinity) on the groundwater flow (Strack, 1995). In this chapter we explore the application of analytic element modeling within a coastal aquifer where fresh and sea water meet. The shallow fresh water aquifer systems of the Delmarva (Delaware-Maryland-Virginia) Peninsula are stratified and multi-layered with alternating sand and clay layers, and are wedge-shaped, thickening to the east and subcropping or pinching-out in the west (Vroblesky and Fleck, 1991). The aquifers are bounded below by bedrock; fresh water meets sea water in the lower aquifers, directly underneath the Chesapeake Bay, and offshore beneath the Atlantic Ocean.

The upper Chesapeake aquifer is considered a single geohydrologic unit at the regional scale, and is bounded below by the St. Mary's confining unit, and above by the upper Chesapeake confining unit. The upper Chesapeake aquifer subcrops into the surficial Columbia aquifer in the western part of Delmarva, and then gently dips to the southeast at a slope of about 0.01 (15 m per 1600 m) (Vroblesky and Fleck, 1991) (See Figures 1.1 and 1.2). The upper Chesapeake aquifer contains three major sand bodies of Miocene and Pliocene age, which are, from lowermost to uppermost, the Manokin, Ocean City, and Pocomoke aquifers, respectively.

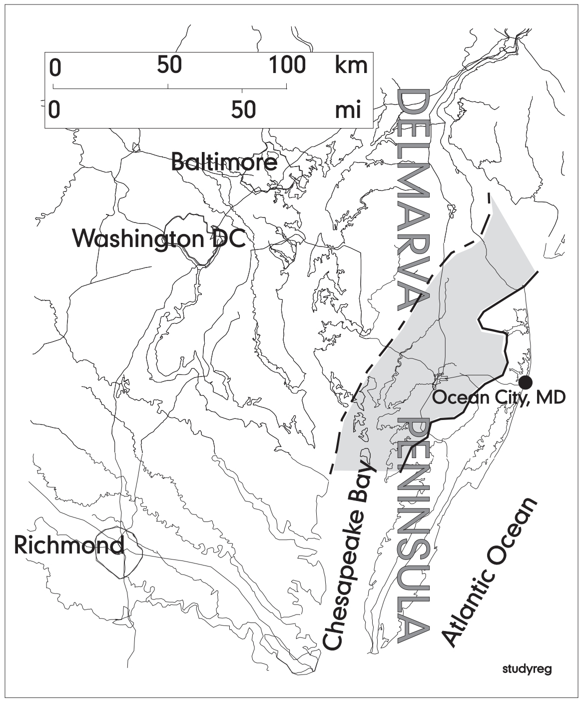

Figure 1.1: The subcrop of the upper Chesapeake aquifer (shaded area) beneath the Delmarva Peninsula USA

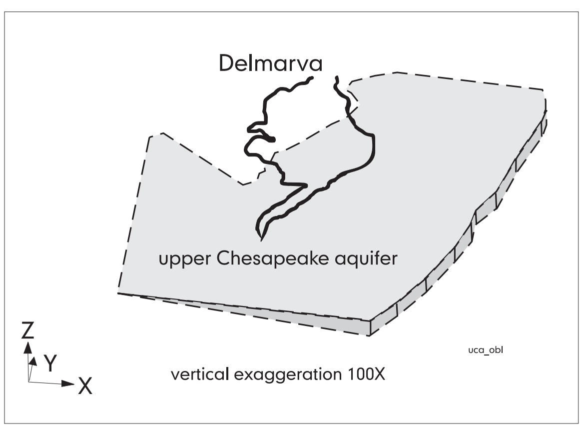

Figure 1.2: Perspective view of the upper Chesapeake aquifer using GMS software (WES, 1997) (vertical exaggeration 100x)

Approach

Groundwater flow in the upper Chesapeake aquifer was simulated using the Multi-layer Variable-density Analytic Element Model (MVAEM Version 1.1 ©1995 Strack Consulting, North Oaks, MN). A description of the mathematical basis of the point, line, and area elements used in MVAEM can be found in Strack (1989), while the extension to include variable density flow is discussed in Chapter 2 of this report, and in Strack (1995), Strack and Bakker (1995). MVAEM solves for the steady–state flow field, and uses the Dupuit approximation; that is, resistance to vertical flow is assumed negligible. The range of applicability of the Dupuit approximation for variable density flow is explored in Chapter 4.

MVAEM computes the influence of variable density flow, or density driven flow, using an estimate of the continuous three-dimensional distribution of density in the aquifer system. The density must be specified at a number of points in the aquifer (referred to as density points); MVAEM interpolates between these points to obtain a continuous density distribution throughout the aquifer. These density points are inferred from measurements of chloride concentration using an empirical relationship. For the upper Chesapeake aquifer model, we used an empirical relationship between chloride concentrations and density (Van Dam, 1973). Assuming the water temperature is 15 degrees Celsius, the density ρ may be written as

$$\rho = 1000 + 1.455[Cl]/1000 - 0.0065(11 + 0.4[Cl]/1000)^2 \tag{1.1}$$

where chloride concentration [Cl] is in mg/l and the resulting density in kg/m^3.

It is essential to evaluate the interpolated density distribution and make sure it is a reasonable representation of what is believed to be the density distribution in the aquifer. If the interpolation of MVAEM does not seem reasonable, additional points must be added where the density is specified to better control the interpolator, for example below the ocean bottom.

The distribution of data points used in the model is shown in Figure 1.3. Many of the chloride data points came from the QWDATA database of the USGS Water Resources Division in Baltimore, MD. Other sources include Meisler (1989), Phelan (1987), Richardson (1992), and Woodruff (1969). Only fairly recent observations (taken after 1940) were used assuming that the chloride (density) distribution did not change significantly during this time period.

The continuous three-dimensional distribution of density was created using a multiquadric interpolator in a procedure described in Chapter 2. It is noted that this interpolation technique is identical to Kriging with a linear variogram. A series of chloride concentration values were added in order to obtain a more realistic density distribution. Specifically, points were added in the upper Chesapeake aquifer beneath the Chesapeake Bay and were given values similar to the lower surface waters, noting that resistance layers in the Bay are partly absent. Data points below the upper Chesapeake aquifer were not used in the calculation, because it is unlikely that the density distributions are related across the separating St. Mary's confining

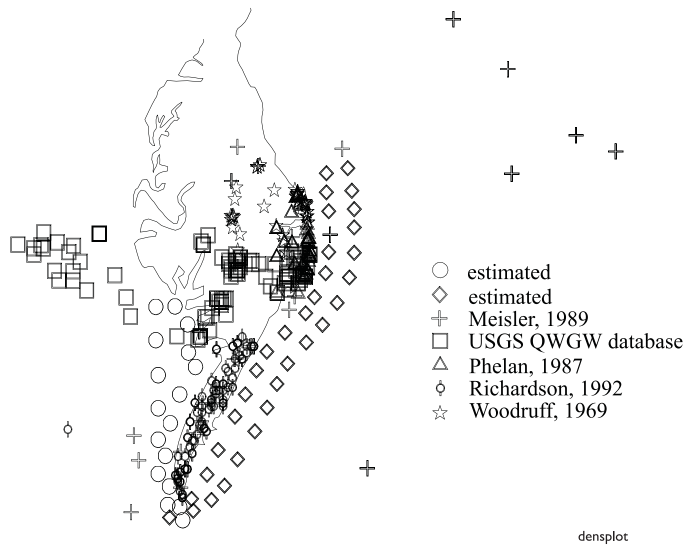

Figure 1.3: Density points used by the interpolator

unit. Another series of points was added in the upper Chesapeake aquifer bounding the coastline of the Atlantic Ocean based on the section model of Achmad and Wilson (1993). These points are shown as "estimated" in Figure 1.3. A total number of 668 data points were used, 148 estimated, see Appendix A1.

A mesh of constant strength area elements was used to simulate the leakage between the surficial unconfined aquifer and the upper Chesapeake aquifer. The leakages of the resistance elements are equal to the difference between the given head above (in the surficial aquifer) and the head in the upper Chesapeake aquifer, divided by the resistance of the upper Chesapeake confining layer. This condition is enforced at the center of each element. The resistance values are based on estimates of the vertical hydraulic conductivity. The resistance is equal to the thickness of the resistance layer divided by its vertical hydraulic conductivity, and has the units of time. (The resistance is the inverse of the conductance, a parameter used in many other models.) The layout of the elements and table of resistances and heads assigned can be found in Appendix A2.

Inhomogeneity polygons were used to represent variable aquifer thickness, variable hydraulic conductivity, and sloping base, as shown in Figure 1.4. Aquifer properties are constant within each polygon. These polygons are composed of line doublet elements which create the appropriate jump in the discharge potential and maintain continuity of flow. The base within each polygon is horizontal, and steps in the base were limited to half the aquifer thickness. The spatial pattern of doublet elements is based on the transmissivity distribution shown by Leahy and Martin (1993), and the estimations of the aquifer base on well logs reported in Vroblesky and Fleck (1991). The two small doublet polygons represent the local increase in thickness and transmissivity reported near Ocean City, Maryland.

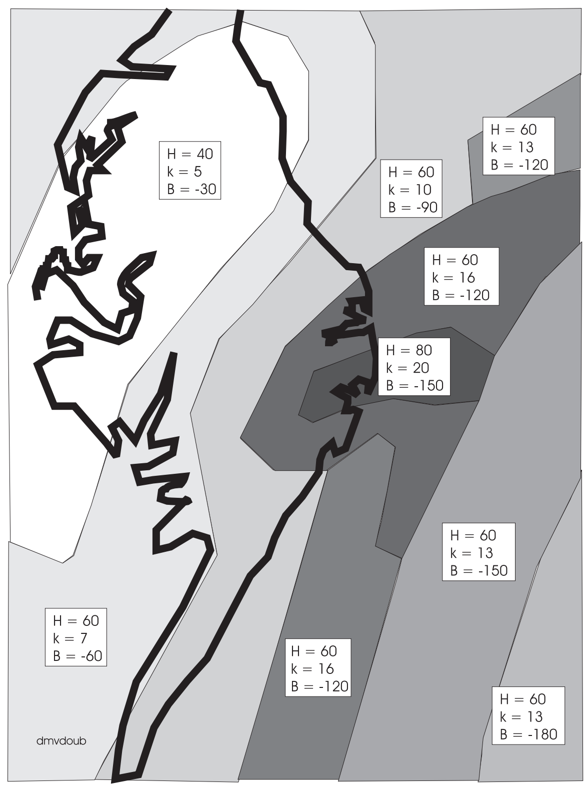

Figure 1.4: MVAEM doublet polygons representing heterogeneous upper Chesapeake aquifer (B, H, k are aquifer base elevation above mean sea level (m), thickness (m) and hydraulic conductivity(m/day)

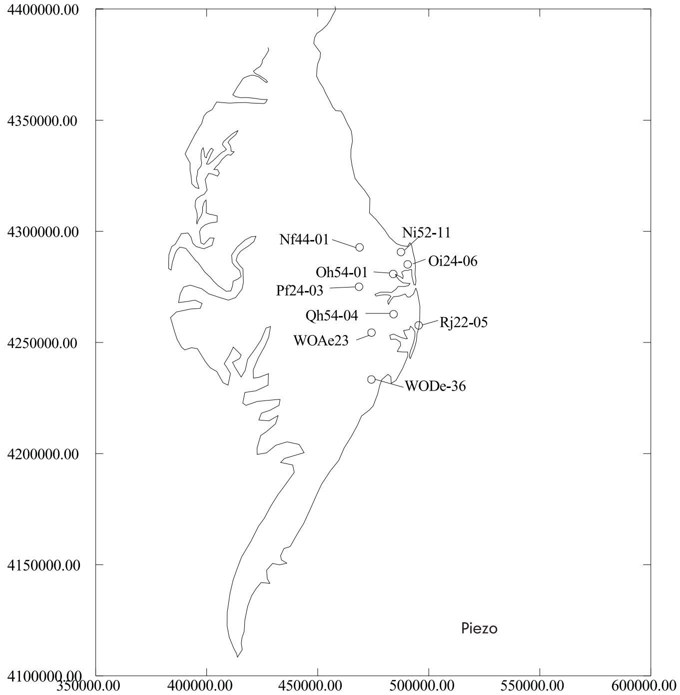

Figure 1.5: Locations of observations wells for fresh water heads

MVAEM was run for two scenarios: (1) variable density – fresh and salt water; and (2) single density – all fresh water. The predictions of fresh water heads were compared to monitoring wells located in Sussex County, Delaware, and Wicomico and Worchester Counties in Maryland (see Figure 1.5). The fresh water head is defined as the elevation to which water rises in a standpipe if the standpipe is filled with fresh water only. The selected observation wells are screened in the upper Chesapeake aquifer, and do not report an influence of nearby pumping wells.

Results

The upper Chesapeake model representing variable density groundwater flow beneath the Delmarva Peninsula has not been extensively calibrated, and results are considered preliminary. Figure 1.6 shows a fence diagram of the density distribution generated with the multiquadric interpolator; notice that the density distribution is continuous in three–dimensions. The transition from fresh to sea water can be seen clearly along the Delmarva shoreline and coastline in the contour map of Figure 1.7. A contour map of the MVAEM fresh water heads (at elevation 50 m below sea level) is shown in Figure 1.8.

The model predicted fresh water heads were compared to observed water levels in nine wells screened in the upper Chesapeake aquifer (See Figure 1.5). The observed water levels are based on a 5 year average over the period 1987-1992 (James et al., 1992) and are based on the density of water at the well screen. It is noted

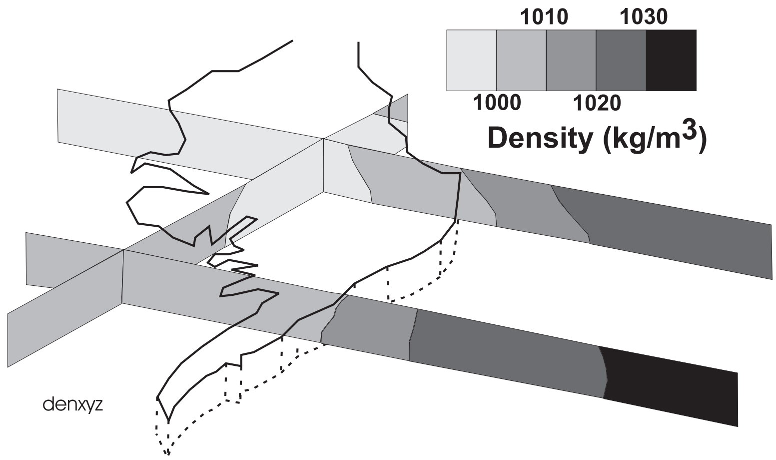

Figure 1.6: Fence diagram of three-dimensional density distribution (kg/m^3) inferred from discrete measurements of chloride concentrations and the multiquadric interpolator

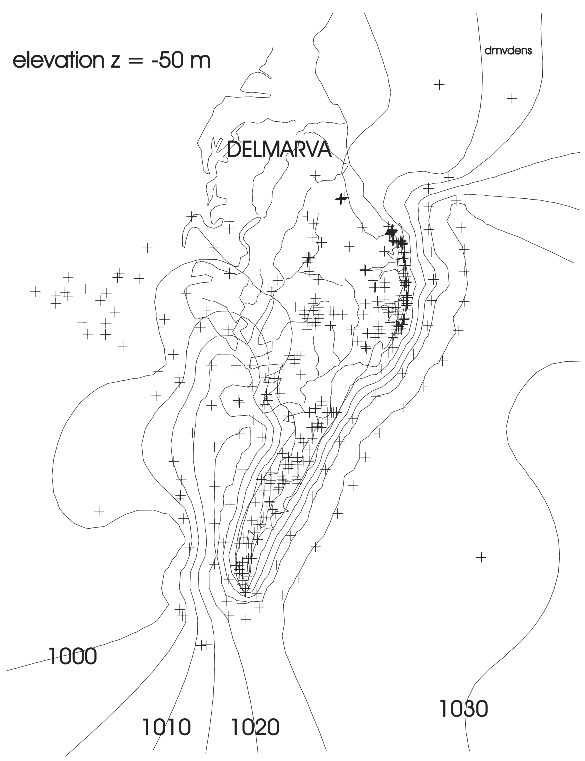

Figure 1.7: Contours of water density at elevation z=-50 m

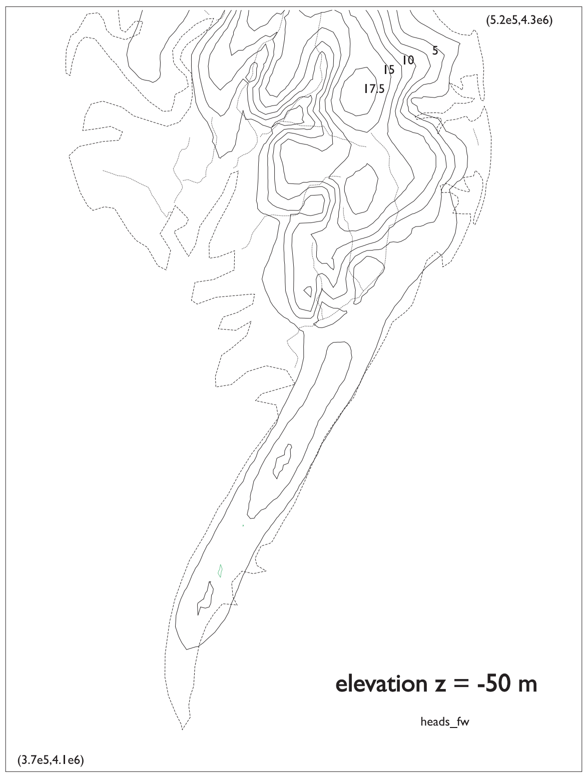

Figure 1.8: Contours of MVAEM fresh water heads at elevation z=-50 m

Table 1.1: Comparison of observed heads with simulated heads. Unit of heads is meters.

					Variable density		Single density	
Well ID	UTM-x	UTM-y	z (m msl)	obs. head	fw head	difference	fw head	difference
Nf44-01	468900	4292706	-30	8.9	9.17	0.27	9.17	0.27
Ni52-11	487572	4290620	-40.8	1.8	2.71	0.91	2.69	0.90
Oh54-01	484053	4280763	-81	2.7	3.01	0.31	3.03	0.34
Oi24-06	490558	4285068	-70.0	1.8	0.032	-1.8	0.0083	-1.8
Pf24-03	468686	4275014	-37.5	13.4	13.8	0.42	13.8	0.43
Qh54-04	484210	4262639	-90.8	4.5	6.38	1.9	6.39	1.9
Rj22-05	495517	4257631	-120	1.0	0.61	-0.39	0.56	-0.43
WOAe23	474254	4254373	-71.6	8.5	12.7	4.3	12.7	4.3
WODe-36	474211	4233291	-89.9	5.2	3.51	-1.7	3.53	-1.7

that, due to the small number of observations, no analysis has been performed to determine whether these values represent regional flow conditions. The difference between the MVAEM model predicted fresh water head and the observed head, for both the variable density and single density (all fresh water) simulations, are shown in Table 1.1.

MVAEM predicts the water exchange between the unconfined surficial aquifer and the upper Chesapeake aquifer. The leakage (m/d) for the area elements is shown in Figure 1.9. The mean value of the leakage is 8.79E-5 m/d (1.3 in/yr), while the maximum leakage entering the aquifer is 2.87E-3 m/d (41.2 in/yr) and the maximum leakage leaving the aquifer is 3.89E-4 m/d (5.6 in/yr). Figure 1.9 shows most of the leakage to the upper Chesapeake aquifer occurs in the uplands of Delmarva, while most of the exchange with the surficial aquifer occurs along the shore. The USGS reports an average flux of 122 ft^3/s through the Upper Chesapeake aquifer layer (4690 mi^2) of their model giving a leakage of 2.457E-5 m/d (0.35 in/yr) (Fleck and Vroblesky, 1996).

Discussion

The definition of the continuous three-dimensional chloride concentration (density) distribution in the upper Chesapeake aquifer is problematic given the paucity of available data. Most of the observation wells reporting a chloride concentration were of the fresh water beneath the Delmarva Peninsula. Only a handful of observation wells were available with a “salty” chloride concentration, and only a couple of these wells reported a chloride concentration that varied with depth. The resulting density contours are essentially

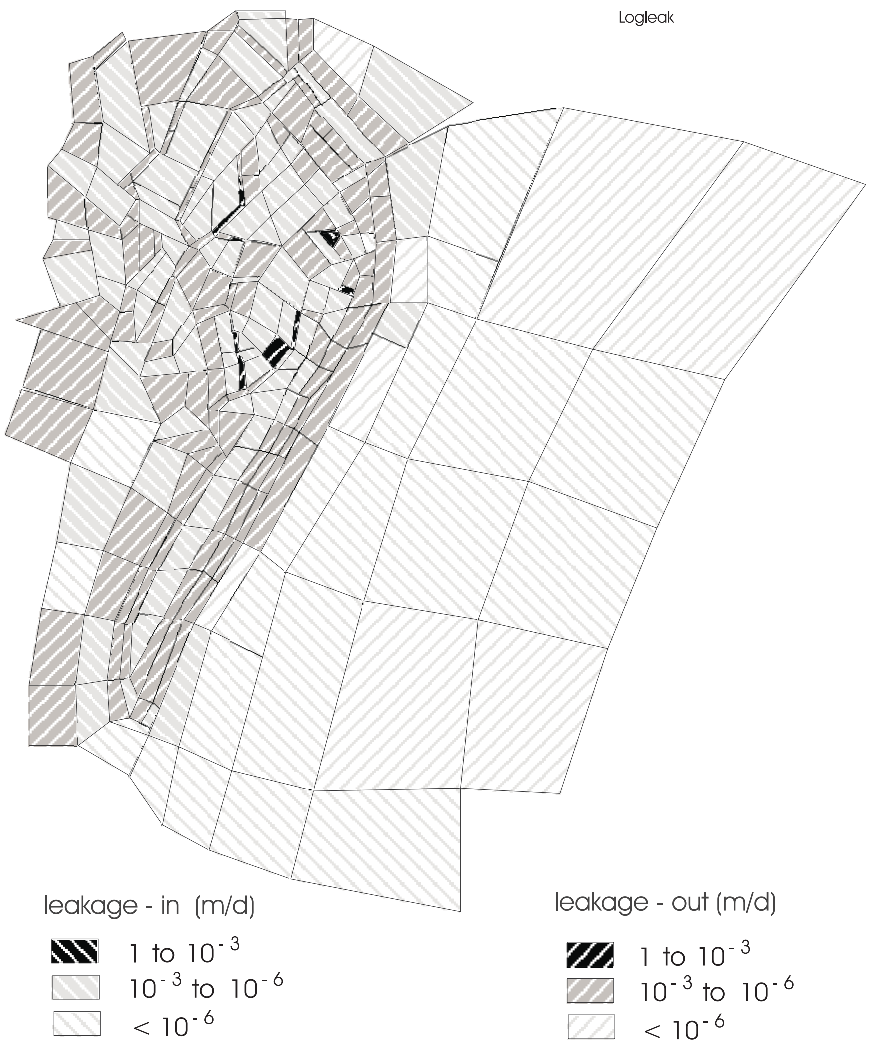

Figure 1.9: Distribution of leakage into and out of the upper Chesapeake aquifer

constant with depth, as shown in Figure 1.6. It is unlikely that this distribution is realistic, especially in the few areas where the density decreases with depth. Also, given the sensitivity of velocity calculations to the density variation, and given the rather questionable predicted density distribution based on so few data points, no calculations of the velocity distribution in the aquifer are presented here. Therefore, no predictions of the movement of the salt water transition zone are offered.

The MVAEM model did a reasonable job in predicting the fresh water heads in the aquifer, based on the comparison to the observed heads in monitoring wells, and the contours of predicted heads. It should be noted that MVAEM is a steady–state model, and the comparison was made to average heads. The heads are known to vary up to 1 m over the seasons. Also, the modeled heads were constrained by the head specified area elements, which were based on published water table contour maps. The solutions for fresh water heads are also relatively insensitive to the density distribution, at least at the observation points, as evidenced in Table 1.1. Further investigation of the reasonableness of the MVAEM fluxes is warranted.

Conclusions

The analytic element method was used to build a groundwater flow model of the upper Chesapeake aquifer of the Delmarva Peninsula, USA. The application of the MVAEM code demonstrated the potential of the analytic element method for representing variable density flow and to increase the understanding of the transition zone between fresh and sea water. No definitive site specific conclusions are offered given the uncertainties involved in this particular model application.

The analytic element method has the potential to simulate a reasonable representation of the fresh water head distribution, given adequate investment in model calibration. However, analytic element models, as with other numerical models, are only as good as the input data and adequacy of the conceptual model. In addition, the appropriateness of using the analytic element method to represent the aquifer base elevation in a piece-wise manner in order to approximate a smoothly sloping base elevation was not examined. More investment is needed to better define the variation of density in space. Better definition of aquifer geometry and properties is needed. More monitoring wells (as opposed to water supply wells) are needed to better define the fresh water head distribution. Measurements of fluxes to tidal rivers and shorelines would be useful. These observations would facilitate a complete water balance analysis.

Additional complexities of the aquifer system may be represented in the future with new developments of the analytic element method. It is possible to build a multi-layer model and better represent the influences of the surficial aquifer. For example, the major streams could be represented as curvilinear line elements, while the minor streams may be lumped into an effective feeding resistance based upon their drainage density (De Lange, 1996). Alternatively, leakage to the upper Chesapeake aquifer from the surficial aquifer could be represented using advanced variable strength area elements (Strack and Janković, 2000). Also, future developments in the analytic element method include functions to represent a continuously sloping aquifer base and a transient aquifer response.

Until these challenges are met, it is too early to assess fully the practical advantages, and disadvantages, of the analytic element method in comparison to numerical techniques such as finite differences and finite elements.

CHAPTER 2

A Dupuit Formulation for Variable Density Flow

Introduction

The Dupuit theory for variable density flow was presented by Strack (1995). The theory is reproduced here, in a slightly different form, for the case of confined flow in a piecewise horizontal aquifer. A Cartesian x_1, x_2, z coordinate system is adopted with the z–axis pointing vertically upward.

The specific discharge vector field for variable density flow is rotational, even if the aquifer is homogeneous and isotropic. Strack (1995) showed, however, that the discharge vector field (the specific discharge integrated over the saturated thickness of the aquifer) is irrotational. Thus, a potential Φ may be defined such that the discharge vector is minus the gradient of this potential. As such, the three–dimensional rotational flow problem is reduced to a two–dimensional potential flow problem. Furthermore, Strack (1995) approximated the pressure distribution in the vertical direction as hydrostatic (the Dupuit approximation) to obtain a relation between the potential and the fresh water head. The fresh water head ϕ is defined as the elevation to which water rises in a standpipe if the standpipe is filled with fresh water only (e.g., Lusczynski, 1961).

Basic Equations

Darcy's law in terms of pressure is

$$\begin{aligned} q_i &= -\frac{\kappa}{\mu}\frac{\partial p}{\partial x_i} \qquad i = 1, 2 \\ q_z &= -\frac{\kappa}{\mu}\frac{\partial p}{\partial z} - \frac{\kappa}{\mu}\rho g \end{aligned} \tag{2.1}$$

where q_1, q_2, q_z are the components of the specific discharge vector in the x_1, x_2, z directions, respectively, κ is the intrinsic permeability, μ is the dynamic viscosity, p is the pressure, ρ is the density of water and g is the acceleration due to gravity. The fresh water head, ϕ, is

$$\phi = \frac{p}{\rho_f g} + Z \tag{2.2}$$

where ρ_f is the density of fresh water and Z is the elevation above an arbitrary datum. Combination of (2.1) and (2.2) gives

$$
\begin{aligned}
q_i &= -k\frac{\partial \phi}{\partial x_i} \\
q_z &= -k\frac{\partial \phi}{\partial z} - k\nu
\end{aligned}
\tag{2.3}
$$

where k is the hydraulic conductivity of fresh water

$$k = \frac{\kappa \rho_f g}{\mu} \tag{2.4}$$

and ν is the dimensionless density

$$\nu = \frac{\rho - \rho_f}{\rho_f} \tag{2.5}$$

The discharge vector is the total flow integrated over the saturated thickness of the aquifer and has components

$$Q_i = \int_{z_b}^{z_t} q_i dz = \int_{z_b}^{z_t} -k\frac{\partial \phi}{\partial x_i} dz \tag{2.6}$$

where z_b and z_t are the bottom and top of the aquifer, respectively. Integration and differentiation may be reversed if z_b and z_t are not a function of x_1 and x_2 (as for a confined aquifer with horizontal base and top)

$$Q_i = -\frac{\partial}{\partial x_i}\left[k\int_{z_b}^{z_t} \phi dz\right] = -\frac{\partial \Phi}{\partial x_i} \tag{2.7}$$

where the potential Φ is defined as

$$\Phi = k\int_{z_b}^{z_t} \phi dz \tag{2.8}$$

Continuity of flow gives

$$\frac{\partial Q_1}{\partial x_1} + \frac{\partial Q_2}{\partial x_2} = \partial_i Q_i = -N_t + N_b \tag{2.9}$$

where N_t is the water leaving the aquifer at the top and N_b is the water entering the aquifer at the bottom; both N_t and N_b may be functions of x_1 and x_2. The partial derivative in the x_i–direction is written as ∂_i and the Einstein summation convention is adopted for repeated indices; only the index i is used to indicate the components of a vector and summation is implied for the horizontal directions only. Substitution of (2.7) for Q_i in (2.9) gives

$$\nabla^2 \Phi = N_t - N_b \tag{2.10}$$

where ∇^2 is the Laplacian in the horizontal directions.

The Dupuit approximation

The Dupuit approximation is adopted, which means that the resistance to flow in the vertical direction is neglected and the pressure distribution is hydrostatic, so that $\partial p/\partial z = -\rho g$ and thus

$$\frac{\partial \phi}{\partial z} = -\nu \tag{2.11}$$

Integration gives

$$\phi = -\int \nu dz + F(x_1, x_2) \tag{2.12}$$

where $F(x_1, x_2)$ is an, as of yet, unknown function of x_1 and x_2. Substitution of (2.12) for ϕ in (2.8) and division by k gives

$$\frac{\Phi}{k} = \int_{z_b}^{z_t} \phi dz = -\int_{z_b}^{z_t} \int \nu dz dz + \int_{z_b}^{z_t} F(x_1, x_2) dz \tag{2.13}$$

Performing the latter integration leads to an expression for F

$$F(x_1, x_2) = \frac{1}{H} \int_{z_b}^{z_t} \int \nu dz dz + \frac{\Phi}{kH} \tag{2.14}$$

Substitution of (2.14) for F into (2.12) gives an expression for the head as a function of the potential

$$\boxed{\phi = \frac{\Phi}{kH} - \int \nu dz + \frac{1}{H} \int_{z_b}^{z_t} \int \nu dz dz} \tag{2.15}$$

or vice versa

$$\boxed{\Phi = kH\phi + kH \int \nu dz - k \int_{z_b}^{z_t} \int \nu dz dz} \tag{2.16}$$

Expressions (2.15) and (2.16) are identical to expressions (40) and (39), respectively, in Strack (1995).

The specific discharge vector

The horizontal components of the specific discharge vector are obtained from differentiation of (2.15)

$$\boxed{q_i = -k\partial_i \phi = \frac{Q_i}{H} + k\partial_i \int \nu dz - \frac{k}{H} \int_{z_b}^{z_t} \partial_i \int \nu dz dz} \qquad i = 1, 2 \tag{2.17}$$

where integration and differentiation are interchanged for the first integral in the last term. The vertical component of flow may be obtained from continuity

$$\partial_i q_i + \frac{\partial q_z}{\partial z} = 0 \tag{2.18}$$

which gives

$$q_z = -\int\limits_{z_b}^{z} \partial_i q_i dz + N_b \tag{2.19}$$

The divergence of q_i may be obtained from (2.17) which gives for (2.19)

$$q_z = -\int\limits_{z_b}^{z} \left[\frac{\partial_i Q_i}{H} + k\nabla^2 \int \nu dz - \frac{k}{H}\partial_i \int\limits_{z_b}^{z_t} \partial_i \int \nu dz dz \right] dz + N_b \tag{2.20}$$

The first and last terms on the right–hand side of (2.20) may be combined, using (2.9)

$$-\int\limits_{z_b}^{z} \frac{\partial_i Q_i}{H} dz + N_b = \frac{z - z_b}{H} N_t - \frac{z - z_t}{H} N_b \tag{2.21}$$

For the case that $N_t = N_b = 0$ integration of (2.20) gives

$$q_z = -k \int\limits_{z_b}^{z} \nabla^2 \int \nu dz dz + \frac{k}{H} \int\limits_{z_b}^{z} \partial_i \int\limits_{z_b}^{z_t} \partial_i \int \nu dz dz dz \tag{2.22}$$

This equation may be simplified by interchanging differentiation and integration and by rearranging terms

$$\begin{aligned} q_z &= \frac{-k(z_t - z_b)}{H} \int\limits_{z_b}^{z} \nabla^2 \int \nu dz dz + \frac{k(z - z_b)}{H} \left[\int\limits_{z_b}^{z} \nabla^2 \int \nu dz dz + \int\limits_{z}^{z_t} \nabla^2 \int \nu dz dz \right] \\ &= \frac{k(z - z_t)}{H} \int\limits_{z_b}^{z} \nabla^2 \int \nu dz dz + \frac{k(z - z_b)}{H} \int\limits_{z}^{z_t} \nabla^2 \int \nu dz dz \end{aligned} \tag{2.23}$$

Combination of (2.20) through (2.23) gives the general expression for q_z

$$\boxed{q_z = \frac{z - z_b}{H} N_t - \frac{z - z_t}{H} N_b + \frac{k(z - z_t)}{H} \int\limits_{z_b}^{z} \nabla^2 \int \nu dz dz + \frac{k(z - z_b)}{H} \int\limits_{z}^{z_t} \nabla^2 \int \nu dz dz} \tag{2.24}$$

It may be verified from equation (2.24) that $q_z(z = z_t) = N_t$ and $q_z(z = z_b) = N_b$, as asserted. The expressions for the specific discharge vector, (2.17) and (2.24), are the same as equations (42) and (50) in Strack (1995).

The three–dimensional multiquadric interpolator

The dimensionless density distribution ν, see (2.5), is represented by a multiquadric interpolator (Hardy, 1971), which is written as follows

$$\nu = \sum_{m=1}^{M} \overset{m}{\alpha} \overset{m}{r} + \overset{0}{\alpha} \tag{2.25}$$

where

$$\overset{m}{r}(x_1, x_2, z) = \sqrt{\beta^2[(x_1 - \overset{m}{x}_1)^2 + (x_2 - \overset{m}{x}_2)^2] + (z - \overset{m}{z})^2 + \overset{m}{\Delta}{}^2} \tag{2.26}$$

and β is the horizontal scale factor. The $M+1$ constants $\overset{m}{\alpha}$ $(m = 0, \ldots, M)$ are determined from $M+1$ conditions. M conditions are obtained by requiring that ν equals a specified value $\overset{m}{\nu}$ at M collocation points $(\overset{m}{x}_1, \overset{m}{x}_2, \overset{m}{z})$

$$\nu(\overset{m}{x}_1, \overset{m}{x}_2, \overset{m}{z}) = \overset{m}{\nu} \qquad m = 1, \ldots, M \tag{2.27}$$

and one condition by requiring that the sum of the $\overset{m}{\alpha}$ $(m = 1, \ldots, M)$ equals zero

$$\sum_{m=1}^{M} \overset{m}{\alpha} = 0 \tag{2.28}$$

The constants $\overset{m}{\Delta}$ $(m = 1, \ldots, M)$ may be chosen arbitrarily, but do affect the shape of the interpolator function. The smaller the value of Δ, the sharper the change of the interpolator function at a collocation point. The multiquadric interpolator is a convenient interpolator for the density distribution, especially when the constants $\overset{m}{\Delta}$ are chosen small (preferably zero) relative to the size of the model domain (VanGerven and Maas, 1994).

Head and Potential

Expressions for the head in terms of the potential and vice versa (equations (2.15) and (2.16)) may be obtained by integration of the dimensionless density distribution (2.25). The variable $\overset{m}{\phi}$ is introduced as

$$\overset{m}{\phi} = -\int \overset{m}{r}\, dz + \frac{1}{H} \int_{z_b}^{z_t} \int \overset{m}{r}\, dz dz \tag{2.29}$$

where

$$\int \overset{m}{r}\, dz = \tfrac{1}{2}[\overset{m}{r}{}^2 - (z - \overset{m}{z})^2] \ln(z - \overset{m}{z} + \overset{m}{r}) + \tfrac{1}{2}(z - \overset{m}{z})\overset{m}{r} \tag{2.30}$$

and

$$\int \int \overset{m}{r}\, dz dz = \tfrac{1}{2}(z - \overset{m}{z})[\overset{m}{r}{}^2 - (z - \overset{m}{z})^2] \ln(z - \overset{m}{z} + \overset{m}{r}) + \tfrac{1}{3}\overset{m}{r}[(z - \overset{m}{z})^2 - \overset{m}{r}{}^2] \tag{2.31}$$

These integrals may be checked by differentiation. After application of the limits of the double integral, $\overset{m}{\phi}$ becomes

$$\boxed{\begin{aligned} \overset{m}{\phi} = & -\tfrac{1}{2}[\overset{m}{r}{}^2 - (z - \overset{m}{z})^2] \ln(z - \overset{m}{z} + \overset{m}{r}) + \tfrac{1}{2}(z - \overset{m}{z})\overset{m}{r} + \\ & + \Big[\tfrac{1}{2}(z_t - \overset{m}{z})[r_{mt}^2 - (z_t - \overset{m}{z})^2] \ln(z_t - \overset{m}{z} + r_{mt}) + \tfrac{1}{2} r_{mt}(z_t - \overset{m}{z})^2 - \tfrac{1}{3} r_{mt}^3 \\ & - \tfrac{1}{2}(z_b - \overset{m}{z})[r_{mb}^2 - (z_b - \overset{m}{z})^2] \ln(z_b - \overset{m}{z} + r_{mb}) - \tfrac{1}{2} r_{mb}(z_b - \overset{m}{z})^2 + \tfrac{1}{3} r_{mb}^3\Big] / H \end{aligned}} \tag{2.32}$$

where

$$r_{mb} = \sqrt{\beta^2[(x_1 - \overset{m}{x}_1)^2 + (x_2 - \overset{m}{x}_2)^2] + (z_b - \overset{m}{z})^2 + \overset{m}{\Delta}{}^2} \tag{2.33}$$

$$r_{mt} = \sqrt{\beta^2[(x_1 - \overset{m}{x}_1)^2 + (x_2 - \overset{m}{x}_2)^2] + (z_t - \overset{m}{z})^2 + \overset{m}{\Delta}{}^2} \tag{2.34}$$

The expression for the head in terms of the potential becomes

$$\boxed{\phi = \frac{\Phi}{kH} + \sum_{m=1}^{M} \overset{m}{\alpha}\overset{m}{\phi} - \overset{0}{\alpha}\left(z - \frac{z_t^2 - z_b^2}{2H}\right)} \tag{2.35}$$

and the expression for the potential in terms of the head is

$$\boxed{\Phi = kH\phi - kH \sum_{m=1}^{M} \overset{m}{\alpha}\overset{m}{\phi} + kH\overset{0}{\alpha}\left(z - \frac{z_t^2 - z_b^2}{2H}\right)} \tag{2.36}$$

The specific discharge vector

The specific discharge vector depends on the first and second derivatives of the density distribution (see equations (2.17) and (2.24)) which may be written as

$$\frac{\partial \nu}{\partial x_i} = \sum_{m=0}^{M} \overset{m}{\alpha} \frac{\partial \overset{m}{r}}{\partial x_i} \qquad i = 1, 2 \tag{2.37}$$

$$\nabla^2 \nu = \frac{\partial^2 \nu}{\partial x_1^2} + \frac{\partial^2 \nu}{\partial x_2^2} = \sum_{m=0}^{M} \overset{m}{\alpha} \left(\frac{\partial^2 \overset{m}{r}}{\partial x_1^2} + \frac{\partial^2 \overset{m}{r}}{\partial x_2^2} \right) \tag{2.38}$$

Differentiation of $\overset{m}{r}$ (2.26) is straightforward and gives:

$$\frac{\partial \overset{m}{r}}{\partial x_i} = \beta^2 \frac{x_i - \overset{m}{x}_i}{\overset{m}{r}} \tag{2.39}$$

$$\frac{\partial^2 \overset{m}{r}}{\partial x_1^2} + \frac{\partial^2 \overset{m}{r}}{\partial^2 x_2} = \frac{\beta^2}{\overset{m}{r}} - \frac{\beta^4 (x_1 - \overset{m}{x}_1)^2}{\overset{m}{r}{}^3} + \frac{\beta^2}{\overset{m}{r}} - \frac{\beta^4 (x_2 - \overset{m}{x}_2)^2}{\overset{m}{r}{}^3} = \frac{2\beta^2}{\overset{m}{r}} - \beta^4 \frac{(x_1 - \overset{m}{x}_1)^2 + (x_2 - \overset{m}{x}_2)^2}{\overset{m}{r}{}^3} \tag{2.40}$$

Expressions for the components of the specific discharge vector may be obtained from equations (2.17) through (2.24) by working out the integrals. The following two integrals are used (these can again be verified by differentiation)

$$\int \frac{\partial \overset{m}{r}}{\partial x_1} dz = \int \beta^2 \frac{x_1 - \overset{m}{x}_1}{\overset{m}{r}} dz = \beta^2 (x_1 - \overset{m}{x}_1) \ln(z - \overset{m}{z} + \overset{m}{r}) \tag{2.41}$$

$$\int\int \frac{\partial \overset{m}{r}}{\partial x_1} dz dz = \int \beta^2 (x_1 - \overset{m}{x}_1) \ln(z - \overset{m}{z} + \overset{m}{r}) dz = \beta^2 (x_1 - \overset{m}{x}_1)[(z - \overset{m}{z}) \ln(z - \overset{m}{z} + \overset{m}{r}) - \overset{m}{r}] \tag{2.42}$$

The contribution of multiquadric point m, with unit strength, to q_i will be called $\overset{m}{q}_i$ and is obtained by combination of (2.1), (2.23), and (2.24)

$$\begin{aligned}\overset{m}{q}_i &= k\beta^2 \int \frac{\partial \overset{m}{r}}{\partial x_i} dz - \frac{k\beta^2}{H} \int\limits_{z_b}^{z_t} \int \frac{\partial \overset{m}{r}}{\partial x_i} dz dz = \\ &= k\beta^2 (x_i - \overset{m}{x}_i) \left[\ln(z - \overset{m}{z} + \overset{m}{r}) - \frac{z_t - \overset{m}{z}}{H} \ln(z_t - \overset{m}{z} + r_{mt}) + \frac{r_{mt}}{H} + \frac{z_b - \overset{m}{z}}{H} \ln(z_b - \overset{m}{z} + r_{mb}) - \frac{r_{mb}}{H} \right]\end{aligned} \tag{2.43}$$

Using that

$$\frac{z_t - \overset{m}{z}}{H} = \frac{z_b - \overset{m}{z}}{H} + 1 \tag{2.44}$$

and rearranging terms gives

$$\boxed{\overset{m}{q}_i = \frac{k\beta^2 (x_i - \overset{m}{x}_i)}{H} \left[H \ln \frac{z - \overset{m}{z} + \overset{m}{r}}{z_t - \overset{m}{z} + r_{mt}} + (z_b - \overset{m}{z}) \ln \frac{z_b - \overset{m}{z} + r_{mb}}{z_t - \overset{m}{z} + r_{mt}} + r_{mt} - r_{mb} \right]} \tag{2.45}$$

An expression for the vertical component of the specific discharge vector may be obtained if the double integral of the Laplacian of the density distribution is carried out. The following integrals are used

$$\int \int \frac{\partial^2 \overset{m}{r}}{\partial x_1^2} dz dz = \beta^2 [(z - \overset{m}{z}) \ln(z - \overset{m}{z} + \overset{m}{r}) - \overset{m}{r}] - \frac{\beta^4 (x_1 - \overset{m}{x}_1)^2}{z - \overset{m}{z} + \overset{m}{r}} \tag{2.46}$$

$$\int \int \frac{\partial^2 \overset{m}{r}}{\partial x_2^2} dz dz = \beta^2 [(z - \overset{m}{z}) \ln(z - \overset{m}{z} + \overset{m}{r}) - \overset{m}{r}] - \frac{\beta^4 (x_2 - \overset{m}{x}_2)^2}{z - \overset{m}{z} + \overset{m}{r}} \tag{2.47}$$

so that

$$\int \int \nabla^2 \overset{m}{r} dz dz = 2\beta^2 [(z - \overset{m}{z}) \ln(z - \overset{m}{z} + \overset{m}{r}) - \overset{m}{r}] - \frac{\beta^4 [(x_1 - \overset{m}{x}_1)^2 + (x_2 - \overset{m}{x}_2)^2]}{z - \overset{m}{z} + \overset{m}{r}} \tag{2.48}$$

which may be simplified, after some algebra, to

$$\int \int \nabla^2 \overset{m}{r} dz dz = 2\beta^2 [(z - \overset{m}{z}) \ln(z - \overset{m}{z} + \overset{m}{r}] + \beta^2 \left[z - \overset{m}{z} - \overset{m}{r} + \frac{\Delta^2}{z - \overset{m}{z} + \overset{m}{r}} \right] \tag{2.49}$$

The vertical component of the specific discharge vector may be obtained by substitution of (2.49) for the double integrals in (2.24) and gives, after a considerable amount of algebra,

$$\boxed{\begin{aligned}\overset{m}{q}_z = 3 &\left[\frac{z_t - z}{H} (r_{mt} - r_{mb}) + \overset{m}{r} - r_{mt} \right] \\ &- 2(z - \overset{m}{z}) \ln \frac{z - \overset{m}{z} + \overset{m}{r}}{z_t - \overset{m}{z} + r_{mt}} + \frac{2(z_b - \overset{m}{z})(z_t - z)}{H} \ln \frac{z_b - \overset{m}{z} + r_{mb}}{z_t - \overset{m}{z} + r_{mt}} \\ &+ \frac{\Delta^2}{H} \left[\frac{z - z_b}{z_t - \overset{m}{z} + r_{mt}} - \frac{z - z_t}{z_b - \overset{m}{z} + r_{mb}} - \frac{H}{z - \overset{m}{z} + \overset{m}{r}} \right]\end{aligned}} \tag{2.50}$$

It is noted that the specific form of (2.50) is chosen so that the logarithms are the same in the expressions for $\overset{m}{q}_i$ and $\overset{m}{q}_z$; this will facilitate computations.

The three components of the discharge vector may now be obtained as follows

$$\boxed{\begin{aligned} q_i &= \frac{Q_i}{H} + \sum_{m=1}^{M} \overset{m}{\alpha}\overset{m}{q}_i \qquad i = 1, 2 \\ q_z &= \frac{z - z_b}{H} N_t - \frac{z - z_t}{H} N_b + \sum_{m=1}^{M} \overset{m}{\alpha}\overset{m}{q}_z \end{aligned}} \tag{2.51}$$

where $\overset{m}{q}_i$ and $\overset{m}{q}_z$ are given by (2.45) and (2.50), respectively.

Rotation

As stated before, the specific discharge field is rotational. It will be shown that, although continuity of flow is met exactly when making the Dupuit approximation (see (2.18)), the curl of the specific discharge vector is represented approximately. Darcy's law may be rewritten as

$$\begin{aligned} q_i &= -\partial_i \chi \qquad i = 1, 2 \\ q_z &= -\frac{\partial \chi}{\partial z} - k\nu \end{aligned} \tag{2.52}$$

where

$$\chi = k\phi \tag{2.53}$$

The curl $\vec{R}$ of the specific discharge vector may be written as

$$\vec{R} = (\partial_2 q_z - \partial_z q_2, \partial_z q_1 - \partial_1 q_z, \partial_1 q_2 - \partial_2 q_1) \tag{2.54}$$

where ∂_z stands for partial differentiation in the z–direction. Differentiation of (2.52) and substitution of the result in (2.54) gives

$$\vec{R} = (-k\partial_2 \nu, k\partial_1 \nu, 0) \tag{2.55}$$

where it is used that χ is single valued ($\partial_1 \partial_2 \chi = \partial_2 \partial_1 \chi$).

The curl of the specific discharge vector obtained with the Dupuit approximation may be computed by differentiation of (2.17) and (2.24). Differentiation gives

$$\partial_z q_1 = k\partial_1 \nu \qquad \partial_z q_2 = k\partial_2 \nu \qquad \partial_2 q_1 = \partial_1 q_2 \tag{2.56}$$

so that the curl of the specific discharge obtained with the Dupuit approximation becomes

$$\vec{R} = (-k\partial_2 \nu + \partial_2 q_z, k\partial_1 \nu + \partial_1 q_z, 0) \tag{2.57}$$

Equation (2.57) is only equal to (2.55) for the case that $\partial_2 q_z = \partial_1 q_z = 0$; this is the case if $\nabla^2 \nu = 0$. For almost all other cases, the curl is represented approximately.

Implementation

The Dupuit formulation for variable density flow may be implemented in any groundwater code for Dupuit flow of a single density fluid. Prior to this study, this theory has been implemented, in a slightly different manner, in the commercial program Multi Layer Analytic Element Model (MLAEM; Strack, 1992) and is called MVAEM (where the V stands for Variable density). The flow field in MLAEM and MVAEM is modeled with analytic elements (Strack, 1989; Haitjema 1995). The implementation of the theory in the analytic element code Single Layer Wells Line–sinks (SLWL; Strack, 1989) is discussed in the next chapter.

CHAPTER 3

Implementation on the Supercomputer

Introduction

The analytic element code Single Layer Wells Line–sinks, SLWL (Strack, 1989), is modified to run on a CrayC916. The Dupuit theory for variable density flow is implemented and the resulting program is called Variable Density SLWL (VDSLWL); VDSLWL is an experimental code.

Implementation

The flow field consists of a potential flow part plus a part due to the variation in density. This may be seen, for example, from the equations for the horizontal components of the specific discharge vector (2.51):

$$q_i = \frac{Q_i}{H} + \sum_{m=1}^{M} \overset{m}{\alpha} \overset{m}{q}_i \qquad i = 1, 2 \tag{3.1}$$

where $\overset{m}{\alpha}$ is the strength of multiquadric point m and $\overset{m}{q}_i$ $(m = 1, \ldots, M)$ depend on the density distribution and aquifer parameters only (see 2.45). It is noted here that this does not mean that the flow field written in the form (3.1) is the sum of single density flow plus variable density flow. The discharge vector Q_i depends on the boundary conditions, which in turn depend on the density distribution.

The flow field is modeled with analytic elements. The analytic elements used here are wells, constant strength line–sinks, and constant strength, circular ponds. Each element may be written as the product of a strength parameter (for example, the discharge of a well) and an influence function that depends on the geometry only. The influence functions for the analytic elements used in this study may be found in Strack (1989). The strength of element n is called $\overset{n}{s}$ and the influence function $\overset{n}{\Lambda}(x_1, x_2)$ so that the potential due to N elements is

$$\Phi(x_1, x_2) = \sum_{n=1}^{N} \overset{n}{s} \overset{n}{\Lambda}(x_1, x_2) \tag{3.2}$$

The derivative of $\overset{n}{\Lambda}$ in the x_i direction is written as $\overset{n}{\lambda}_i$ so that the discharge vector may be written as

$$Q_i = -\partial_i \Phi = -\sum_{n=1}^{N} \overset{n}{s} \overset{n}{\lambda}_i \tag{3.3}$$

and the specific discharge vector becomes

$$q_i = -\frac{1}{H}\sum_{n=1}^{N} \overset{n}{s}\overset{n}{\lambda}_i + \sum_{m=1}^{M} \overset{m}{\alpha}\overset{m}{q}_i \qquad i = 1, 2 \tag{3.4}$$

Hence, the specific discharge vector consists of two large sums. These sums are represented by do–loops in FORTRAN subroutines. The contribution of the analytic elements is divided into three parts, one each for wells, line–sinks and ponds. The listing of the code may be found in Strack (1989). The computation of heads may also be written as the sum of a potential flow part plus a density part (see 2.35), both existing of large sums.

The program SLWL was modified to run on the vector machine CRAY C916 at the Minnesota Supercomputer Institute. The C916 is a vector machine with 9 processors. Each processor is capable of 960 Mflops (10^6 floating point operations per second) at peak performance. The program SLWL was transported to the C916 and modified to run under cf77, the Cray FORTRAN compiler, and using vectorization. As the do–loops for the analytic elements and the density all have the same format (a parameter times an influence function), the design for each module is the same. The design of the line–sink module will be discussed here.

The code of SLWL was transferred to the C916 and was run with only minor changes (to comply with Cray FORTRAN). The performance of the code was evaluated by running a test case of 80 head specified line–sinks. The calculation part of the test case consisted of the computation of 3 grids of 80*80, which corresponds to 3*80*80*80=153600 evaluations of the line–sink function. The initial performance test showed that the code ran at 24.84 Mflops. A performance trace showed that 94.76% of the time was spent in two functions: `COMLS` (78.63%) and `CFLSU` (16.14%). The solution of a 81 by 81 matrix used 0.07% of the time.

`CFLSU` consists of a do–loop that sums up the contribution to the complex potential of all head specified line–sinks. `COMLS` is the complex potential due to a line–sink of unit strength (the function $\overset{n}{\Lambda}$ for a line–sink). The code of `CFLSU` and `COMLS` is (see Strack, 1989)

```
      COMPLEX FUNCTION CFLSU(CZ)
      IMPLICIT COMPLEX (C), LOGICAL (L)
      INCLUDE 'SLLS.CMN'
      CFLSU=(.0,.0)
      DO 100 ILSF=1,NLSF
        IAD=ILSPTF(ILSF)
        CFLSU=CFLSU+RLSDIS(IAD)*COMLS(CZ,CLSZS(IAD),CLSZE(IAD))
  100 CONTINUE
      RETURN
      END
```

```
COMPLEX FUNCTION COMLS(CZ,CZS,CZE)
IMPLICIT COMPLEX (C), LOGICAL (L)
DATA RPI /3.1415926/
CBZ=(2.0*CZ-(CZS+CZE))/(CZE-CZS)
COM1=(.0,.0)
COM2=(.0,.0)
IF(CABS(CBZ+1.).GT..0001) COM1=(CBZ+1.)*CLOG(CBZ+1.)
IF(CABS(CBZ-1.).GT..0001) COM2=(CBZ-1.)*CLOG(CBZ-1.)
COMLS=COM1-COM2+2.*CLOG(.5*(CZE-CZS))-2.
COMLS=.25/RPI*CABS(CZE-CZS)*COMLS
RETURN
END
```

The vectorization on the C916 is automatic, provided that the code is in a vectorizable form. Only inner do–loops can be vectorized and the do–loop cannot contain calls to other subroutines or external functions. In addition, a recurrence relation, like the line

```
CFLSU=CFLSU+RLSDIS(IAD)*COMLS(CZ,CLSZS(IAD),CLSZE(IAD))
```

in `CFLSU`, is not guaranteed to be vectorized correctly.

The do–loop in `CFLSU` is not vectorizable because it has a call to an external function `COMLS`. Furthermore, problems are anticipated because of the presence of a recurrence relation in the do–loop. The do–loop will be vectorizable if the function `COMLS` is brought inline with the function `CFLSU`.

The program fpp (FORTRAN pre processor) on the C916 may be used to bring `COMLS` inline with `CFLSU`. This results in a do–loop that is indeed vectorizable, but does not modify the recurrence relation at the end of the do–loop. As such, the code does not give correct results.

The code was rewritten to bring `COMLS` inline with `CFLSU`, instead of using fpp. The recurrence relation at the end of the do–loop was moved to a separate do–loop. Compiler directives were added to obstruct cf77 from vectorizing the latter do–loop. The modified code is

```
COMPLEX FUNCTION CFLSU(CZ)
IMPLICIT COMPLEX (C), LOGICAL (L)
INCLUDE 'SLLS.CMN'
DIMENSION CSCR(100)
DATA RPI /3.1415926/
```

Table 3.1: Bench mark results

Machine	Wallclock (seconds)	CPU time (seconds)
486PC,50MHz	130	–
C916 w/o vectorization	30.25	22.22
C916 w/ vectorization	2.65	2.49

```
      CFLSU=(.0,.0)
      DO 100 ILSF=1,NLSF
        IAD=ILSPTF(ILSF)
        CZS=CLSZS(IAD)
        CZE=CLSZE(IAD)
        CBZ=(2.0*CZ-(CZS+CZE))/(CZE-CZS)
        COM1=(.0,.0)
        COM2=(.0,.0)
        IF(CABS(CBZ+1.).GT..0001) COM1=(CBZ+1.)*CLOG(CBZ+1.)
        IF(CABS(CBZ-1.).GT..0001) COM2=(CBZ-1.)*CLOG(CBZ-1.)
        COM=COM1-COM2+2.*CLOG(.5*(CZE-CZS))-2.
        COM=.25/RPI*CABS(CZE-CZS)*COM
        CSCR(ILSF)=RLSDIS(IAD)*COM
  100 CONTINUE
CDIR$ NOVECTOR
      DO I=1,NLSF
         CFLSU=CFLSU+CSCR(I)
      ENDDO
CDIR$ VECTOR
      RETURN
      END
```

The vectorized code ran at 293.95 Mflops. A performance of over 300 Mflops may be obtained by replacing the second do–loop in `CFLSU` by a library call that sums up the `CSCR` array. Results of a benchmark for the outlined problem are shown in Table 3.1.

It may be concluded from Table 3.1 that vectorization gives a significant increase in performance. To enable vectorization, the code has to be rewritten to create do–loops that do not call any external functions or subroutines and do not include recurrence relations. This influences the modular structure of the program. The use of fpp to inline code has to be used with caution, because fpp does not consider the presence of recurrence relations.

Performance

The change of the salinity distribution over time may be approximated using consecutive steady–state approximations. Given the initial density distribution, points where the density is specified (referred to as density points here) are moved with the flow over a certain time interval. The velocity field is fixed over the time interval. As a first order approximation, the density at a point that moves with the flow is assumed not to change; processes such as diffusion and dispersion are not taken into account. At the end of the time interval, the new locations of the density points may be used to compute a new density distribution and thus a new velocity field. This process is repeated until the desired time is reached.

The computational effort of transient simulations may be separated into two parts: (1) the computation of the density distribution and (2) the advection of points during a time interval with a suitable particle tracking technique. The computation of the density distribution consists of solving the system of linear equations presented by equations (2.27) and (2.28). Such a system may be solved using a standard routine and is not used as a bench mark.

The advection of the density points requires the repeated evaluation of the three components of the specific discharge vector given by (2.51). The parts of equations (2.51) that represent the influence of the variation in density consist of simple sums, which are easily vectorizable. Computations have been performed on a PC with an Intel Pentium Pro 200 MHz processor and a Cray C916 with 9 processors and a clockspeed of 238 MHz. The computer program is written in FORTRAN77, using the Lahey F77L-EM/32 compiler on the PC and the CrayCFT77 compiler on the C916.

A benchmark is performed for a hypothetical problem where the flow is caused by density differences only (hence $Q_1 = Q_2 = N_b = N_t = 0$). The components of the specific discharge vector were computed ten times at each density point (representing a procedure that needs 10 evaluations of the velocity over a time interval). The results are presented in Table 3.2. Column 1 is the number of points where the density is specified, column 2 the computation time (in seconds) on the PC, Column 3 the computation time on the CrayC916 without vectorization, and column 4 the computation time on the CrayC916 with vectorization and autotasking, using 1 processor. The computational speed on the PC and the CrayC916 without vectorization are similar while the computation time on the CrayC916 with vectorization is an order of magnitude smaller. The CrayC916 with vectorization runs at a speed of 363 Mflops for the case of 1600 density points.

It is of interest to note that the computation time to solve the system of equations is comparable to

Table 3.2: Comparison of performance with time in seconds

Number of points	PC	CrayC916 w/o vectorization	CrayC916 w/ vectorization
200	2.31	2.39	0.39
400	9.01	9.22	1.20
600	20.38	20.48	2.37
800	35.87	35.95	3.95
1000	55.97		5.88
1200	80.63		8.32
1400	109.74		11.08
1600	143.52		14.43
3200			54.92

the computation time of the evaluation of the discharge vector as discussed above. The system was solved using LDU–decomposition. This procedure is known to be inefficient and hard to vectorize. It may have an advantage, however, if the procedure to simulate the change of the density is modified as follows. Instead of following a density point with the flow, it is determined what density will arrive at the density point. Thus the location of the density point is fixed, but the density will change. If the location remains the same, so will the system of equations (2.27) and (2.28) that has to be solved; this system depends only on the location of the points. Hence, the matrix equation has to be inverted only once and the LDU–decomposition stored. Back substitution using the LDU–decomposition consists of the two matrix multiplications and the computation time involved is insignificant.

The evaluation of the specific discharge vector at the M density points is an M^2 process (M evaluations at M locations). Hence, a graph of the number of points versus the computation time should be a straight line on log–log paper; this graph is presented in Figure 3.1 for the PC and the CrayC916 with vectorization. The slopes of the lines represent the real powers of the process. The computations on the PC are approximately an $M^{1.99}$ process and on the CrayC916 an $M^{1.74}$ process.

The benchmark shows that vectorization results in an order of magnitude increase in speed. Use of a vector machine makes it possible to solve problems with thousands of density points, as needed in regional modeling, in a timely manner. Much larger systems of equations can be handled on the Cray than on the PC.

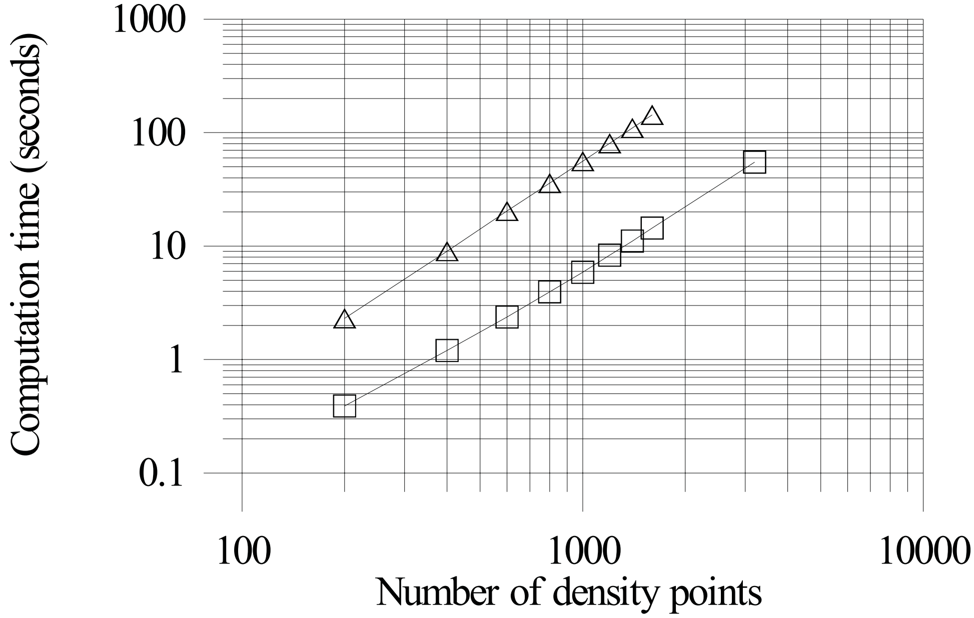

Figure 3.1: Comparison of computation times; PC (triangles), CrayC916 (squares).

Instructions for use of the density module in VDSLWL

VDSLWL has a command line interface. Commands can be typed in or read from an input file. If VDSLWL is run on the supercomputer, instructions are read from the file IN.SL, output is written to the file OUT.SL (unless specified differently) and messages are written to the file MES.SL. The input of aquifer parameters and analytic elements is described in Strack (1989). The only change that has been made is that when a head is specified, either for a head specified well, a head specified line–sink or the reference point, both the head and an elevation have to be specified. A horizontal grid of the density distribution may be obtained with the command `<GRID>(N)<NU>(Z)` where Z is the elevation in the aquifer where the grid is computed.

The check module includes three new commands: `<DENSITY>`, `<SDIS>(x,y,z)`, `<NU>(x,y,z)`. These commands will return input density information, specific discharge at a point and dimensionless density at a point. The same convention is adopted for the density module. The command `<DENS>` accesses the density module. The following commands are available in the density module

```
(x,y,z,nu,delta)..<BETA>(b)..<SOLVE>..<CONTROL>
<COIN>(tol)..<QUIT>
```

The first command specifies the data at a point. Specify the dimensionless density (ν) not the density (ρ). A separate Δ may be specified for each point. The factor β is the horizontal scale factor. All density data should be entered consecutively. After all density data is entered solve the system of equations by typing `<SOLVE>`. The command `<CONTROL>` provides data to check whether the solution is correct. The command <COIN> finds all the points within a specified tolerance from each other. And finally, <QUIT> returns command to the main menu. An example data file with the following three data points

x	y	z	ν	Δ
1000	1000	-20	0.02	1
1000	2000	-30	0.01	1
2000	2000	-10	0.005	1

would look as follows

```
DENS
BETA .01
1000 1000 -20 0.02  1
1000 2000 -30 0.01  1
2000 2000 -10 0.005 1
SOLVE
CONTROL
QUIT
```

The CONTROL statement returns the following information

```
I,ALPHA,NUCOMPUTED,NUGIVEN    1 -6.52104E-04  2.00000E-02  2.00000E-02
I,ALPHA,NUCOMPUTED,NUGIVEN    2  2.57503E-04  1.00000E-02  1.00000E-02
I,ALPHA,NUCOMPUTED,NUGIVEN    3  3.94602E-04  5.00000E-03  5.00000E-03
NUO,SUM OF ALPHA-S   1.01553E-02  0.00000E+00
```

Some notes on modification of the code

Details of the analytic element part of the code are given in Strack (1989). The listing of the density module of VDSLWL is presented in Appendix B. Two issues are of interest for VDSLWL.

1) In the top part of the file SLMN.FOR, the input and output are directed to either a file (for use on the supercomputer) or the console (for use on a PC).

2) The maximum number of density points is specified in the common block vardens.cmn and in the routine `ludcmp` (in the file ludcmp.for).

CHAPTER 4

The Dupuit Approximation for Variable Density Flow in Coastal Aquifers

Introduction

The implications of the Dupuit approximation for variable density flow in coastal aquifers are investigated. The density distribution in the aquifer is represented by a number of surfaces of constant density. The elevations of the surfaces are approximated with multiquadric interpolators; the density varies linearly between them. A new exact solution is derived for two–dimensional flow in the vertical plane, and is compared to the Dupuit solution. The problem used for comparison consists of a bell-shaped transition zone between fresh and salt water (as may be expected from upconing under a pumping well).

The density distribution changes with time because the salt moves with the groundwater. The change of the density distribution is simulated by computing the change of the surfaces of constant density through time. A transient simulation is presented for a hypothetical problem.

Representation of the density distribution

In practice, the density distribution as a function of x_1, x_2, and z is unknown. Rather, the density is known at a number of isolated points in the aquifer. The integrals in the expressions for the head, potential, and specific discharge vector, derived in Chapter 2, may be carried out when a functional form is chosen to represent the density distribution. In light of the expressions for the specific discharge vector, (2.17) and (2.24), the function that represents the density distribution needs to have continuous first derivatives and Laplacian in the two horizontal directions to ensure a continuous flow field.

Strack (1995) proposed to represent the density distribution using a three–dimensional radial basis interpolator function; such functions have an infinite number of continuous derivatives (except for some special cases). This approach has been implemented in the commercial software package MVAEM, and for this project in the program VDSLWL, and has been used successfully to simulate the distribution of fresh water heads in parts of The Netherlands (e.g., Van Gerven and Maas, 1994; Minnema and van der Meij, 1997).

Radial basis functions, such as the multiquadric interpolator (Hardy, 1971), are nicely behaved functions

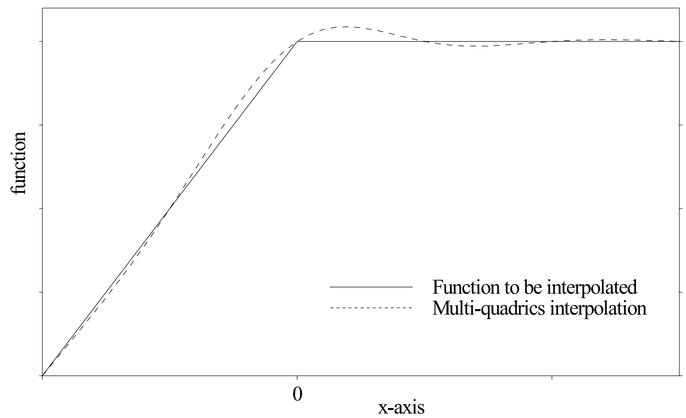

Figure 4.1: Overshoot and fluctuation of the interpolator function

that are suitable for the representation of continuously varying functions. However, radial basis functions, as well as most other interpolation functions, are not suitable for the representation of a function that has discontinuities in its derivatives; for example, a function that varies in one part of a domain and is constant in another part. Consider, for example, a one–dimensional function that varies linearly for $x < 0$ and is constant for $x > 0$ (the solid line in figure 4.1). When this function is approximated by a multiquadric interpolator a problem arises near $x = 0$, because the interpolator cannot make a sharp bend (the derivative of the interpolator is continuous). As a result, the interpolator will fluctuate around the function that it represents over a considerable distance from the sharp bend (the dashed line in Figure 4.1). Such a behavior is undesirable if the interpolator is to be used for the representation of the density distribution. Another problem with the three–dimensional interpolator function is the shape factor Δ. In practice, this shape factor is often set close to zero to obtain a reasonable representation of the density distribution (Van Gerven and Maas, 1994). This results in a reasonable variation of the fresh water head, but the resulting velocity field appears to be physically unrealistic. (It turns out that for Δ approaching zero, the Laplacian of the interpolator function ($\nabla^2\nu$) tends to infinity, as will be explained later in this chapter.)

As an alternative functional representation, it is proposed to divide the aquifer up in a number, say $N+1$, of regions (see Figure 4.2). The n^{th} region is bounded below by surface n of constant density $\nu = \nu_n$ and on top by surface $n+1$ with density $\nu = \nu_{n+1}$. The density in region n varies linearly from ν_n to ν_{n+1} in the vertical direction. If the elevation of surface n is represented by the function $\zeta_n(x_1, x_2)$, then the density may be written as

$$\nu(x_1, x_2, z) = \begin{cases} \nu_N & z \geq \zeta_N(x_1, x_2) \\ \nu_n + \dfrac{z - \zeta_n}{\zeta_{n+1} - \zeta_n}(\nu_{n+1} - \nu_n) & \zeta_n(x_1, x_2) \leq z \leq \zeta_{n+1}(x_1, x_2) \\ \nu_1 & z \leq \zeta_1(x_1, x_2) \end{cases} \tag{4.1}$$

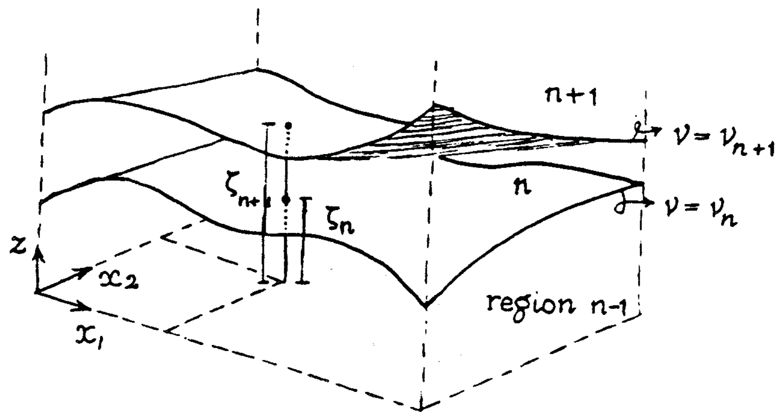

Figure 4.2: Surfaces of constant density

The elevation of surface n, $\zeta_n(x_1, x_2)$, may be represented by a two–dimensional interpolation function. In practice, salinities are measured in nested observation wells, such that the density is known at a number of elevations at one location. These measurements may be used to estimate the elevations of surfaces of constant density; the interpolation function is fitted through these elevations.

The advantage of representation (4.1) is that the change from constant density (in the salt and fresh water zones) to varying density (in the transition zone) is represented accurately. Also, it is convenient to have explicit expressions for the elevations of surfaces of constant density while doing transient simulations, as will become apparent in the final part of this chapter. A third advantage is that the integrations in the expressions of the head, potential, and specific discharge vector may be carried out independent of the choice of the functions ζ_n, since they do not depend on z.

The new representation is, however, more restrictive, since the density is approximated as piecewise linear in the vertical direction. This restriction may be overcome somewhat by approximating the vertical variation by a second or third order polynomial, but that has not been explored. In addition, representation (4.1) will have to be modified if surface n intersects the base (or top) of the aquifer. Such a modification is possible, but falls outside the scope of this chapter.

The integrations and differentiations for the specific discharge vector are carried out in chapter 5. It is noted that as a result of the choice of this particular representation, the vertical variation of q_x is quadratic in the transition zone and is constant in the fresh and salt water zones; the vertical variation of q_z is linear in the constant density areas and is a third order polynomial in the transition zone (where the vertical variation of ν is linear).

Comparison with exact solution

Strack and Bakker (1995) showed that solutions obtained with the Dupuit approximation for variable density flow compare well with exact solutions for problems where the density varies in the x_1 direction only. In this section, a comparison is made to problems where the density varies in x_1 and z directions. Flow is considered in the vertical x, z plane (the index 1 is dropped from x_1 for notational convenience in this section). The problem used for comparison is a transition zone that has a bell–shape, representing, for example, the upconing under a well. It will be shown that the Dupuit approximation overestimates the specific discharge vector and becomes inaccurate when the horizontal size of the bell–shape becomes small.

Consider the following hypothetical situation of an aquifer in which the density varies linearly from salt ($\nu_1 = \nu_s$) at $z = \zeta_1$ to fresh ($\nu_2 = 0$) at $z = \zeta_2$. The thickness of the transition zone is constant and equal to h so that the density in the transition zone may be written as

$$\nu = \nu_s - \frac{z - \zeta_1}{h}\nu_s \qquad \zeta_1 < z < \zeta_2 \tag{4.2}$$

The elevation of the top and bottom of the transition zone are

$$\zeta_1 = Ae^{-(x/\sigma)^2} - \tfrac{1}{2}h \qquad \zeta_2 = \zeta_1 + h \tag{4.3}$$

where A and σ are chosen as: $\sigma = 2h$, $A = 0.2h$ and $\nu_s = 0.025$.

An exact solution is derived for the case that the aquifer is infinitely thick. It will be shown that the flow caused by the density variation only has a limited extent in the vertical direction if the resistance to flow in the vertical direction is not neglected. The continuity equation may be written, with the aid of Darcy's law, as

$$\frac{\partial q_x}{\partial x} + \frac{\partial q_z}{\partial z} = -\frac{\partial^2 \chi}{\partial x^2} - \frac{\partial^2 \chi}{\partial z^2} - k\frac{\partial \nu}{\partial z} = 0 \tag{4.4}$$

or

$$\frac{\partial^2 \chi}{\partial x^2} + \frac{\partial^2 \chi}{\partial z^2} = -k\frac{\partial \nu}{\partial z} \tag{4.5}$$

where $\chi = k\phi$ (equation (2.53)). The term $-k\partial\nu/\partial z$, and thus the Laplacian of χ, equals zero in the fresh and salt water zones and $k\nu_s/h$ in the transition zone.

The function χ is modeled with analytic elements (Strack, 1989). The transition zone is represented by an area–sink of constant extraction rate $k\nu_s/h$; the boundary of the transition zone is approximated with a polygon. The transition zone is infinitely long. Far away, where the transition zone becomes horizontal, the area–sink is approximated by long line–sinks of strength $k\nu_s$. When z approaches positive infinity, $\frac{\partial \chi}{\partial z}$ approaches $\frac{1}{2}k\nu_s$ (half the "water" extracted by the area–sink comes from the top, the other half from the bottom of the aquifer); for z approaching negative infinity, $\frac{\partial \chi}{\partial z}$ approaches $-\frac{1}{2}k\nu_s$. The desired behavior at

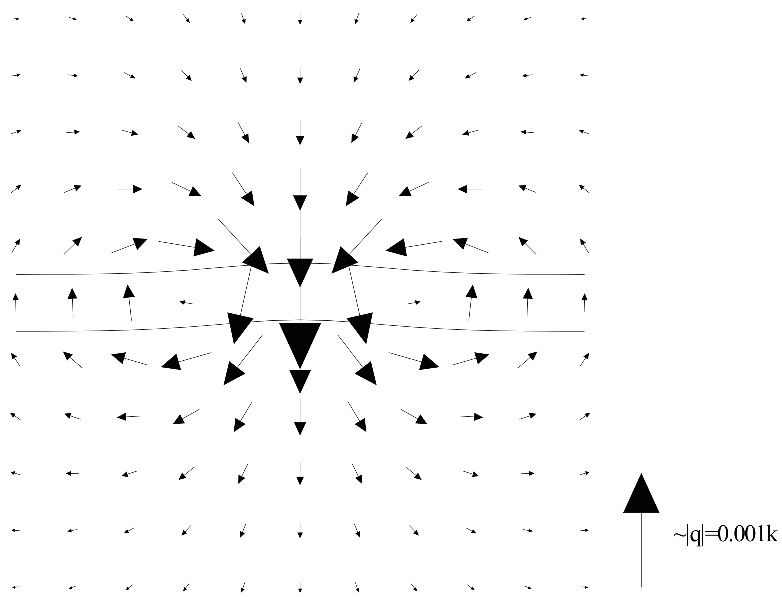

Figure 4.3: Exact solution for variable density flow in an infinite aquifer with the boundary of the transition zone consisting of straight segments

infinity is that q_z equals zero. In terms of derivatives of χ this becomes, with equation (2.52) for q_z, and using that $\nu = 0$ in the fresh water zone and $\nu = \nu_s$ in the salt water zone

$$\lim_{z \to +\infty} \frac{\partial \chi}{\partial z} = 0 \qquad \lim_{z \to -\infty} \frac{\partial \chi}{\partial z} = -k\nu_s \tag{4.6}$$

A term $\chi = -\frac{1}{2}k\nu_s z$ (of which the Laplacian is zero) is added to the solution to obtain the correct behavior at infinity. The flow field for the exact solution may now be obtained with Darcy's law (2.52). Note that the specific discharge vector is not just the gradient of χ, but that an extra term $-k\nu$ must be added to q_z. The flow field and transition zone are shown in Figure 4.3.

An exact solution for an aquifer of finite thickness H may be obtained as follows. (The solution is exact in the sense that the vertical resistance to flow is not neglected; the boundary condition along the base of the aquifer will be met approximately.) The area–sink and the two line–sinks that represent the area–sink far away are imaged through the line $z = H/2$; this will create an impermeable upper boundary. The impermeable base is approximated by a long line–sink with a polynomial strength; this line–sink is also imaged through $z = H/2$. The coefficients of the polynomial are computed such that $\partial\chi/\partial z = -k\nu_s$ along the base, using the procedure proposed by Janković and Barnes (1997). For this solution the extra term $\chi = -\frac{1}{2}k\nu_s z$ is not needed.

The flow field obtained with the Dupuit approximation for an aquifer of finite thickness H may be obtained using the expressions presented in the next chapter with (4.2) for the density distribution. The

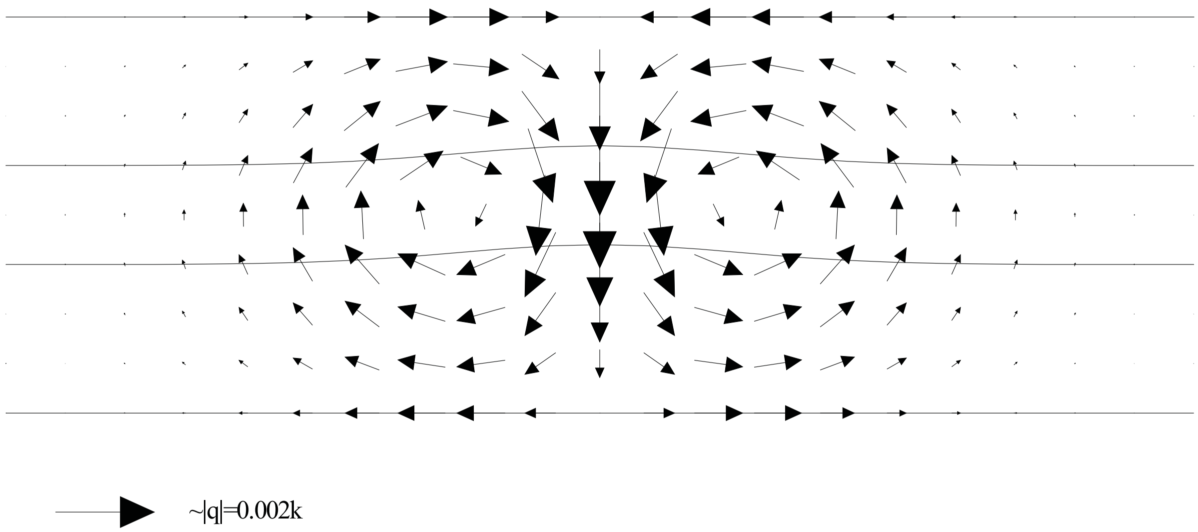

Figure 4.4: Flow field for Dupuit solution ($\sigma = H/2$, $h = H/4$)

functions ζ_1 and ζ_2 are given by (4.3) and the derivatives and Laplacians are

$$\begin{aligned} \frac{\partial \zeta_1}{\partial x} &= \frac{\partial \zeta_2}{\partial x} = -2A\frac{x}{\sigma^2}e^{-(x/\sigma)^2} \\ \frac{\partial^2 \zeta_1}{\partial x^2} &= \frac{\partial^2 \zeta_2}{\partial x^2} = \left(\frac{4x^2}{\sigma^4} - \frac{2}{\sigma^2}\right) Ae^{-(x/\sigma)^2} \end{aligned} \tag{4.7}$$

Solutions are obtained for two cases. Case 1 is characterized by the following values: $\sigma = H$, $h = H/2$; case 2 is characterized by: $\sigma = H/2$, $h = H/4$. The flow field for case 2 is shown in Figure 4.4.

The value of q_x at $z = -h/2$ is plotted versus x for the exact (solid line) and the Dupuit solution (dashed line) for case 2 (see Figure 4.5). The vertical component of flow is plotted versus z at $x = 0$ (Figure 4.6). The solid lines represent the exact solution and the dashed lines the Dupuit solution. The thin lines correspond to case 1, and the thick lines to case 2. The dotted line is the exact solution for an infinite aquifer. It is concluded from Figures 4.5 and 4.6 that a solution obtained with the Dupuit approximation overestimates the specific discharge vector. Such a behavior has also been observed for Dupuit interface flow (see, e.g., Bear, 1972).

The value of σ is a measure of the horizontal size of the upconing; the horizontal size of the upconing is approximately 4σ and the transition zone is essentially horizontal at $|x| > 2\sigma$ (see equation (4.3)). The Dupuit solution becomes inaccurate when the horizontal size of the bell shape is smaller than twice the thickness of the aquifer, as may be seen from Figure 4.6. Further research is needed to draw general conclusions about the range of applicability of the Dupuit approximation.

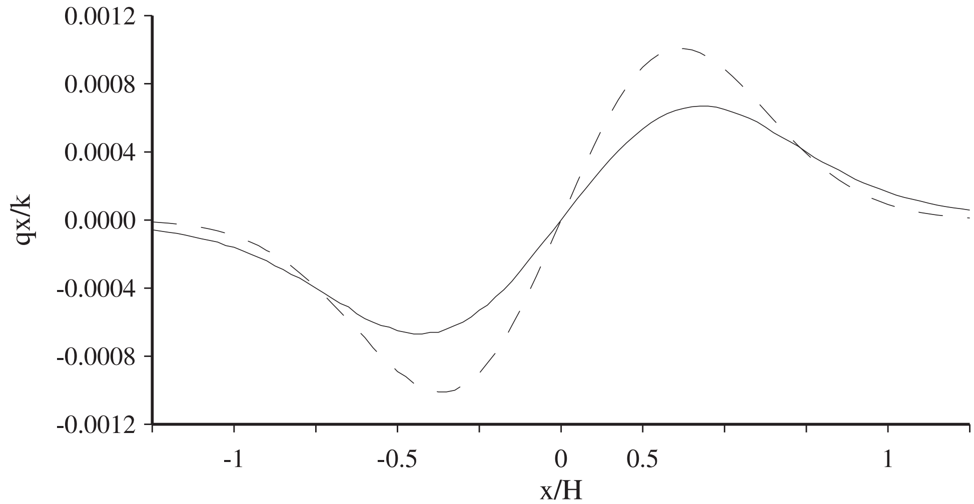

Figure 4.5: Comparison of q_x versus x for exact (solid) and Dupuit (dashed) solutions

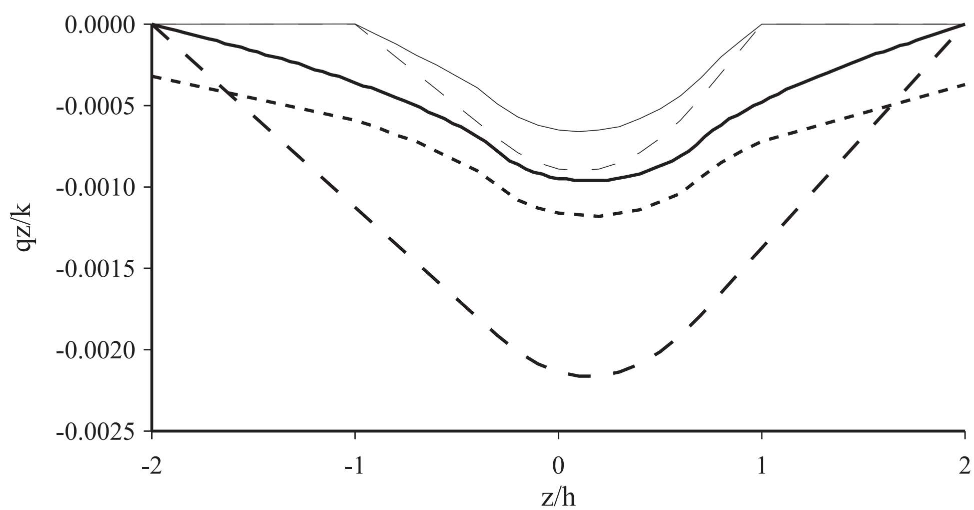

Figure 4.6: Comparison of q_z versus z for exact and Dupuit solutions; (thick lines), $H = 4h$ (thin lines); exact (solid lines) approximate (dashed lines) exact solution for semi–infinite aquifer (dotted line)

Choice of the shape factor Δ

A procedure is outlined to simulate the change of the salinity distribution over time due to advection of the salt with the groundwater. If one is interested in relatively small times (on the order of 25 years, as is the case for most engineering purposes) it might be reasonable to neglect other processes that affect the salinity distribution, such as diffusion and microscopic dispersion. The flow in the aquifer is approximated as incompressible.

The elevation of surface n is represented by a multiquadric interpolator function (Hardy, 1971), which may be written as

$$\zeta_n(x_1, x_2) = \sum_{m=1}^{M} \overset{m}{\alpha}_n \sqrt{(x_1 - \overset{m}{x}_1)^2 + (x_2 - \overset{m}{x}_2)^2 + \Delta^2} + \overset{0}{\alpha}_n \tag{4.8}$$

The constant Δ controls the smoothness of the interpolator. The $M+1$ constants $\overset{m}{\alpha}_n$ $(m = 0, \ldots, M)$ are determined from $M+1$ conditions. M conditions are that ζ_n equals a specified value $\overset{m}{\zeta}_n$ at M collocation points $(\overset{m}{x}_1, \overset{m}{x}_2)$, and one condition is that the sum of the $\overset{m}{\alpha}_n$ $(m = 1, \ldots, M)$ equals zero.

To obtain accurate expressions for the specific discharge vector, the multiquadric interpolator must not only represent the elevations of the surfaces of constant density accurately, but also the first and second derivatives of the elevations of the surfaces. This puts a constraint on the choice of the smoothness parameter Δ. Consider, for example, flow in the vertical plane where the multiquadric function is a function of one variable (x). If Δ is chosen equal to zero, the multiquadric function reduces to a piecewise linear interpolator. The derivative of a piecewise linear interpolator is discontinuous and the second derivative becomes infinite at the collocation points and is zero between them. If Δ is reduced, the derivatives approach the behavior of the derivatives of a piecewise linear interpolator.

It was found that an accurate representation may be obtained if Δ is chosen equal to the distance between the (regularly spaced) collocation points. (In practice, Δ may be chosen equal to the average distance between collocation points, for example.) Figure 4.7 shows the function ζ_1 (solid line) of equation (4.3) and two multiquadric representations. The collocation points are spaced a distance $\sigma/2$ apart and Δ is chosen equal to $\sigma/2$ (dashed line) and $\sigma/20$ (dotted line), respectively. The first and second derivatives of the function and the two multiquadric representations are also shown in Figure 4.7. The case for which Δ is equal to the distance between the collocation points is almost indistinguishable from the function it represents; the interpolator with smaller Δ gives poor results for the derivatives. A similar behavior is observed if the multiquadric interpolator is a function of two or three variables. It is noted that a collocation point is located at the maximum of the function; in practice the location of the maximum is not known and the representation of the density distribution is less accurate.

Transient simulations

Expressions for the movement of the surfaces of constant density through time are obtained by applying continuity of flow in every region separately. The salt water region is bounded below by the aquifer base and on top by surface 1. The salt water zone is called region 0 and the discharge vector in the salt water zone is represented by $\overset{0}{Q}_i$, so that continuity of flow in the salt region gives

$$\partial_i \overset{0}{Q}_i = -\theta \frac{\partial \zeta_1}{\partial t} + N_b \tag{4.9}$$

where θ is the effective porosity. A superscript is added to the specific discharge vector; a superscript n indicates evaluation at $z = \zeta_n$. The horizontal components of the specific discharge vector do not vary with z in the salt water region, so that

$$\overset{0}{Q}_i = \overset{1}{q}_i(\zeta_1 - z_b) \tag{4.10}$$

Substitution of (4.10) for $\overset{0}{Q}_i$ in (4.9) and differentiation gives

$$\theta \frac{\partial \zeta_1}{\partial t} = -\overset{1}{q}_i \partial_i \zeta_1 - \partial_i \overset{1}{q}_i(\zeta_1 - z_b) + N_b \tag{4.11}$$

The sum of the latter two terms equals $q_z(z = \zeta_1) = \overset{1}{q}_z$, as may be seen from (2.19), and (4.11) may be written as

$$\theta \frac{\partial \zeta_1}{\partial t} = -\overset{1}{q}_i \partial_i \zeta_1 + \overset{1}{q}_z \tag{4.12}$$

A similar equation may be derived for the movement of surface 2. Continuity of flow in region 1 states

$$\partial_i \overset{1}{Q}_i = \theta \frac{\partial \zeta_1}{\partial t} - \theta \frac{\partial \zeta_2}{\partial t} \tag{4.13}$$

and the divergence of the discharge vector may be written as

$$\partial_i \overset{1}{Q}_i = \partial_i \int_{\zeta_1}^{\zeta_2} q_i dz = \int_{\zeta_1}^{\zeta_2} \partial_i q_i dz + \overset{2}{q}_i \partial_i \zeta_2 - \overset{1}{q}_i \partial_i \zeta_1 \tag{4.14}$$

where use is made of Leibniz's rule. Substitution of (4.14) for $\partial_i \overset{1}{Q}_i$ in (4.13) and using that

$$\int_{\zeta_1}^{\zeta_2} \partial_i q_i dz = -\overset{2}{q}_z + \overset{1}{q}_z \tag{4.15}$$

gives, after rearrangement of terms

$$\theta \frac{\partial \zeta_2}{\partial t} = -\overset{2}{q}_i \partial_i \zeta_2 + \overset{2}{q}_z \tag{4.16}$$

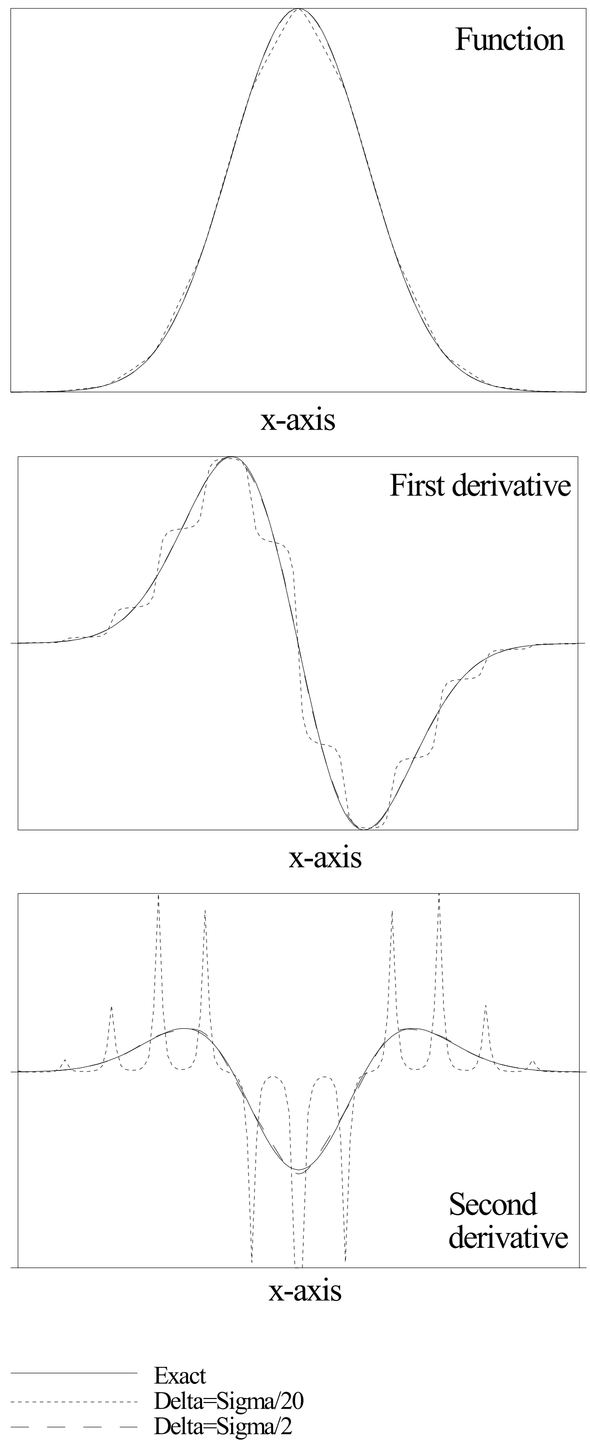

Figure 4.7: Behavior of the multiquadric interpolator

In general, the differential equation for the movement of surface n may be written as

$$\theta \frac{\partial \zeta_n}{\partial t} = -\overset{n}{q}_i \partial_i \zeta_n + \overset{n}{q}_z \tag{4.17}$$

or as

$$\frac{D\zeta_n}{Dt} = \frac{\overset{n}{q}_z}{\theta} \tag{4.18}$$

where $\frac{D}{Dt}$ is the material time derivative for the two horizontal directions. Equations (4.16) and (4.17) are equivalent to the equations for a moving interface as obtained by, e.g., Bear (1972) and De Josselin de Jong (1981).

The movement of a surface of constant density through time may be approximated by numerical integration of either (4.17) or (4.18), where the specific discharge vector is taken constant during a time step. At the end of the time step, a new specific discharge field is computed, based on the new density distribution. The accuracy may be improved by using a predictor–corrector procedure and/or smaller time steps.

For general cases, (4.18) is probably preferred, especially in the presence of leakage or in the neighborhood of inhomogeneities in the aquifer properties. It may also be beneficial to choose the collocation points for the multiquadric interpolator on a regular grid. Equation (4.18) should then be integrated by determining what elevation will arrive at a grid point during a time step, instead of where the elevation of a grid point moves to.

As an example, the change through time of the density distribution of a hypothetical problem is computed. Consider an aquifer of hydraulic conductivity $k = 1$m/d and thickness $H = 40$m. The aquifer is divided into 3 regions. The density in the salt and fresh regions are $\nu_1 = 0.025$ and $\nu_2 = 0$, respectively. The density in the transition zone at $t = 0$ is

$$\nu = \nu_1 - \frac{z - \zeta_1}{\zeta_2 - \zeta_1}\nu_1 \qquad \zeta_1 < z < \zeta_2 \tag{4.19}$$

where

$$\zeta_1 = -Ae^{-(x+2\sigma)^2/\sigma^2} - \tfrac{1}{2}h \qquad \zeta_2 = Ae^{-(x-2\sigma)^2/\sigma^2} + \tfrac{1}{2}h \tag{4.20}$$

where $h = H/4$, $\sigma = H/2$, $A = H/8$. The top and bottom of the transition zone are represented by multiquadric interpolators. The collocation points are spaced a distance $\sigma/2$ apart; Δ is chosen equal to this distance. The flow field and position of the transition zone at $t = 0$ is shown in Figure 4.8a. The change of the transition zone through time is computed through numerical integration of equation (4.17) where $\theta = 0.3$; the time step is 20d. The flow field and position of the transition zone at $t = 500$d and $t = 4000$d are shown in Figures 4.8b and 4.8c, respectively.

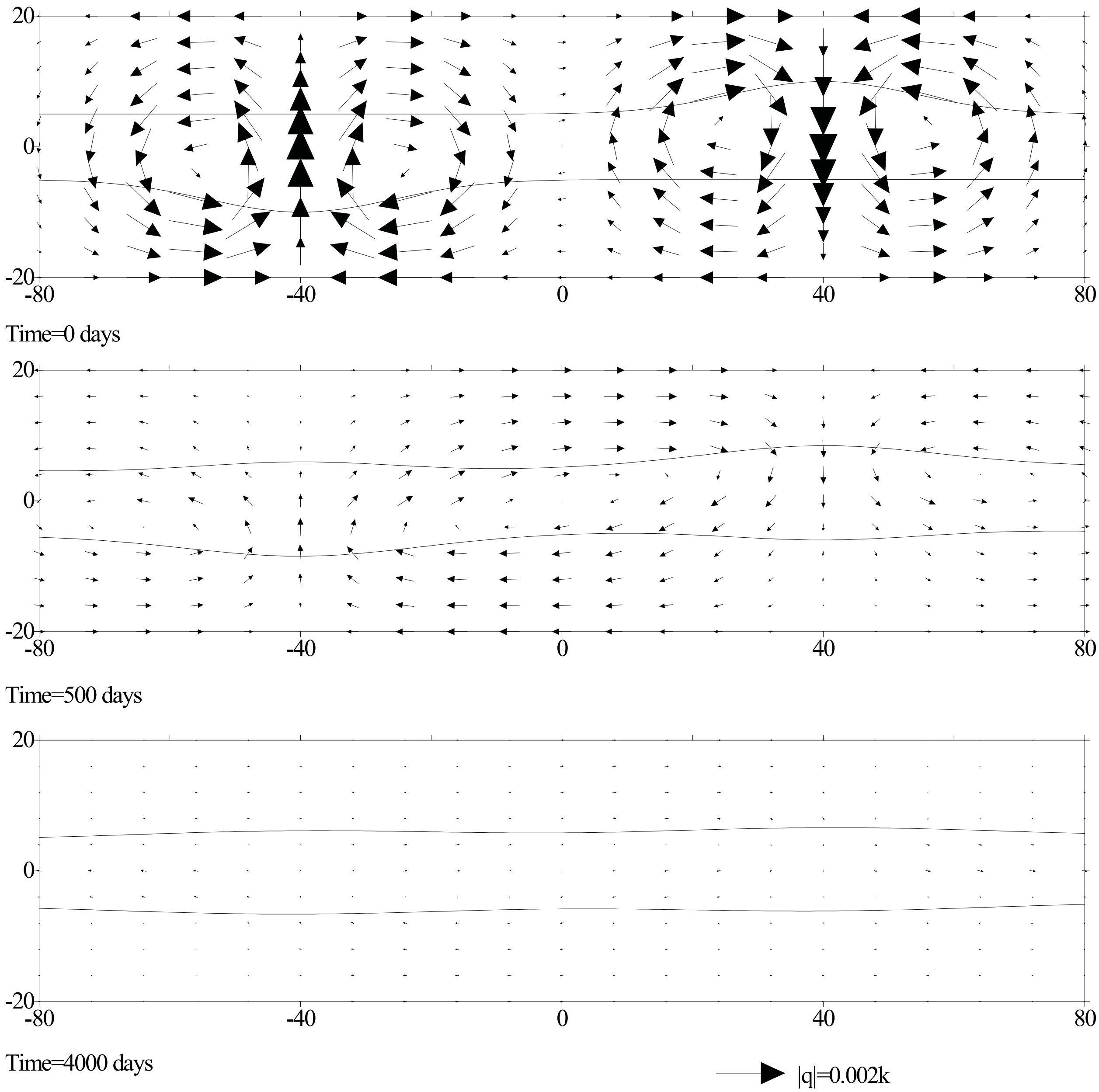

Figure 4.8: Results of transient simulation

Conclusions

The implications of the Dupuit approximation for variable density flow in coastal aquifers were investigated. The density distribution was represented by a number of surfaces of constant density; the elevations of the surfaces were approximated with multiquadric interpolators and the density varies linearly between them. It was shown that the smoothness parameter Δ in the multiquadric interpolator must be of the order of the average distance between control points to obtain reasonable results for the gradient and Laplacian of the density distribution; this is required to obtain accurate specific discharges (and thus velocities). A new exact solution was derived for two–dimensional, variable density flow in the vertical plane. The exact solution was compared to the Dupuit solution. The problem chosen for comparison consisted of a bell shaped transition zone. The comparison showed that the Dupuit approximation overestimates the specific discharge vector and that the flow field becomes inaccurate when horizontal size of the upconing is smaller than two times the aquifer thickness for the specific case investigated. Additional research is needed to draw general conclusions on the range of application of the Dupuit approximation for variable density flow. The new density distribution was highly useful for the comparison of Dupuit solutions to exact solutions. Equations were derived for the movement of surfaces of constant density through time. The equations were used for a simple transient simulation.

Acknowledgment

The computations for the exact solutions in Figures 4.3, 4.5, and 4.6 were obtained with the program Split written by Igor Janković.

CHAPTER 5

The Specific Discharge Vector for a Vertically Piecewise–Linear Density Distribution

Introduction

Expressions are derived for the specific discharge vector resulting from the new density distribution introduced in the previous chapter. First, expressions are derived for the simple case of a transition zone consisting of two constant density planes ($N = 2$). General expressions for arbitrary N are derived in the second part. The expressions for the specific discharge vector are reproduced here from Chapter 2 for completeness

$$\boxed{q_i = -k\partial_i\phi = \frac{Q_i}{H} + k\partial_i \int \nu dz - \frac{k}{H}\int_{z_b}^{z_t} \partial_i \int \nu dz dz} \qquad i = 1, 2 \tag{5.1}$$

$$\boxed{q_z = \frac{z - z_b}{H}N_t - \frac{z - z_t}{H}N_b + \frac{k(z - z_t)}{H}\int_{z_b}^{z} \nabla^2 \int \nu dz dz + \frac{k(z - z_b)}{H}\int_{z}^{z_t} \nabla^2 \int \nu dz dz} \tag{5.2}$$

A simple transition zone

The integrations in the expressions for the specific discharge vector may be carried out when a functional form is chosen for the dimensionless density distribution. As an example, the density is taken to vary linearly from ν_1 to ν_2 between $\zeta_1(x, y)$ and $\zeta_2(x, y)$. For $z < \zeta_1$ the density is equal to ν_1 and for $z > \zeta_2$ the density is ν_2. In functional form this becomes

$$\nu(x, y, z) = \begin{cases} \nu_2 & z > \zeta_2(x, y) \\ \nu_1 + \dfrac{z - \zeta_1}{\zeta_2 - \zeta_1}(\nu_2 - \nu_1) & \zeta_1(x, y) < z < \zeta_2(x, y) \\ \nu_1 & z < \zeta_1(x, y) \end{cases} \tag{5.3}$$

The integrations in (5.1) may be carried out without knowing the functions $\zeta_1(x, y)$ and $\zeta_2(x, y)$, because they are independent of z.

$$\int \nu dz = \begin{cases} \nu_2(z-\zeta_2) + \nu_1(\zeta_2 - z_b) + \frac{1}{2}(\nu_2-\nu_1)(\zeta_2-\zeta_1) & z > \zeta_2 \\ \nu_1(z-\zeta_1) + \dfrac{(z-\zeta_1)^2(\nu_2-\nu_1)}{2(\zeta_2-\zeta_1)} + \nu_1(\zeta_1 - z_b) & \zeta_1 < z < \zeta_2 \\ \nu_1(z-z_b) & z < \zeta_1 \end{cases} \tag{5.4}$$

It may be verified from (5.4) that the function $\int \nu dz$ is continuous. Differentiation of (5.4) gives

$$\partial_i \int \nu dz = \begin{cases} \frac{1}{2}(\nu_1-\nu_2)\,(\partial_i\zeta_1 + \partial_i\zeta_2) & z > \zeta_2 \\ \frac{1}{2}(\nu_1-\nu_2)\dfrac{2(z-\zeta_1)\partial_i\zeta_1(\zeta_2-\zeta_1) + (z-\zeta_1)^2(\partial_i\zeta_2 - \partial_i\zeta_1)}{(\zeta_2-\zeta_1)^2} & \zeta_1 < z < \zeta_2 \\ 0 & z < \zeta_1 \end{cases} \tag{5.5}$$

where it is assumed that z_b is constant. Expression (5.5) may be integrated from z_b to z_t

$$\begin{aligned} \int_{z_b}^{z_t} \partial_i \int \nu dz dz &= \frac{(\nu_1-\nu_2)}{2(\zeta_2-\zeta_1)^2}\left[(z-\zeta_1)^2\partial_i\zeta_1(\zeta_2-\zeta_1) + \tfrac{1}{3}(z-\zeta_1)^3(\partial_i\zeta_2-\partial_i\zeta_1)\right]_{\zeta_1}^{\zeta_2} \\ &+ \tfrac{1}{2}(\nu_1-\nu_2)(\partial_i\zeta_1+\partial_i\zeta_2)(z_t-\zeta_2) \\ &= \tfrac{1}{2}(\nu_1-\nu_2)[\tfrac{1}{3}(\zeta_2-\zeta_1)(2\partial_i\zeta_1+\partial_i\zeta_2) + (z_t-\zeta_2)(\partial_i\zeta_1+\partial_i\zeta_2)] \end{aligned} \tag{5.6}$$

The horizontal components of the discharge vector become, with (5.1), (5.5), and (5.6)

$$\begin{aligned} q_i = \frac{Q_i}{H} &- \frac{k}{2H}(\nu_1-\nu_2)[\tfrac{1}{3}(\zeta_2-\zeta_1)(2\partial_i\zeta_1+\partial_i\zeta_2) + (z_t-\zeta_2)(\partial_i\zeta_1+\partial_i\zeta_2)] \\ &+ \frac{k}{2}(\nu_1-\nu_2)\begin{cases} \partial_i\zeta_1+\partial_i\zeta_2 & z > \zeta_2 \\ \dfrac{2(z-\zeta_1)\partial_i\zeta_1(\zeta_2-\zeta_1) + (z-\zeta_1)^2(\partial_i\zeta_2-\partial_i\zeta_1)}{(\zeta_2-\zeta_1)^2} & \zeta_1 < z < \zeta_2 \\ 0 & z < \zeta_1 \end{cases} \end{aligned} \tag{5.7}$$

The vertical component of flow is obtained from (5.2) which may be written as

$$q_z = -k\int_{z_b}^{z} \nabla^2 \int \nu dz dz + \frac{k}{H}\int_{z_b}^{z}\int_{z_b}^{z_t} \nabla^2 \int \nu dz dz dz \tag{5.8}$$

The derivation of $\nabla^2 \int \nu dz$, which requires differentiation of (5.5), is messy for the region $\zeta_1 < z < \zeta_2$. The vector $f_i(x, y, z)$ is introduced for convenience as

$$\partial_i \int \nu dz = \tfrac{1}{2}(\nu_1-\nu_2) f_i \qquad \zeta_1 < z < \zeta_2 \tag{5.9}$$

where f_i is

$$f_i = \frac{2(z-\zeta_1)\partial_i\zeta_1}{\zeta_2-\zeta_1} + \frac{(z-\zeta_1)^2(\partial_i\zeta_2-\partial_i\zeta_1)}{(\zeta_2-\zeta_1)^2} = g_i + h_i \tag{5.10}$$

where g_i is the first fraction in (5.10) and h_i is the second fraction. Differentiation of g_i gives

$$\begin{aligned}\partial_i g_i &= \frac{[-2\partial_i\zeta_1\partial_i\zeta_1 + 2(z-\zeta_1)\nabla^2\zeta_1](\zeta_2-\zeta_1) - 2(z-\zeta_1)\partial_i\zeta_1(\partial_i\zeta_2-\partial_i\zeta_1)}{(\zeta_2-\zeta_1)^2} \\ &= \frac{-2\partial_i\zeta_1\partial_i\zeta_1}{\zeta_2-\zeta_1} + \frac{2\nabla^2\zeta_1(\zeta_2-\zeta_1) - 2\partial_i\zeta_1(\partial_i\zeta_2-\partial_i\zeta_1)}{(\zeta_2-\zeta_1)^2}(z-\zeta_1)\end{aligned} \tag{5.11}$$

And differentiation of h_i

$$\begin{aligned}\partial_i h_i =& \left\{[-2(z-\zeta_1)\partial_i\zeta_1(\partial_i\zeta_2-\partial_i\zeta_1) + (z-\zeta_1)^2(\nabla^2\zeta_2-\nabla^2\zeta_1)](\zeta_2-\zeta_1)^2\right. \\ &\left. -2(z-\zeta_1)^2(\partial_i\zeta_2-\partial_i\zeta_1)(\zeta_2-\zeta_1)(\partial_i\zeta_2-\partial_i\zeta_1)\right\}/(\zeta_2-\zeta_1)^4 \\ =& \frac{(\zeta_2-\zeta_1)(\nabla^2\zeta_2-\nabla^2\zeta_1) - 2(\partial_i\zeta_2-\partial_i\zeta_1)^2}{(\zeta_2-\zeta_1)^3}(z-\zeta_1)^2 - \frac{2\partial_i\zeta_1(\partial_i\zeta_2-\partial_i\zeta_1)}{(\zeta_2-\zeta_1)^2}(z-\zeta_1)\end{aligned} \tag{5.12}$$

Combination of (5.11) and (5.12) gives

$$\begin{aligned}\partial_i f_i =& \frac{-2\partial_i\zeta_1\partial_i\zeta_1}{(\zeta_2-\zeta_1)} + \frac{2\nabla^2\zeta_1(\zeta_2-\zeta_1) - 4\partial_i\zeta_1(\partial_i\zeta_2-\partial_i\zeta_1)}{(\zeta_2-\zeta_1)^2}(z-\zeta_1) \\ &+ \frac{(\zeta_2-\zeta_1)(\nabla^2\zeta_2-\nabla^2\zeta_1) - 2(\partial_i\zeta_2-\partial_i\zeta_1)^2}{(\zeta_2-\zeta_1)^3}(z-\zeta_1)^2\end{aligned} \tag{5.13}$$

This gives for $\nabla^2\int\nu dz$

$$\nabla^2\int\nu dz = \tfrac{1}{2}(\nu_1-\nu_2)\begin{cases}\nabla^2\zeta_1+\nabla^2\zeta_2 & z>\zeta_2 \\ \partial_i f_i & \zeta_1<z<\zeta_2 \\ 0 & z<\zeta_1\end{cases} \tag{5.14}$$

Integration of (5.14) gives for $\zeta_1<z<\zeta_2$

$$\begin{aligned}\int_{\zeta_1}^{z}\partial_i f_i dz =& \frac{-2\partial_i\zeta_1\partial_i\zeta_1}{(\zeta_2-\zeta_1)}(z-\zeta_1) + \frac{\nabla^2\zeta_1(\zeta_2-\zeta_1) - 2\partial_i\zeta_1(\partial_i\zeta_2-\partial_i\zeta_1)}{(\zeta_2-\zeta_1)^2}(z-\zeta_1)^2 \\ &+ \frac{(\zeta_2-\zeta_1)(\nabla^2\zeta_2-\nabla^2\zeta_1) - 2(\partial_i\zeta_2-\partial_i\zeta_1)^2}{3(\zeta_2-\zeta_1)^3}(z-\zeta_1)^3\end{aligned} \tag{5.15}$$

so that

$$\begin{aligned}\int_{\zeta_1}^{\zeta_2}\partial_i f_i dz =& -2\partial_i\zeta_1\partial_i\zeta_1 + \nabla^2\zeta_1(\zeta_2-\zeta_1) - 2\partial_i\zeta_1(\partial_i\zeta_2-\partial_i\zeta_1) \\ &+ \tfrac{1}{3}(\zeta_2-\zeta_1)(\nabla^2\zeta_2-\nabla^2\zeta_1) - \tfrac{2}{3}(\partial_i\zeta_2-\partial_i\zeta_1)^2 \\ =& -\tfrac{2}{3}(\partial_i\zeta_2\partial_i\zeta_2 + \partial_i\zeta_1\partial_i\zeta_2 + \partial_i\zeta_1\partial_i\zeta_1) + \nabla^2\zeta_1(\zeta_2-\zeta_1) + \tfrac{1}{3}(\zeta_2-\zeta_1)(\nabla^2\zeta_2-\nabla^2\zeta_1)\end{aligned} \tag{5.16}$$

and

$$\int_{\zeta_2}^{z}(\nabla^2\zeta_1+\nabla^2\zeta_2)dz = (\nabla^2\zeta_1+\nabla^2\zeta_2)(z-\zeta_2) \tag{5.17}$$

Combining the previous three equations gives

$$\int_{z_b}^{z} \nabla^2 \int \nu dz dz = \tfrac{1}{2}(\nu_1 - \nu_2) \begin{cases} \nabla^2\zeta_1(z-\zeta_1) + \nabla^2\zeta_2(z-\zeta_2) + \frac{1}{3}(\zeta_2-\zeta_1)(\nabla^2\zeta_2 - \nabla^2\zeta_1) + \\ -\frac{2}{3}(\partial_i\zeta_2\partial_i\zeta_2 + \partial_i\zeta_1\partial_i\zeta_2 + \partial_i\zeta_1\partial_i\zeta_1) & z > \zeta_2 \\ \dfrac{-2\partial_i\zeta_1\partial_i\zeta_1}{(\zeta_2-\zeta_1)}(z-\zeta_1) + \dfrac{\nabla^2\zeta_1(\zeta_2-\zeta_1) - 2\partial_i\zeta_1(\partial_i\zeta_2 - \partial_i\zeta_1)}{(\zeta_2-\zeta_1)^2}(z-\zeta_1)^2 + \\ + \dfrac{(\zeta_2-\zeta_1)(\nabla^2\zeta_2 - \nabla^2\zeta_1) - 2(\partial_i\zeta_2 - \partial_i\zeta_1)^2}{3(\zeta_2-\zeta_1)^3}(z-\zeta_1)^3 & \zeta_1 < z < \zeta_2 \\ 0 & z < \zeta_1 \end{cases} \tag{5.18}$$

Differentiation of (5.6) gives

$$\begin{aligned} \int_{z_b}^{z_t} \nabla^2 \int \nu dz dz &= \tfrac{1}{2}(\nu_1 - \nu_2)\left[\tfrac{1}{3}(\partial_i\zeta_2 - \partial_i\zeta_1)(2\partial_i\zeta_1 + \partial_i\zeta_2) + \tfrac{1}{3}(\zeta_2-\zeta_1)(2\nabla^2\zeta_1 + \nabla^2\zeta_2) - \right. \\ &\qquad \left. \partial_i\zeta_2(\partial_i\zeta_1 + \partial_i\zeta_2) + (z_t - \zeta_2)(\nabla^2\zeta_1 + \nabla^2\zeta_2)\right] \\ &= \tfrac{1}{2}(\nu_1 - \nu_2)\left[-\tfrac{2}{3}(\partial_i\zeta_2\partial_i\zeta_2 + \partial_i\zeta_1\partial_i\zeta_2 + \partial_i\zeta_1\partial_i\zeta_1) + \right. \\ &\qquad \left. \tfrac{1}{3}(\zeta_2-\zeta_1)(2\nabla^2\zeta_1 + \nabla^2\zeta_2) + (z_t - \zeta_2)(\nabla^2\zeta_1 + \nabla^2\zeta_2)\right] \end{aligned} \tag{5.19}$$

and consecutive integration

$$\begin{aligned} \int_{z_b}^{z}\int_{z_b}^{z_t} \nabla^2 \int \nu dz dz dz = \tfrac{1}{2}(\nu_1 - \nu_2)(z - z_b)\left[-\tfrac{2}{3}(\partial_i\zeta_2\partial_i\zeta_2 + \partial_i\zeta_1\partial_i\zeta_2 + \partial_i\zeta_1\partial_i\zeta_1) + \right. \\ \left. \tfrac{1}{3}(\zeta_2-\zeta_1)(2\nabla^2\zeta_1 + \nabla^2\zeta_2) + (z_t - \zeta_2)(\nabla^2\zeta_1 + \nabla^2\zeta_2)\right] \end{aligned} \tag{5.20}$$

The vertical component of the discharge vector may now be computed with (5.8), (5.18) (with (5.15), (5.16), and (5.17)) and (5.20) which gives

$$\begin{aligned} q_z =& \frac{z - z_b}{H} N_t - \frac{z - z_t}{H} N_b + \tfrac{1}{2}\frac{k}{H}(\nu_1 - \nu_2)(z - z_b) \\ & * \left[-\tfrac{2}{3}(\partial_i\zeta_2\partial_i\zeta_2 + \partial_i\zeta_1\partial_i\zeta_2 + \partial_i\zeta_1\partial_i\zeta_1) + \tfrac{1}{3}(\zeta_2-\zeta_1)(2\nabla^2\zeta_1 + \nabla^2\zeta_2) + (z_t - \zeta_2)(\nabla^2\zeta_1 + \nabla^2\zeta_2)\right] \\ & - \tfrac{1}{2}k(\nu_1 - \nu_2) \begin{cases} \nabla^2\zeta_1(z-\zeta_1) + \nabla^2\zeta_2(z-\zeta_2) + \frac{1}{3}(\zeta_2-\zeta_1)(\nabla^2\zeta_2 - \nabla^2\zeta_1) + \\ -\frac{2}{3}(\partial_i\zeta_2\partial_i\zeta_2 + \partial_i\zeta_1\partial_i\zeta_2 + \partial_i\zeta_1\partial_i\zeta_1) & z \geq \zeta_2 \\ \dfrac{-2\partial_i\zeta_1\partial_i\zeta_1}{(\zeta_2-\zeta_1)}(z-\zeta_1) + \dfrac{\nabla^2\zeta_1(\zeta_2-\zeta_1) - 2\partial_i\zeta_1(\partial_i\zeta_2 - \partial_i\zeta_1)}{(\zeta_2-\zeta_1)^2}(z-\zeta_1)^2 + \\ + \dfrac{(\zeta_2-\zeta_1)(\nabla^2\zeta_2 - \nabla^2\zeta_1) - 2(\partial_i\zeta_2 - \partial_i\zeta_1)^2}{3(\zeta_2-\zeta_1)^3}(z-\zeta_1)^3 & \zeta_1 \leq z \leq \zeta_2 \\ 0 & z \leq \zeta_1 \end{cases} \end{aligned} \tag{5.21}$$

A general transition zone

Consider a transition zone that varies linearly from $\nu = \nu_1$ at $z = \zeta_1$ to $\nu = \nu_2$ at $z = \zeta_2$, then varies linearly from $\nu = \nu_2$ at $z = \zeta_2$ to $\nu = \nu_3$ at $z = \zeta_3$ and so on until the fresh water at $z = \zeta_N$. Hence the density varies linearly in the vertical direction over $N-1$ sections, or written as an equation:

$$\nu(x,y,z) = \begin{cases} \nu_N & z > \zeta_N(x,y) \\ \nu_n + \dfrac{z-\zeta_n}{\zeta_{n+1}-\zeta_n}(\nu_{n+1}-\nu_n) \qquad \zeta_n(x,y) < & z < \zeta_{n+1}(x,y) \\ \nu_1 & z < \zeta_1(x,y) \end{cases} \tag{5.22}$$

The integrations in (5.1) are carried out in what follows. Since the expressions become lengthy, they are not combined into one expression.

$$\int \nu dz = \begin{cases} \nu_N(z-\zeta_N) + \nu_1(\zeta_1 - z_b) + \sum_{m=1}^{N-1}\frac{1}{2}(\nu_m+\nu_{m+1})(\zeta_{m+1}-\zeta_m) & z > \zeta_N \\ \nu_n(z-\zeta_n) + \dfrac{(z-\zeta_n)^2(\nu_{n+1}-\nu_n)}{2(\zeta_{n+1}-\zeta_n)} + \nu_1(\zeta_1 - z_b) + \sum_{m=1}^{n-1}\frac{1}{2}(\nu_m+\nu_{m+1}) & (\zeta_{m+1}-\zeta_m) \\ & \zeta_n < z < \zeta_{n+1} \\ \nu_1(z-z_b) & z < \zeta_1 \end{cases} \tag{5.23}$$

$$\partial_i \int \nu dz = \begin{cases} \nu_1\partial_i\zeta_1 - \nu_N\partial_i\zeta_N + \sum_{m=1}^{N-1}\frac{1}{2}(\nu_m+\nu_{m+1})(\partial_i\zeta_{m+1}-\partial_i\zeta_m) & z > \zeta_N \\ \nu_1\partial_i\zeta_1 - \nu_n\partial_i\zeta_n + \sum_{m=1}^{n-1}\frac{1}{2}(\nu_m+\nu_{m+1})(\partial_i\zeta_{m+1}-\partial_i\zeta_m) + & \\ +\frac{1}{2}(\nu_n-\nu_{n+1})\dfrac{2(z-\zeta_n)\partial_i\zeta_n(\zeta_{n+1}-\zeta_n)+(z-\zeta_n)^2(\partial_i\zeta_{n+1}-\partial_i\zeta_n)}{(\zeta_{n+1}-\zeta_n)^2} & \\ & \zeta_n < z < \zeta_{n+1} \\ 0 & z < \zeta_1 \end{cases} \tag{5.24}$$

$$\begin{aligned} \int_{z_b}^{z_t} \partial_i \int \nu dz =& \nu_1\partial_i\zeta_1(z_t-\zeta_1) - \sum_{m=1}^{N-1}\nu_m\partial_i\zeta_m(\zeta_{m+1}-\zeta_m) - \nu_N\partial_i\zeta_N(z_t-\zeta_N) \\ &+ \sum_{m=1}^{N-1}\tfrac{1}{2}(\nu_m+\nu_{m+1})(\partial_i\zeta_{m+1}-\partial_i\zeta_m)(z_t-\zeta_{m+1}) \\ &+ \sum_{m=1}^{N-1}\tfrac{1}{6}(\nu_m-\nu_{m+1})(2\partial_i\zeta_m+\partial_i\zeta_{m+1})(\zeta_{m+1}-\zeta_m) \end{aligned} \tag{5.25}$$

The expressions for q_z include the integral $\nabla^2 \int \nu dz$. The derivation of $\nabla^2 \int \nu dz$, which requires differentiation of (5.24), is messy for the region $\zeta_n < z < \zeta_{n+1}$. The vector $\overset{n}{f}_i(x,y,z)$ is introduced for convenience as

$$\partial_i \int \nu dz = \tfrac{1}{2}(\nu_n - \nu_{n+1})\overset{n}{f}_i \qquad \zeta_n < z < \zeta_{n+1} \tag{5.26}$$

where $\overset{n}{f}_i$ is

$$\overset{n}{f}_i = \frac{2(z-\zeta_n)\partial_i\zeta_n}{\zeta_{n+1}-\zeta_n} + \frac{(z-\zeta_n)^2(\partial_i\zeta_{n+1}-\partial_i\zeta_n)}{(\zeta_{n+1}-\zeta_n)^2} = \overset{n}{g}_i + \overset{n}{h}_i \tag{5.27}$$

where $\overset{n}{g}_i$ is the first fraction in (5.27) and $\overset{n}{h}_i$ is the second fraction. Differentiation of $\overset{n}{g}_i$ gives

$$\begin{aligned}\partial_i\overset{n}{g}_i &= \frac{[-2\partial_i\zeta_n\partial_i\zeta_n + 2(z-\zeta_n)\nabla^2\zeta_n](\zeta_{n+1}-\zeta_n) - 2(z-\zeta_n)\partial_i\zeta_n(\partial_i\zeta_{n+1}-\partial_i\zeta_n)}{(\zeta_{n+1}-\zeta_n)^2}\\ &= \frac{-2\partial_i\zeta_n\partial_i\zeta_n}{\zeta_{n+1}-\zeta_n} + \frac{2\nabla^2\zeta_n(\zeta_{n+1}-\zeta_n) - 2\partial_i\zeta_n(\partial_i\zeta_{n+1}-\partial_i\zeta_n)}{(\zeta_{n+1}-\zeta_n)^2}(z-\zeta_n)\end{aligned} \tag{5.28}$$

And differentiation of $\overset{n}{h}_i$

$$\begin{aligned}\partial_i\overset{n}{h}_i =& \big\{[-2(z-\zeta_n)\partial_i\zeta_n(\partial_i\zeta_{n+1}-\partial_i\zeta_n) + (z-\zeta_n)^2(\nabla^2\zeta_{n+1}-\nabla^2\zeta_n)](\zeta_{n+1}-\zeta_n)^2\\ &-2(z-\zeta_n)^2(\partial_i\zeta_{n+1}-\partial_i\zeta_n)(\zeta_{n+1}-\zeta_n)(\partial_i\zeta_{n+1}-\partial_i\zeta_n)\big\}/(\zeta_{n+1}-\zeta_n)^4\\ =&\frac{(\zeta_{n+1}-\zeta_n)(\nabla^2\zeta_{n+1}-\nabla^2\zeta_n) - 2(\partial_i\zeta_{n+1}-\partial_i\zeta_n)^2}{(\zeta_{n+1}-\zeta_n)^3}(z-\zeta_n)^2 - \frac{2\partial_i\zeta_n(\partial_i\zeta_{n+1}-\partial_i\zeta_n)}{(\zeta_{n+1}-\zeta_n)^2}(z-\zeta_n)\end{aligned} \tag{5.29}$$

Combination of (5.28) and (5.4) gives

$$\begin{aligned}\partial_i\overset{n}{f}_i =& \frac{-2\partial_i\zeta_n\partial_i\zeta_n}{(\zeta_{n+1}-\zeta_n)} + \frac{2\nabla^2\zeta_n(\zeta_{n+1}-\zeta_n) - 4\partial_i\zeta_n(\partial_i\zeta_{n+1}-\partial_i\zeta_n)}{(\zeta_{n+1}-\zeta_n)^2}(z-\zeta_n)\\ &+ \frac{(\zeta_{n+1}-\zeta_n)(\nabla^2\zeta_{n+1}-\nabla^2\zeta_n) - 2(\partial_i\zeta_{n+1}-\partial_i\zeta_n)^2}{(\zeta_{n+1}-\zeta_n)^3}(z-\zeta_n)^2\end{aligned} \tag{5.30}$$

This gives for $\nabla^2 \int \nu dz$

$$\nabla^2 \int \nu dz = \begin{cases} \nu_1\nabla^2\zeta_1 - \nu_N\nabla^2\zeta_N + \sum_{m=1}^{N-1}\frac{1}{2}(\nu_m+\nu_{m+1})(\nabla^2\zeta_{m+1}-\nabla^2\zeta_m) & z > \zeta_N\\ \nu_1\nabla^2\zeta_1 - \nu_n\nabla^2\zeta_n + \sum_{m=1}^{n-1}\frac{1}{2}(\nu_m+\nu_{m+1})(\nabla^2\zeta_{m+1}-\nabla^2\zeta_m) + \frac{1}{2}(\nu_n & -\nu_{n+1})\partial_i\overset{n}{f}_i\\ & \zeta_n < z < \zeta_{n+1}\\ 0 & z < \zeta_n \end{cases} \tag{5.31}$$

Integration of (5.30) gives

$$\begin{aligned}\int_{\zeta_n}^{z}\partial_i\overset{n}{f}_i dz =& \frac{-2\partial_i\zeta_n\partial_i\zeta_n}{(\zeta_{n+1}-\zeta_n)}(z-\zeta_n) + \frac{\nabla^2\zeta_n(\zeta_{n+1}-\zeta_n) - 2\partial_i\zeta_n(\partial_i\zeta_{n+1}-\partial_i\zeta_n)}{(\zeta_{n+1}-\zeta_n)^2}(z-\zeta_n)^2\\ &+ \frac{(\zeta_{n+1}-\zeta_n)(\nabla^2\zeta_{n+1}-\nabla^2\zeta_n) - 2(\partial_i\zeta_{n+1}-\partial_i\zeta_n)^2}{3(\zeta_{n+1}-\zeta_n)^3}(z-\zeta_n)^3\end{aligned} \tag{5.32}$$

so that

$$
\begin{aligned}
\int\limits_{\zeta_m}^{\zeta_{m+1}} \partial_i \overset{m}{f}_i dz =& -2\partial_i\zeta_m\partial_i\zeta_m + \nabla^2\zeta_m(\zeta_{m+1}-\zeta_m) - 2\partial_i\zeta_m(\partial_i\zeta_{m+1}-\partial_i\zeta_m) \\
&+ \tfrac{1}{3}(\zeta_{m+1}-\zeta_m)(\nabla^2\zeta_{m+1}-\nabla^2\zeta_m) - \tfrac{2}{3}(\partial_i\zeta_{m+1}-\partial_i\zeta_m)^2 \\
=& -\tfrac{2}{3}(\partial_i\zeta_{m+1}\partial_i\zeta_{m+1} + \partial_i\zeta_m\partial_i\zeta_{m+1} + \partial_i\zeta_m\partial_i\zeta_m) \\
&+ \tfrac{1}{3}(\zeta_{m+1}-\zeta_m)(2\nabla^2\zeta_m + \nabla^2\zeta_{m+1})
\end{aligned}
\tag{5.33}
$$

Combining equations (5.26) through (5.33) gives

$$
\int\limits_{z_b}^{z} \nabla^2 \int \nu dz dz = \begin{cases}
\nu_1\nabla^2\zeta_1(z-\zeta_1) - \sum_{m=1}^{N-1}\nu_m\nabla^2\zeta_m(\zeta_{m+1}-\zeta_m) - \nu_N\nabla^2\zeta_N(z-\zeta_N) + & \\
+\sum_{m=1}^{N-1}\frac{1}{2}(\nu_m+\nu_{m+1})(\nabla^2\zeta_{m+1}-\nabla^2\zeta_m)(z-\zeta_{m+1}) & \\
+\sum_{m=1}^{N-1}\frac{1}{2}(\nu_m-\nu_{m+1})\int_{\zeta_m}^{\zeta_{m+1}}\partial_i\overset{m}{f}_i dz & z > \zeta_N \\
\nu_1\nabla^2\zeta_1(z-\zeta_1) - \sum_{m=1}^{n-1}\nu_m\nabla^2\zeta_m(\zeta_{m+1}-\zeta_m) - \nu_n\nabla^2\zeta_n(z-\zeta_n) + & \\
+\sum_{m=1}^{n-1}\frac{1}{2}(\nu_m+\nu_{m+1})(\nabla^2\zeta_{m+1}-\nabla^2\zeta_m)(z-\zeta_{m+1}) & \\
+\sum_{m=1}^{n-1}\frac{1}{2}(\nu_m-\nu_{m+1})\int_{\zeta_m}^{\zeta_{m+1}}\partial_i\overset{m}{f}_i dz + \frac{1}{2}(\nu_n-\nu_{n+1})\int_{\zeta_n}^{z}\partial_i\overset{n}{f}_i dz & \zeta_n < z < \zeta_{n+1} \\
0 & z < \zeta_1
\end{cases}
\tag{5.34}
$$

All integrals are now computed and the specific discharge vector may be computed. The expressions have been implemented in a FORTRAN program, which has been used in Chapter 4 to assess the implications of the Dupuit approximation.

CHAPTER 6

Results and Conclusions

The objective of this report is to investigate the performance of the Dupuit theory for variable density flow combined with analytic elements to model groundwater flow in coastal aquifers. Four areas of study were identified in the introduction. The conclusions pertaining to these four areas of study are summarized in this chapter.

Study area 1.

The analytic element modeling of groundwater flow in the first confined aquifer beneath the Delmarva Peninsula.

An analytic element model was presented for groundwater flow in the shallow aquifers beneath the Delmarva peninsula, in Chapter 1. The modeling of the Delmarva peninsula is greatly hampered by the unavailability of measurements of the salinity of the groundwater, especially near the shore. Only six measurements were found of brackish or salt water. All other measurements indicated fresh water. The six measurements were insufficient to construct a three–dimensional picture of the salinity distribution below the Delmarva peninsula. To overcome this problem, publications of salinity in the Chesapeake Bay and the Atlantic Ocean were used to construct a conceptual model of the salinity distribution below the peninsula. This distribution results in a horizontal variation from fresh water on the peninsula to salt water in the bay and ocean. The variation in the vertical direction is assumed to be negligible. This is known to be unrealistic, but there are not enough data to propose otherwise.

The resulting model of the fresh water head was compared to nine measurements of the head on the eastern part of the peninsula (the counties of Sussex, DE, Wicomico, MD, and Worchester, MD). The comparison showed that the simulation of fresh water heads in that area is reasonable, but general conclusions for the entire model cannot be drawn. Additional data (head, discharge and chloride measurements) are necessary to calibrate the model and to improve the conceptual model of the density distribution.

The modeling study demonstrated the many challenges in building groundwater models of flow systems in coastal aquifers. The biggest constraints in the Chesapeake Bay area are the availability of density data and water table measurements. To assess the full capabilities of the approach, it should be applied to an area where more data are available, perhaps an area outside the United States.

Study area 2

The reduction of computation time by the use of a supercomputer.

The second area of study was addressed in Chapter 3. The Dupuit approximation for variable density flow was implemented in an analytic element model. The resulting program was written to run on the CrayC916, a vector machine. The Dupuit formulation for variable density flow, as well as the analytic element formulation for groundwater flow, are suited ideally for implementation on supercomputers. Both formulations result in large sums of complicated functions that are easily vectorizable. The performance of the vectorized code was an order of magnitude better than the unvectorized code. The vecorized code performed at a speed of over 300 billion floating point operations per second (300 Mflops), which is a significant improvement over the non–vectorized code. It is noted that high performance computing seems to move away from vector machines to massively parallel machines. This will have no adverse effect on the implementation of analytic element codes on supercomputers. The large sums of complicated functions can just as easy be modified to run on massively parallel machines as on vector machines. An analytic element code written specifically for use of a massively parallel machine is presented by Haitjema et al. (1997).

Study area 3

The accurate representation of the density distribution.

In Chapters 1, 2 and 3, the density distribution was represented by the three-dimensional multiquadric interpolator function. It was noted that the shape factor Δ of the interpolator was chosen close to zero. The main reason for this choice was to improve control of the interpolator, especially at the transition from brackish water of variable density to fresh or salt water of constant density. It was shown in Chapter 4 that this will result in reasonable simulations of the density (and thus the fresh water head, as was the objective of the modeling study in Chapter 1), but that the resulting velocity vector was unrealistic near the points where the density is specified. This makes it difficult to simulate the change of the salinity distribution through time; during such a simulation the salt moves with the groundwater and the velocities have to be accurate.

A new function to represent the density was introduced to solve this problem. The representation consists of a number of surfaces of constant density; the elevations of the surfaces are approximated with the multiquadric interpolator and the density varies linearly between them. It was shown that the smoothness parameter Δ in the multiquadric interpolator must be of the order of the average distance between control points to obtain reasonable results for the velocity field. It is noted that this was not practical for the original three–dimensional interpolator.

Study area 4

The implications of adopting the Dupuit approximation for variable density flow.

The new density distribution was used to compare a Dupuit solution with an exact solution, a solution in which the vertical resistance to flow is not neglected. The problem chosen for comparison consisted of a bell shaped transition zone. The comparison showed that the Dupuit approximation overestimates the specific discharge vector and that the flow field becomes inaccurate when the width of the bell–shaped transition zone is less than two times the thickness of the aquifer.

The new density distribution represents the transition from variable density zones (brackish water) to constant density zones (fresh or salt water) accurately. The new distribution does introduce complications that remain to be solved, however, such as the intersection of the transition zone with the base or top of the aquifer. The new density distribution is highly useful for the comparison between Dupuit solutions and exact solutions, because it is relatively easy to obtain exact solutions for flow in the vertical plane corresponding to the new density distribution. A comparison between exact and Dupuit solutions may be used to determine the full range of applicability of the Dupuit approximation for variable density flow.

References

Achmad, G., and J.M. Wilson, 1993. Hydrogeologic framework and the distribution and movement of brackish water in the Ocean City-Manokin aquifer system at Ocean City, Maryland, Maryland Geological Survey Report of Investigations No. 57.

Bear, J. 1972. *Dynamics of fluids in porous media.* Dover Publications, Inc., New York, NY.

De Josselin de Jong, G. 1981. The simultaneous flow of fresh and salt water in aquifers of large horizontal extension determined by shear flow and vortex theory. In: *Flow and transport in porous media.* A. Verruijt and F.B.J. Barends, Editors. A.A. Balkema, Rotterdam, The Netherlands. pp. 75–82.

De Lange, W.J., 1996. Groundwater modeling of large domains with analytic elements, Ph.D. dissertation, Delft University of Technology, published as RIZA note 96.028, Lelystad.

De Lange, W.J. 1997. On the effects of three–dimensional density variation in groundwater flow on the head and flow distribution in a multi–aquifer system. In: Conference companion Part 1. International conference Analytic–based modeling of groundwater flow. April 1997. Nunspeet, The Netherlands.

Fleck, W.B., and D.A. Vroblesky, 1996. Simulation of ground-water flow of the Coastal Plain aquifers in parts of Maryland, Delaware, and the District of Columbia, USGS Professional Paper 1404-J.

Haitjema, H., V. Kelson, and K. Luther. 1997. Modeling three–dimensional groundwater flow on a regional scale using the analytic element method. Report to the US EPA pursuant to project number CR 823637-01-1.

Haitjema, H. 1995. *Analytic Element Modeling of Groundwater Flow.* Academic Press, San Diego, CA.

Hardy, R.L. 1971. Multiquadric equations of topography and other irregular surfaces. *J. Geophys. Res.* 76, 1905–1915.

James R.W., R.H. Simmons and B.F. Strain. 1992. Water Resources Data – Maryland and Delaware, Volume 2. U.S. Geological Survey Water-Data Report MD-DE-92-2, Towson, MD.

Janković, I., and R.J. Barnes. 1997. High order line elements for two–dimensional groundwater flow. In: *Proceedings of the Analytic–based modeling of groundwater flow conference.* Nunspeet, The Netherlands. April 1997.

Kipp, K.L. Jr. 1986. HST3D. A computer code for simulation of heat and solute transport in three–dimensional groundwater flow systems. IGWMC, USGS Water–Resources Investigations Report 86-4095.

Konikow, L.F., and J.D. Bredehoeft. 1978. Computer model of two–dimensional solute transport and dispersion in ground water. Techniques and Water–Resources Investigations, Book 7.

Konikow, L.F., D.J. Goode, G.Z. Hornberger. 1996. A three–dimensional method-of-characteristics solute–transport model (MOC3D), USGS Water–Resources Investigations Report 96-67406.

Leahy, P. P., and M. Martin, 1993. Geohydrology and simulation of ground-water flow in the Northern Atlantic Coastal Plain aquifer system, USGS Professional Paper 1404-K.

Lester, B. 1991. SWICHA. A three–dimensional finite element code for analyzing seawater intrusion in coastal aquifers. Version 5.05. GeoTrans, Inc., Sterling VA.

Lusczynski, N.S. 1961. Head and flow of ground water of variable density. *J. Geophys. Res.* 12(66), 4247–4256.

Maas, C and M.J. Emke. 1988. Solving varying density groundwater problems with a single density computer program. Natuurwetenschappelijk Tijdschrift 1989, Vol 70, p143–154.

McDonald, M.G. and A.W. Harbaugh. 1984. A modular three–dimensional finite–difference groundwater flow model. USGS Open–File Report 83-875.

Meisler, H., 1981. Preliminary delineation of salty ground water in the northern Atlantic Coastal Plain, USGS Open-File Report 81-71.

Meisler, H., 1989. The occurrence and geochemistry of salty ground water in the Northern Atlantic Coastal Plain, USGS Professional Paper 1404-D.

Minnema, B. and J.L. Van Der Meij. 1997. Three–dimensional density–dependent groundwater flow. In: Conference companion Part 1. International conference Analytic–based modeling of groundwater flow. April 1997. Nunspeet, The Netherlands.

Olsthoorn, T.N. 1996. Variable density groundwater flow modelling with MODFLOW. In: 14th Salt Water Intrusion Meeting, 16-21 June, 1996. Malmö, Sweden. Rapporter och meddelanden nr. 87. Geological Survey of Sweden, Uppsala, Sweden.

Oude Essink, G.H.P., and R.H. Boekelman. 1996. Problems of large–scale modelling of salt water intrusion in 3D. *Proc.* 14^{th} *Salt Water Intrusion Meeting,* Malmö, Sweden, June 1996. pp. 16–31.

Oude Essink, G.H.P. 1998. MOC3D adapted to simulate 3D density-dependent groundwater flow. Paper presented at the MODFLOW'98 Conference, October 1998, Golden, CO.

Phelan, D.J., 1987. Water levels, chloride concentrations, and pumpage in the coastal aquifers of Delaware and Maryland, USGS Water-Resources Investigations Report 87-4229.

Richardson, D.L., 1992. Hydrogeology and analysis of the ground-water flow system of the Eastern Shore, Virginia, USGS Open File Report 91-490.

Strack, O.D.L. 1989. *Groundwater Mechanics.* Prentice Hall, Englewood Cliffs, NJ.

Strack, O.D.L. 1995. A Dupuit-Forchheimer model for three–dimensional flow with variable density. *Water Resources Research*, 31 (12), pp. 3007–3017.

Strack, O.D.L., and M. Bakker. 1995. A validation of a Dupuit-Forchheimer formulation for flow with variable density. *Water Resources Research*, 31(12), 3019–3024.

Strack, O.D.L., 1997. Principles of the analytic element method. In: Conference companion Part 1. International conference Analytic–based modeling of groundwater flow. April 1997. Nunspeet, The Netherlands.

Strack, O.D.L., 1997. In: Conference companion Part 2. International conference Analytic–based modeling of groundwater flow. April 1997. Nunspeet, The Netherlands.

Strack, O.D.L., and I. Janković. 2000. A multi-quadric area-sink for analytic element modeling of groundwater flow. *Journal of Hydrology.* In press.

Strack, O.E., 1992. *MLAEM User's Manual*. Strack Engineering, North Oaks, MN.

Sanford, W.E. and L.F. Konikow. 1985. A two–constiuent solute–transport model for ground water having variable density. USGS Water Resources Investigations Report 85-4279.

Van Dam, J.C., 1973. Lecture notes to Geohydrology (F15b), Delft University of Technology, Department of Civil Engineering, Delft, The Netherlands.

Van Gerven, M.W.., and C. Maas. 1994. Testing the new variable density module of MLAEM in the dune water catchment of the Amsterdam Municipal Waterworks (in dutch). KIWA-report SWO 94.212, KIWA, Nieuwegein, The Netherlands.

Voss, C.I. 1984. SUTRA – A finite element simulation for saturated–unsaturated , fluid–density–dependent ground–water flow with energy transport or chemically reactive single–species solute transport. USGS Water–Resources Investigations Report 84-4369.

Vroblesky, D.A., and W.B. Fleck, 1991. Hydrogeologic framework of the coastal plain of Maryland, Delaware, and the District of Columbia, USGS Professional Paper 1404-E.

WES, 1997. The Groundwater Modeling System version 2.0, US Army Corps of Engineers, Waterways Experiment Station, Vicksburg, MS.

Woodruff, K.D., 1969. The occurrence of saline ground water in Delaware aquifers, Delaware Geological Survey Report of Investigations No. 13.

Appendix A1

x (m)	y (m)	z (m)	ρ (kg/m^3)	x (m)	y (m)	z (m)	ρ (kg/m^3)
424108	4204046	-347.5	999.3	435778	4173864	-6.7	999.2
425613	4205912	-299.9	999.4	437272	4173853	-4.6	999.2
425613	4205912	-295.4	999.4	449394	4201970	-7.9	999.2
425613	4205912	-151.5	999.4	455317	4196295	-10.4	999.3
425613	4205912	-341.7	999.4	446405	4200109	-7.6	999.2
410711	4206061	-1.1	999.3	458315	4200040	-4.6	999.2
425613	4205912	-106.7	1001.2	459804	4200032	-11.3	999.2
431596	4209651	-13.4	999.3	411298	4121447	-36.0	999.2
428688	4217197	-173.7	999.2	412806	4119552	-30.2	999.2
428688	4217197	-342.9	999.2	411303	4119567	-29.6	999.2
430174	4217184	-8.7	999.3	412806	4119552	-31.4	999.3
381120	4217752	-2.1	999.3	411462	4134606	-40.2	999.2
442072	4218971	-9.1	999.3	415888	4127040	-34.1	999.2
433191	4222799	-15.2	999.2	412864	4125191	-41.2	999.2
439144	4224633	-62.5	999.3	415964	4134560	-38.7	999.2
439158	4226513	-16.0	999.2	417576	4145824	-35.1	999.3
437674	4226524	-12.2	999.2	419020	4140170	-34.8	999.2
439158	4226513	-32.3	999.3	420555	4143915	-36.6	999.2
442139	4228371	-7.2	999.2	419166	4155209	-29.9	999.2
439172	4228393	-9.8	999.2	429597	4149474	-45.1	999.3
436205	4228416	-18.3	999.2	420484	4136396	-47.6	999.2
436205	4228416	-19.2	999.2	428115	4151366	-32.0	999.2
378318	4229077	-4.7	999.2	426700	4160779	-41.5	999.2
440656	4228382	-14.9	999.2	428115	4151366	-37.5	999.3
353163	4233256	-19.8	999.2	422266	4166460	-28.0	999.3
474791	4231964	-4.6	999.2	432745	4168248	-31.4	999.2
474791	4231964	-13.7	999.2	440205	4166311	-44.8	999.2
482209	4233824	-7.0	999.2	434285	4173876	-43.3	999.2
470356	4235739	-11.7	999.2	435764	4171984	-41.8	999.2
479254	4237592	-17.5	999.2	435808	4177624	-36.0	999.2
344373	4239063	-1.5	999.2	440286	4177590	-35.1	999.2
335481	4239239	-2.3	999.3	440191	4164431	-36.6	999.2
488145	4237574	-14.3	999.2	446245	4175669	-43.3	999.2
488145	4237574	-27.1	999.2	452316	4192552	-41.2	999.2
480740	4239468	-4.6	999.2	446282	4181309	-36.6	999.2
480740	4239468	-12.3	999.2	449394	4201970	-36.3	999.2
489629	4239452	-14.6	999.2	452393	4205712	-33.8	999.2
482222	4239465	-12.6	999.2	459804	4200032	-37.8	999.2
371109	4242354	-2.9	999.3	411298	4121447	-60.4	999.2
445196	4241511	-8.4	999.2	420484	4136396	-60.4	999.2
467414	4241391	-4.9	999.2	409815	4123343	-57.3	999.5
480745	4241348	-16.5	999.3	409815	4123343	-48.2	999.6
482226	4241345	-16.3	999.2	411318	4123327	-54.3	999.5
482226	4241345	-26.4	999.2	409815	4123343	-63.7	999.5
491113	4241330	-17.5	999.2	412747	4113912	-58.8	999.2
492594	4241329	-22.9	999.2	412806	4119552	-50.3	999.2
492594	4241329	-12.2	999.2	415888	4127040	-64.6	999.2
480749	4243228	-32.6	999.2	417390	4127025	-54.9	999.2
480749	4243228	-32.8	999.2	417390	4127025	-55.8	999.2
449651	4243362	-22.6	999.2	417390	4127025	-55.2	999.2

x	y	z	ρ	x	y	z	ρ
491115	4243210	-22.9	999.2	417390	4127025	-54.6	999.2
491115	4243210	-25.9	999.2	412864	4125191	-61.0	999.2
344482	4244704	-4.0	999.2	419166	4155209	-61.9	1001.2
491115	4243210	-36.7	999.2	429597	4149474	-65.2	999.7
448170	4243372	-23.2	999.2	423588	4147647	-63.4	999.2
449651	4243362	-14.0	999.2	420484	4136396	-59.1	999.2
332633	4244941	-6.1	999.2	428115	4151366	-54.9	999.3
486676	4245097	-28.0	999.2	423709	4160806	-45.7	999.2
449663	4245243	-7.6	999.2	426634	4153259	-59.1	999.3
449663	4245243	-8.5	999.2	425137	4153273	-49.4	999.2
449663	4245243	-25.6	999.2	426734	4164539	-56.4	999.2
449663	4245243	-13.1	999.2	426784	4170179	-54.6	999.2
449663	4245243	-10.7	999.2	432837	4179528	-39.6	999.3
448182	4245252	-10.7	999.2	440286	4177590	-56.4	999.2
449663	4245243	-9.3	999.2	440218	4168191	-64.0	999.2
448182	4245252	-9.9	999.2	434210	4164476	-56.1	999.2
448182	4245252	-14.0	999.2	441845	4186979	-46.3	999.2
448182	4245252	-8.7	999.2	443324	4185089	-56.1	999.2
445221	4245271	-11.7	999.2	435969	4198304	-33.5	999.2
451155	4247114	-22.1	999.2	435969	4198304	-33.5	999.3
494079	4246968	-82.6	999.3	446245	4175669	-64.6	999.2
445234	4247152	-19.2	999.2	452316	4192552	-61.3	999.2
443767	4249042	-12.2	999.2	447810	4186939	-58.8	999.2
349030	4250260	-1.2	999.2	449394	4201970	-50.9	999.3
458565	4248952	-1.8	999.2	450837	4194441	-60.4	999.2
473363	4248890	-1.8	999.3	455338	4200055	-47.2	999.2
463005	4248931	-28.3	999.2	459804	4200032	-72.2	999.5
451166	4248994	-25.9	999.2	459804	4200032	-63.7	999.3
486682	4248857	-24.4	999.2	459804	4200032	-71.0	999.4
458575	4250832	-1.8	999.2	459804	4200032	-77.4	999.4
449698	4250883	-20.1	999.2	458315	4200040	-67.4	999.3
443780	4250922	-18.3	999.2	411298	4121447	-75.6	999.7
448219	4250892	-45.7	999.2	412806	4119552	-77.4	999.3
448219	4250892	-57.9	999.2	415888	4127040	-86.0	999.4
448219	4250892	-38.7	999.2	412864	4125191	-83.8	999.2
448219	4250892	-36.6	999.2	412864	4125191	-96.0	1000.1
448219	4250892	-24.4	999.2	417576	4145824	-66.5	999.6
448219	4250892	-2.0	999.2	422054	4143901	-79.9	999.2
489644	4250733	-12.3	999.2	419166	4155209	-81.7	1007.8
457096	4250840	-2.4	999.2	341188	4150692	-91.4	1002.1
489646	4252613	-10.7	999.2	428115	4151366	-86.3	1001.9
488167	4252615	-27.7	999.2	431204	4162621	-68.6	999.2
439356	4252835	-10.4	999.3	432715	4164488	-67.7	999.2
451189	4252754	-6.1	999.2	432730	4166368	-74.7	999.2
451189	4252754	-21.0	999.2	422266	4166460	-51.2	999.6
480772	4252629	-17.5	999.2	432745	4168248	-72.2	999.2
319490	4254631	-5.8	999.2	440205	4166311	-78.9	999.2
485209	4252620	-21.3	999.2	440205	4166311	-74.1	999.3
341741	4256043	-4.6	999.2	440205	4166311	-76.8	999.3
495564	4254487	-1.2	999.3	435808	4177624	-84.4	1000.3

x	y	z	ρ	x	y	z	ρ
486691	4254497	-33.2	999.2	435808	4177624	-65.8	999.2
448243	4254653	-6.9	999.2	440286	4177590	-82.3	999.7
495564	4254487	-11.0	999.3	435969	4198304	-57.9	999.8
483737	4256383	-16.8	999.2	443259	4175689	-86.0	999.2
319575	4258392	-5.2	999.2	452316	4192552	-91.4	999.2
325514	4258260	-2.9	999.2	447846	4192579	-69.8	999.2
324052	4260174	-4.0	999.3	449394	4201970	-69.8	1001.2
344772	4259746	-2.0	999.3	446405	4200109	-101.8	1002.1
309269	4260511	-5.3	999.2	446405	4200109	-68.3	1000.3
334463	4261834	-6.1	999.2	461901	4306639	-52.4	999.2
427591	4260453	-15.7	999.2	461901	4306639	-57.3	999.2
427591	4260453	-4.4	1002.1	463727	4307713	-198.7	1000.0
426130	4262347	-4.1	999.2	463727	4307713	-233.0	1000.0
430595	4266068	-19.8	999.2	461901	4306639	-57.3	999.2
325718	4267663	-3.7	999.2	448528	4294466	0.0	999.2
361163	4266970	-7.9	999.2	472855	4292711	-4.3	999.2
361163	4266970	-7.0	999.2	486014	4293091	-9.5	1008.0
361163	4266970	-9.4	999.6	487792	4291790	-8.8	999.3
361163	4266970	-8.2	999.5	487792	4291790	-0.6	1000.7
587112	4394561	-31.4	1021.6	487979	4290942	-6.9	999.2
587112	4394561	-73.5	1021.6	487792	4291790	-8.8	1000.1
587112	4394561	-93.3	1010.3	487792	4291790	-9.0	999.5
587112	4394561	-93.0	1000.4	486665	4289088	4.0	999.3
587112	4394561	-102.7	1001.7	486665	4289088	-18.0	999.2
587112	4394561	-140.2	1001.4	486665	4289088	-36.0	999.2
621912	4364874	-46.9	1019.9	486665	4289088	-14.0	999.2
621912	4364874	-64.3	1016.9	487297	4290811	-9.1	999.2
621912	4364874	-73.2	1014.3	487320	4290250	-15.2	999.2
621912	4364874	-82.9	1004.8	487320	4290250	-15.2	999.2
624253	4302710	-64.9	1022.7	487320	4290250	-19.8	999.2
624253	4302710	-74.1	1024.3	487320	4290250	-17.4	999.2
624253	4302710	-83.2	1014.8	447699	4287420	-19.7	999.2
624253	4302710	-92.7	1008.0	466391	4283041	-22.6	999.2
624253	4302710	-102.1	1006.4	488562	4286213	-23.0	999.2
624253	4302710	-102.1	1004.4	488562	4286213	-24.1	999.2
624253	4302710	-130.8	1004.5	489844	4285214	0.8	999.2
624253	4302710	-140.2	1004.1	487987	4285866	-9.9	999.2
624253	4302710	-140.2	1003.6	492643	4285876	-16.8	999.2
624253	4302710	-149.7	1003.9	492100	4285465	-20.7	999.2
624253	4302710	-159.1	1004.1	492643	4285876	-16.8	999.2
624253	4302710	-168.9	1004.5	492100	4285465	-19.5	999.3
624253	4302710	-187.8	1005.9	492396	4284776	-8.5	999.2
624253	4302710	-197.2	1006.1	492990	4285238	-16.8	999.3
624253	4302710	-216.1	1007.1	493300	4284625	-3.8	999.3
624253	4302710	-235.0	1009.4	492863	4283933	-33.2	999.2
624253	4302710	-253.6	1007.8	492863	4283933	-10.7	999.2
624253	4302710	-282.2	1011.8	492863	4283933	-4.1	1002.4
624253	4302710	-310.3	1009.2	493794	4279961	-5.7	1007.6
624253	4302710	-329.5	1014.4	493794	4279961	-13.3	1002.6
624253	4302710	-338.9	1018.9	493794	4279961	-17.9	1000.5

x	y	z	ρ	x	y	z	ρ
665369	4325474	-84.1	1023.5	493794	4279961	-2.7	1001.3
665369	4325474	-102.1	1021.0	493794	4279961	-2.7	1008.2
665369	4325474	-121.0	1018.6	446152	4276339	-16.9	999.2
665369	4325474	-159.1	1020.6	445164	4277572	-19.5	999.3
665369	4325474	-178.3	1033.0	445935	4277613	-18.3	999.2
665369	4325474	-235.3	1018.4	447103	4276882	-19.8	999.2
665369	4325474	-253.6	1017.8	446572	4277674	-12.2	999.2
665369	4325474	-291.7	1017.5	445440	4275266	-19.8	999.2
665369	4325474	-310.6	1017.9	445440	4275266	-16.5	999.2
665369	4325474	-329.5	1017.8	446266	4270594	-23.6	999.2
665369	4325474	-348.7	1018.7	474096	4271638	-18.4	999.2
665369	4325474	-377.0	1024.0	493342	4277288	-8.8	1009.0
690651	4315899	-305.1	1023.5	493342	4277288	-2.7	1000.1
690651	4315899	-308.8	1024.0	493342	4277288	-4.2	1000.5
690651	4315899	-313.3	1024.6	493342	4277288	-5.0	1003.4
690651	4315899	-326.8	1024.2	493342	4277288	-8.8	1009.0
690651	4315899	-364.5	1037.5	493342	4277288	-10.3	1008.9
690651	4315899	-383.4	1037.5	493342	4277288	-11.8	1006.3
690651	4315899	-431.0	1024.3	493342	4277288	-14.1	1000.2
690651	4315899	-457.8	1021.3	493833	4277324	-4.2	999.5
690651	4315899	-498.0	1024.0	493833	4277324	-2.7	1006.2
690651	4315899	-526.7	1024.0	493833	4277324	-3.4	1002.7
690651	4315899	-555.0	1024.3	493833	4277324	-4.2	1001.9
508463	4266409	-29.9	1019.7	493833	4277324	-5.0	1002.9
508463	4266409	-39.0	1031.5	493833	4277324	-8.0	1007.1
508463	4266409	-48.2	1011.2	493833	4277324	-9.5	1010.3
508463	4266409	-57.3	1005.5	494351	4273698	-3.4	1022.9
508463	4266409	-78.9	999.5	494351	4273698	-5.7	1017.6
508463	4266409	-92.7	1001.3	494351	4273698	-6.5	1021.9
508463	4266409	-102.1	999.5	494351	4273698	-8.8	1018.6
508463	4266409	-111.6	1000.4	494351	4273698	-11.8	1019.4
532263	4127653	-93.9	1026.8	450877	4266554	-1.7	999.2
532263	4127653	-111.0	1021.0	478216	4265970	5.5	999.3
532263	4127653	-129.8	1017.6	478216	4265970	5.5	999.3
532263	4127653	-139.3	1017.5	478907	4262483	-5.8	999.2
532263	4127653	-148.7	1018.4	492257	4258722	-17.8	999.2
532263	4127653	-158.2	1019.7	493613	4269682	-19.8	999.3
532263	4127653	-177.4	1020.1	449497	4257141	-21.3	999.2
532263	4127653	-196.6	1020.5	480455	4255757	-17.7	999.2
532263	4127653	-215.5	1021.9	480455	4255757	-65.7	999.3
532263	4127653	-233.5	1022.7	420080	4109399	-25.0	1020.0
532263	4127653	-252.7	1023.8	421216	4102296	-25.0	1020.0
532263	4127653	-271.6	1024.0	406017	4098318	-25.0	1020.0
532263	4127653	-300.5	1023.4	429953	4123746	-25.0	1020.0
532263	4127653	-310.3	1024.6	437055	4138449	-25.0	1020.0
532263	4127653	-319.7	1036.2	447781	4158265	-25.0	1020.0
449343	4318613	-137.2	999.2	454386	4171476	-25.0	1020.0
462482	4307222	-146.3	999.3	461489	4185682	-25.0	1020.0
462482	4307222	-195.1	1000.0	468094	4196905	-25.0	1020.0
462482	4307222	-237.7	1000.0	479672	4208128	-25.0	1020.0

x	y	z	ρ	x	y	z	ρ
445513	4298316	-103.6	999.2	492883	4219704	-25.0	1020.0
445513	4298316	-170.7	999.4	498494	4229291	-25.0	1020.0
445513	4298316	-213.4	999.6	505597	4243496	-25.0	1020.0
492063	4285982	-75.6	999.3	507585	4256066	-25.0	1020.0
493692	4266053	-106.7	999.3	507585	4280355	-25.0	1020.0
484073	4264973	-91.4	999.3	506094	4291578	-25.0	1020.0
495022	4258646	-88.4	999.2	506094	4302946	-25.0	1020.0
495022	4258646	-137.2	999.9	441110	4117217	-25.0	1025.0
424959	4209049	-91.4	999.2	449436	4132847	-25.0	1025.0
424959	4209049	-152.4	999.7	460465	4149499	-25.0	1025.0
424959	4209049	-91.4	999.3	468280	4163596	-25.0	1025.0
485824	4229800	-42.7	999.3	474561	4177692	-25.0	1025.0
482322	4221801	-48.8	999.3	481353	4189743	-25.0	1025.0
494761	4253464	-128.0	999.5	493258	4202304	-25.0	1025.0
494761	4253464	-140.2	999.6	503629	4212819	-25.0	1025.0
516177	4317494	-106.7	999.3	512978	4225892	-25.0	1025.0
452647	4203684	-70.1	999.3	520793	4241010	-25.0	1025.0
457483	4199978	-61.0	999.3	523860	4255617	-25.0	1025.0
447299	4192577	-67.1	999.2	523860	4270736	-25.0	1025.0
450352	4192929	-54.9	999.2	523860	4281620	-25.0	1025.0
440191	4175551	-73.2	999.3	522327	4292504	-25.0	1025.0
427199	4165917	-54.9	999.2	519770	4305945	-25.0	1025.0
433276	4166160	-73.2	999.2	432784	4108747	-25.0	1025.0
426371	4155489	-73.2	1000.2	420080	4109399	-50.0	1020.0
423192	4148222	-61.0	999.3	421216	4102296	-50.0	1020.0
413230	4137301	-39.6	999.2	406017	4098318	-50.0	1020.0
413131	4116059	-57.9	999.2	429953	4123746	-50.0	1020.0
381495	4101481	-42.7	1000.5	437055	4138449	-50.0	1020.0
386349	4132317	-45.7	999.3	447781	4158265	-50.0	1020.0
383287	4146958	-30.5	999.3	454386	4171476	-50.0	1020.0
474432	4233178	-89.9	999.2	461489	4185682	-50.0	1020.0
488153	4232525	-91.1	999.2	468094	4196905	-50.0	1020.0
474407	4254373	-71.6	999.2	479672	4208128	-50.0	1020.0
485926	4249917	-90.2	999.2	492883	4219704	-50.0	1020.0
490649	4248877	-125.0	999.2	498494	4229291	-50.0	1020.0
492203	4241833	-117.0	999.2	505597	4243496	-50.0	1020.0
492203	4241833	-124.7	999.2	507585	4256066	-50.0	1020.0
492203	4241833	-134.9	999.2	507585	4280355	-50.0	1020.0
492963	4243841	-121.9	999.2	506094	4291578	-50.0	1020.0
493622	4246664	-119.8	999.3	506094	4302946	-50.0	1020.0
493622	4246664	-125.9	999.2	441110	4117217	-50.0	1025.0
493622	4246664	-132.0	999.2	449436	4132847	-50.0	1025.0
493622	4246664	-141.4	999.2	460465	4149499	-50.0	1025.0
493622	4246664	-150.1	999.2	468280	4163596	-50.0	1025.0
494771	4251403	-103.9	999.2	474561	4177692	-50.0	1025.0
495139	4254651	-105.8	999.2	481353	4189743	-50.0	1025.0
495139	4254651	-119.8	999.2	493258	4202304	-50.0	1025.0
495139	4254651	-120.4	999.3	503629	4212819	-50.0	1025.0
495139	4254651	-114.3	999.2	512978	4225892	-50.0	1025.0
495546	4254637	-125.6	999.2	520793	4241010	-50.0	1025.0

x	y	z	ρ	x	y	z	ρ
495546	4254637	-141.1	999.2	523860	4255617	-50.0	1025.0
493571	4256188	-106.7	999.3	523860	4270736	-50.0	1025.0
495582	4257574	-136.4	999.8	523860	4281620	-50.0	1025.0
494158	4263600	-105.9	999.3	522327	4292504	-50.0	1025.0
494158	4263600	-104.4	999.2	519770	4305945	-50.0	1025.0
494158	4263600	-114.0	999.2	432784	4108747	-50.0	1025.0
494158	4263600	-107.1	999.2	420080	4109399	-100.0	1020.0
494158	4263600	-105.6	999.2	421216	4102296	-100.0	1020.0
494360	4264920	-110.5	999.2	406017	4098318	-100.0	1020.0
494962	4265185	-107.9	999.2	429953	4123746	-100.0	1020.0
494962	4265185	-110.3	999.2	437055	4138449	-100.0	1020.0
484226	4262435	-90.8	999.3	447781	4158265	-100.0	1020.0
474380	4271053	-63.4	999.2	454386	4171476	-100.0	1020.0
474380	4271053	-61.3	999.2	461489	4185682	-100.0	1020.0
483958	4280699	-81.4	999.2	468094	4196905	-100.0	1020.0
491043	4284865	-65.2	999.2	479672	4208128	-100.0	1020.0
489843	4241777	-65.5	999.2	492883	4219704	-100.0	1020.0
492246	4241853	-78.8	999.3	498494	4229291	-100.0	1020.0
492246	4241853	-81.2	999.2	505597	4243496	-100.0	1020.0
492246	4241853	-68.1	999.2	507585	4256066	-100.0	1020.0
489952	4243705	-69.5	999.2	507585	4280355	-100.0	1020.0
492978	4243920	-78.3	999.2	506094	4291578	-100.0	1020.0
492978	4243920	-70.3	999.2	506094	4302946	-100.0	1020.0
492978	4243920	-69.7	999.2	441110	4117217	-100.0	1025.0
493678	4246382	0.0	999.2	449436	4132847	-100.0	1025.0
493678	4246382	0.0	999.2	460465	4149499	-100.0	1025.0
493761	4246617	-81.1	999.2	468280	4163596	-100.0	1025.0
493761	4246617	-80.8	999.2	474561	4177692	-100.0	1025.0
493761	4246617	-80.9	999.6	481353	4189743	-100.0	1025.0
493761	4246617	-86.6	999.2	493258	4202304	-100.0	1025.0
493761	4246617	-68.4	999.2	503629	4212819	-100.0	1025.0
490663	4248925	-78.6	999.3	512978	4225892	-100.0	1025.0
495633	4257666	-87.6	999.2	520793	4241010	-100.0	1025.0
494202	4263601	-86.3	999.2	523860	4255617	-100.0	1025.0
494340	4265003	-67.1	999.2	523860	4270736	-100.0	1025.0
494989	4265170	-58.4	999.2	523860	4281620	-100.0	1025.0
494725	4265417	0.0	999.2	522327	4292504	-100.0	1025.0
484163	4262483	-61.7	999.2	519770	4305945	-100.0	1025.0
479438	4262824	-50.8	999.2	432784	4108747	-100.0	1025.0
474489	4254337	-50.3	999.2	405022	4105633	-25.0	1023.0
493639	4246598	-57.2	999.3	397422	4203579	-25.0	1018.0
485941	4249891	-51.5	999.2	397422	4223395	-25.0	1017.0
474385	4254362	-22.3	999.2	398914	4124099	-25.0	1022.0
493540	4256130	-51.8	999.2	398914	4144413	-25.0	1021.0
495589	4257595	-54.1	999.3	398914	4163094	-25.0	1020.0
495589	4257595	-61.0	999.2	398914	4182769	-25.0	1019.0
494151	4263613	-60.7	999.2	414611	4096541	-25.0	1025.0
484139	4262404	-36.0	999.2	412622	4171333	-25.0	1020.0
479328	4262832	-25.9	999.2	406656	4154144	-25.0	1021.0
494596	4268212	0.0	999.2	403531	4134825	-25.0	1021.0

x	y	z	ρ	x	y	z	ρ
493526	4270344	-61.0	999.2	406017	4116641	-25.0	1022.0
493835	4273600	-61.0	999.2	422708	4187669	-25.0	1019.0
483888	4280701	-50.6	999.2	418233	4196265	-25.0	1018.0
486730	4289419	-19.7	999.2	417736	4212955	-25.0	1017.0
486730	4289419	-28.7	999.2	409639	4223681	-25.0	1017.0
486730	4289419	-34.8	999.2	412622	4104427	-25.0	1024.0
486730	4289419	-41.6	999.2	405022	4105633	-50.0	1023.0
486730	4289419	-33.2	999.2	397422	4203579	-50.0	1018.0
486730	4289419	-28.7	999.2	397422	4223395	-50.0	1017.0
487544	4290685	-40.8	999.2	398914	4124099	-50.0	1022.0
488017	4291125	-39.9	999.2	398914	4144413	-50.0	1021.0
493785	4246695	-23.9	999.3	398914	4163094	-50.0	1020.0
485998	4249923	-17.2	999.2	398914	4182769	-50.0	1019.0
495676	4257637	-32.8	1012.4	414611	4096541	-50.0	1025.0
484264	4262431	-23.8	999.2	412622	4171333	-50.0	1020.0
491081	4284799	-23.5	999.2	406656	4154144	-50.0	1021.0
488728	4285570	-22.0	999.2	403531	4134825	-50.0	1021.0
487637	4290618	-18.0	999.2	406017	4116641	-50.0	1022.0
488016	4291137	0.0	999.2	422708	4187669	-50.0	1019.0
488016	4291137	0.0	999.2	418233	4196265	-50.0	1018.0
474398	4271104	0.0	999.2	417736	4212955	-50.0	1017.0
411298	4121447	-9.1	999.3	409639	4223681	-50.0	1017.0
414233	4112017	-19.5	999.3	412622	4104427	-50.0	1024.0
414214	4110137	-15.2	999.2	405022	4105633	-100.0	1023.0
414214	4110137	-15.9	999.2	397422	4203579	-100.0	1018.0
414214	4110137	-16.8	999.3	397422	4223395	-100.0	1017.0
414233	4112017	-11.0	999.3	398914	4124099	-100.0	1022.0
415888	4127040	-1.8	999.3	398914	4144413	-100.0	1021.0
412864	4125191	-16.8	999.2	398914	4163094	-100.0	1020.0
417576	4145824	-6.1	999.2	398914	4182769	-100.0	1019.0
419166	4155209	-4.6	999.2	414611	4096541	-100.0	1025.0
428115	4151366	-5.2	999.2	412622	4171333	-100.0	1020.0
426651	4155139	-7.0	999.3	406656	4154144	-100.0	1021.0
422266	4166460	-10.7	999.7	403531	4134825	-100.0	1021.0
432745	4168248	-1.5	999.2	406017	4116641	-100.0	1022.0
440259	4173830	-0.9	999.2	422708	4187669	-100.0	1019.0
435808	4177624	-4.6	999.2	418233	4196265	-100.0	1018.0
440286	4177590	1.5	999.2	417736	4212955	-100.0	1017.0
412622	4104427	-100.0	1024.0	409639	4223681	-100.0	1017.0

Appendix A2

This appendix contains information on the area element mesh used in the MVAEM model in Chapter 1. The area mesh is shown in figure A.1, and the values used in the mesh are presented in the following pages. Resistances are given in days and heads in meters.

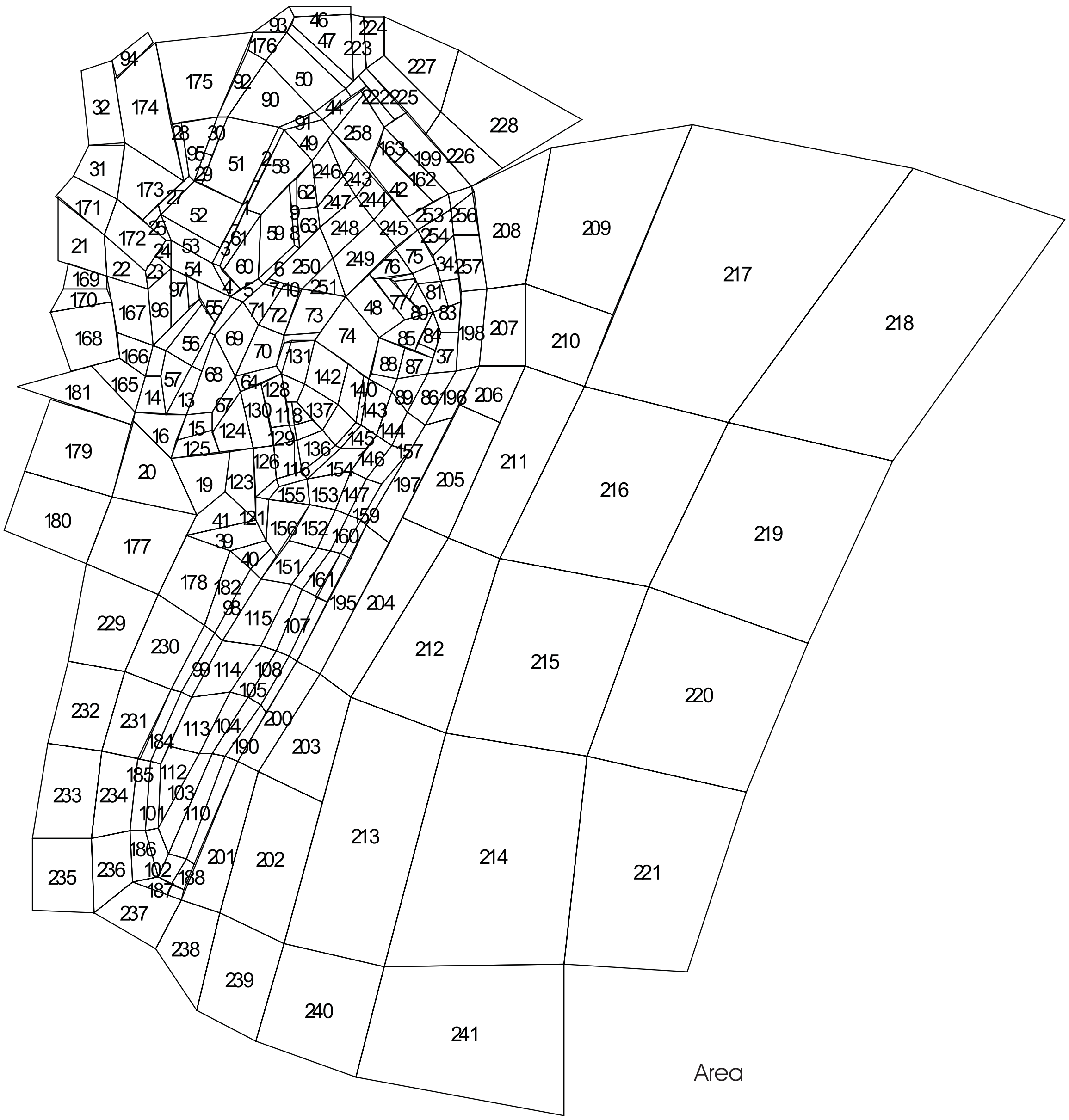

Figure A.1. MVAEM area element mesh

No.	utm-x_1	y_1	x_2	y_2	x_3	y_3	x_4	y_4	resist.	head
1	433220	4286003	435173	4286006	440764	4297782	439241	4297942	10	8
2	440764	4297782	447465	4312086	446067	4312409	439241	4297942	10	12
3	435173	4286006	429761	4274915	428131	4275111	433220	4286003	10	3
4	428131	4275111	432568	4266489	435344	4268341	429761	4274915	10	2
5	432568	4266489	435973	4265048	441553	4269590	440610	4271652	10	1
6	441553	4269590	451967	4279639	450018	4280091	440610	4271652	10	2
7	441553	4269590	446537	4268735	447365	4270023	443040	4271006	10	2
8	450018	4280091	451967	4279639	450598	4290322	449382	4290209	10	5
9	449382	4290209	450598	4290322	450582	4298617	448931	4296935	10	12
10	446537	4268735	447365	4270023	452230	4268919	451862	4267999	10	3
11	432568	4266489	435973	4265048	428815	4256138	427133	4256644	10	1
12	422342	4247730	425210	4246293	428815	4256138	427133	4256644	10	0
13	425210	4246293	422342	4247730	415363	4234389	420660	4233973	10	0
14	415363	4234389	414223	4244657	409693	4244589	406859	4234854	10	0
15	427676	4235401	427671	4229854	418346	4227663	420660	4233973	10	0
16	406859	4234854	420660	4233973	416411	4222745	406365	4232987	10	0
17	414223	4244657	409693	4244589	411914	4253217	415552	4252008	10	1
18	415552	4252008	411914	4253217	424043	4266090	425354	4264322	10	2
19	416411	4222745	432937	4224553	431594	4213072	423494	4207347	10	0
20	423494	4207347	400658	4212037	406365	4232987	416411	4222745	10	0
21	385735	4293428	385735	4276099	398956	4272169	398197	4282902	10	0
22	398197	4282902	398956	4272169	410677	4268704	409796	4273103	10	0
23	409746	4273196	410677	4268704	416636	4273992	412222	4277673	10	0
24	412222	4277673	416636	4273992	416579	4282082	415025	4282082	10	0
25	415025	4282082	416579	4282082	413997	4288474	410936	4285544	10	0
26	408882	4287449	410936	4285544	413997	4288474	413021	4291294	10	0
27	413021	4291294	413997	4288474	423383	4297662	421593	4299495	10	0
28	419907	4297912	421593	4299495	419360	4313699	416874	4313389	10	1.5
29	423383	4297662	424966	4296877	428132	4305133	426031	4305443	10	1
30	426031	4305443	428132	4305133	431988	4315315	429571	4315556	10	2
31	390463	4298992	402007	4293151	404276	4308027	394374	4308027	10	0
32	394374	4308027	392592	4327831	400711	4330306	404226	4308073	10	0
33	421554	4263514	424029	4265990	423597	4270681	421061	4271751	10	3
34	493426	4282994	487736	4277542	490122	4270814	495219	4271111	1.00E4	0
35	488474	4275356	490122	4270814	483730	4269772	482081	4272564	1.00E3	0
36	482081	4272564	482843	4271238	477098	4270741	476238	4271706	1.00E2	0
37	490325	4256887	494895	4256450	494158	4246224	486188	4245921	1.00E4	0
38	482720	4251518	487595	4249699	488372	4251707	483847	4253880	1.00E3	0
39	420876	4201229	439812	4205689	442706	4199795	432516	4197233	1.00E2	0
40	432516	4197233	442706	4199795	444106	4197909	438696	4192215	1.00E4	1
41	420876	4201229	439812	4205689	431594	4213072	423494	4207347	10	1
42	480984	4287644	488291	4291960	472855	4307687	470175	4300987	40	2
43	464099	4323201	467777	4326581	469842	4323878	465791	4320773	10	2.5
44	465791	4320773	464099	4323201	456030	4316628	457771	4314661	10	3
45	465952	4324945	464191	4323184	448142	4338509	449350	4340753	10	2
46	448841	4345494	465310	4345494	465310	4342844	449833	4342514	10	3
47	449833	4342514	449350	4340753	465952	4324945	465310	4342844	10	3
48	463972	4266612	470712	4273000	480634	4260083	473403	4255105	10	12
49	447465	4312086	457771	4314661	460740	4311384	455090	4303334	10	15
50	442584	4330811	448142	4338509	464191	4323184	456030	4316628	10	10

PolyID	utm-x_1	y_1	x_2	y_2	x_3	y_3	x_4	y_4	resist.	head
51	431988	4315315	446067	4312409	436075	4291403	424966	4296877	10	15
52	423383	4297662	436075	4291403	430143	4279426	413997	4288474	10	10
53	413997	4288474	416579	4282082	428131	4275111	430143	4279426	10	8
54	416636	4273992	432568	4266489	428131	4275111	416579	4282082	10	6
55	423597	4270681	424055	4266131	428567	4259506	432568	4266489	10	3
56	428647	4259425	425364	4264259	415535	4252033	422342	4247730	10	2
57	415363	4234389	414223	4244657	415504	4251845	422342	4247730	10	1
58	441255	4288711	437244	4290234	447465	4312086	455090	4303334	10	15
59	448931	4296935	450018	4280091	440610	4271652	441255	4288711	10	12
60	441255	4288711	440610	4271652	435409	4268344	430805	4273642	10	12
61	430805	4273642	429761	4274915	437244	4290234	441255	4288711	10	9
62	450598	4290322	450582	4298617	455090	4303334	456743	4290675	10	13
63	456743	4290675	450598	4290322	451967	4279639	457437	4285020	10	10
64	435414	4240535	434239	4244910	445262	4247235	446919	4245303	10	3
65	446919	4245303	445262	4247235	447181	4254113	449258	4254205	10	5
66	447181	4254113	447549	4255888	457240	4256467	456043	4254600	20	12
67	434239	4244910	427676	4235401	427662	4229685	435414	4240535	10	1
68	420660	4233973	427676	4235401	434239	4244910	428815	4256138	10	1.5
69	428815	4256138	435973	4265048	440383	4259112	434239	4244910	10	3
70	434239	4244910	440220	4258949	447549	4255888	445262	4247235	10	9
71	440383	4258997	446537	4268735	441553	4269590	435973	4265048	10	10
72	446537	4268735	440336	4258949	447549	4255888	451862	4267999	10	11
73	452230	4268919	447549	4255888	457240	4256467	463972	4266612	20	11
74	463972	4266612	456043	4254600	470389	4244091	473403	4255105	20	15
75	483498	4284490	488474	4275356	482081	4272564	477427	4279538	100	3
76	477427	4279538	482081	4272564	472174	4271117	470712	4273000	80	3
77	480634	4260083	472174	4271117	476238	4271706	485238	4261525	80	10
78	483115	4270806	480569	4266813	481431	4265829	483730	4269772	90	3
79	482843	4271238	483115	4270806	480569	4266813	477098	4270741	90	5
80	483730	4269772	488212	4262439	485238	4261525	481431	4265829	100	4
81	483730	4269772	490122	4270814	492347	4263908	488212	4262439	1.00E3	2
82	492347	4263908	490122	4270814	495219	4271111	495541	4265045	1.00E4	1
83	495541	4265045	494895	4256450	490325	4256887	488212	4262439	1.00E4	1
84	488212	4262439	483847	4253880	488372	4251707	490325	4256887	5.00E3	3
85	488212	4262439	482720	4251518	473403	4255105	480634	4260083	1.00E2	10
86	494158	4246224	485965	4231759	480777	4234875	486188	4245921	1.00E4	2
87	486188	4245921	487595	4249699	480269	4252477	478045	4243868	5.00E3	5
88	478045	4243868	470810	4245395	473403	4255105	480269	4252477	1.00E3	10
89	478045	4243868	476553	4240827	480777	4234875	486188	4245921	1.00E4	6
90	431988	4315315	442584	4330811	456030	4316628	446067	4312409	10	10
91	446067	4312409	447465	4312086	457771	4314661	456030	4316628	10	5
92	429571	4315556	437303	4333126	442584	4330811	431988	4315315	10	10
93	439236	4338338	448651	4345402	449833	4342514	448142	4338509	10	3
94	400659	4330364	410405	4338000	411811	4335824	401764	4325542	10	0
95	419360	4313699	429571	4315556	423383	4297662	421593	4299495	10	3
96	411914	4253217	410677	4268704	416636	4273992	416392	4257966	10	0
97	416636	4273992	421061	4271751	421542	4263299	416300	4258057	10	1
98	438696	4192215	441421	4189956	431054	4172799	428517	4174922	1.00E4	1
99	428517	4174922	431054	4172799	422250	4157769	419220	4158598	2.00E4	1
100	411090	4140378	413876	4139660	422250	4157769	419220	4158598	2.00E4	1

PolyID	utm-x_1	y_1	x_2	y_2	x_3	y_3	x_4	y_4	resist.	head
101	411090	4140378	413876	4139660	413278	4121933	409620	4121694	2.00E4	1
102	409620	4121694	413278	4121933	415757	4115128	413158	4108616	2.00E4	1
103	413278	4121933	415757	4115128	427825	4141935	424201	4142110	2.00E4	1
104	424201	4142110	427825	4141935	437702	4157548	432877	4158598	2.00E4	1
105	432877	4158598	437702	4157548	445042	4170312	440853	4171804	2.00E4	1
106	440853	4171804	445042	4170312	452474	4186880	449279	4188040	2.00E4	1
107	452474	4186880	456167	4184679	448522	4168489	445042	4170312	2.00E4	0
108	445042	4170312	448522	4168489	440806	4155449	437869	4157771	2.00E4	0
109	437869	4157771	440806	4155449	431124	4141336	427825	4141935	2.00E4	0
110	427825	4141935	431124	4141336	421124	4113505	415757	4115128	2.00E4	0
111	415757	4115128	421124	4113505	416714	4106787	413278	4108616	2.00E4	0
112	413278	4121933	413876	4139660	415979	4144037	424257	4142110	2.00E4	7
113	424257	4142110	415979	4144037	422250	4157769	432877	4158598	2.00E4	7
114	432877	4158598	422250	4157769	431054	4172799	440853	4171804	2.00E4	7
115	440853	4171804	431054	4172799	441421	4189956	449279	4188040	1.00E4	10
116	449889	4218087	452380	4218954	451269	4227621	449919	4227346	150	3
117	449919	4227346	451269	4227621	449919	4231399	448483	4231160	100	5
118	448483	4231160	449919	4231399	449373	4237968	447818	4238221	80	8
119	445390	4216573	452380	4218954	453457	4217245	446364	4214735	1.00E3	1.5
120	446364	4214735	445390	4216573	439596	4212270	443081	4211482	1.00E3	1
121	443081	4211482	439596	4212270	439812	4205689	442706	4199795	1.00E3	0
122	452380	4218954	461588	4225893	462907	4225179	453457	4217245	1.00E3	2
123	432937	4224553	439064	4225314	439812	4205689	431594	4213072	80	1
124	429864	4224174	427775	4229826	435414	4240535	439064	4225314	50	2
125	416411	4222745	418346	4227663	427773	4229893	429864	4224174	50	1
126	439064	4225314	444910	4225673	445390	4216573	439596	4212270	80	4
127	444910	4225673	449919	4227346	449889	4218087	445390	4216573	60	10
128	443822	4230736	441225	4243079	446919	4245303	448483	4231160	30	10
129	448483	4231160	443822	4230736	444910	4225673	449919	4227346	60	10
130	444910	4225673	441225	4243079	435414	4240535	439064	4225314	40	4
131	446919	4245303	452823	4242397	456043	4254600	449258	4254205	80	4
132	446919	4245303	452823	4242397	450679	4237662	447818	4238221	80	10
133	449919	4231399	449373	4237968	450679	4237662	455165	4232682	100	12
134	470810	4245395	478045	4243868	476553	4240827	470389	4244091	1.00E3	5
135	451269	4227621	449919	4231399	455165	4232682	457631	4230131	100	10
136	457631	4230131	461588	4225893	452380	4218954	451269	4227621	200	7
137	450679	4237662	452823	4242397	462487	4237137	457631	4230131	100	10
138	457631	4230131	462487	4237137	467122	4232488	461588	4225893	200	0
139	461588	4225893	462907	4225179	468269	4231882	467122	4232488	1.00E3	3
140	467122	4232488	468269	4231882	470389	4244091	468864	4245130	1.00E3	4
141	462487	4237137	464573	4248351	468864	4245130	467122	4232488	500	10
142	462487	4237137	464573	4248351	456043	4254600	452823	4242397	200	15
143	470389	4244091	476510	4240852	472596	4229050	468269	4231882	1.00E4	5
144	472596	4229050	476510	4240852	480777	4234875	476553	4225958	1.00E4	3
145	462907	4225179	468269	4231882	472596	4229050	469785	4225093	1.00E4	5
146	472596	4229050	476553	4225958	470130	4217071	465545	4219017	1.00E4	3
147	470130	4217071	465545	4219017	461415	4208465	464941	4206973	1.00E4	3
148	464941	4206973	461415	4208465	456312	4198367	459924	4197567	1.00E4	3
149	459924	4197567	456312	4198367	449279	4188040	452474	4186880	1.00E4	3
150	438696	4192215	444106	4197909	445600	4195834	441421	4189956	1.00E4	3

PolyID	utm-x_1	y_1	x_2	y_2	x_3	y_3	x_4	y_4	resist.	head
151	441421	4189956	448492	4199888	456312	4198367	449279	4188040	1.00E4	7
152	448492	4199888	454623	4209957	461415	4208465	456312	4198367	1.00E4	7
153	454623	4209957	453457	4217245	465545	4219017	461415	4208465	1.00E4	5
154	453457	4217245	462907	4225179	469785	4225093	465545	4219017	1.00E4	3
155	443081	4211482	454623	4209957	453457	4217245	446364	4214735	1.00E4	5
156	443081	4211482	454623	4209957	445600	4195834	442706	4199795	1.00E4	3
157	480777	4234875	485965	4231759	481787	4224492	476553	4225958	2.00E4	0
158	476553	4225958	481787	4224492	473829	4215579	470130	4217071	2.00E4	0
159	470130	4217071	473829	4215579	468441	4205394	464941	4206973	2.00E4	0
160	464941	4206973	468441	4205394	462629	4196653	459924	4197567	2.00E4	0
161	459924	4197567	462629	4196653	456167	4184679	452474	4186880	2.00E4	0
162	488143	4291984	491815	4294130	481067	4306013	477747	4302691	20	0
163	477747	4302691	472855	4307687	474924	4312862	481067	4306013	20	0
164	467990	4322463	474924	4312862	477342	4314349	469842	4323878	10	0
165	406859	4234854	394994	4247458	402835	4250013	409693	4244589	10	1
166	409693	4244589	402835	4250013	401852	4256813	411914	4253217	10	2
167	411914	4253217	401852	4256813	398956	4272169	410677	4268704	10	2
168	400418	4265167	383757	4262334	389766	4246083	402835	4250013	10	1
169	387155	4268619	399588	4268659	398956	4272169	388507	4275160	10	1
170	387228	4268619	383830	4262334	400418	4265167	399588	4268659	10	0
171	402007	4293151	390371	4298879	385438	4293432	398197	4282902	10	1
172	402007	4293151	415025	4282082	409739	4273112	398197	4282902	10	3
173	402007	4293151	408882	4287449	419907	4297912	404294	4308050	10	4
174	404294	4308050	419907	4297912	412625	4335168	401663	4325484	10	4
175	412625	4335168	439236	4338338	429571	4315556	416874	4313389	10	4
176	437303	4333126	439236	4338338	448142	4338509	442584	4330811	10	6
177	400658	4212037	393307	4193969	413418	4185822	423494	4207347	5.00E3	0
178	420876	4201229	432516	4197233	425522	4177353	413418	4185822	10	0
179	405851	4231213	383622	4238669	377151	4219258	400658	4212037	1.00E2	0
180	400658	4212037	393307	4193969	371584	4203157	377001	4218731	1.00E3	0
181	375045	4241675	394994	4247458	406859	4234854	405851	4231213	10	0
182	425522	4177353	428538	4174889	438696	4192215	432516	4197233	1.00E4	0
183	425522	4177353	428420	4174877	419220	4158598	416317	4159357	2.00E4	0
184	416317	4159357	419220	4158598	411090	4140378	407999	4140773	2.00E4	0
185	407999	4140773	411090	4140378	409620	4121694	405363	4121334	2.00E4	0
186	405363	4121334	406509	4107141	413158	4108616	409620	4121694	2.00E4	0
187	406509	4107141	413158	4108616	420133	4104958	419107	4102497	2.00E4	0
188	416714	4106787	420133	4104958	423039	4112155	421124	4113505	2.00E4	0
189	421124	4113505	431124	4141336	434714	4140019	423039	4112155	2.00E4	0
190	431124	4141336	434714	4140019	442841	4153533	440806	4155449	2.00E4	0
191	440806	4155449	442841	4153533	450889	4167283	448522	4168489	2.00E4	0
192	448522	4168489	450889	4167283	459333	4183566	456167	4184679	2.00E4	0
193	462629	4196653	465437	4195349	470108	4204359	468441	4205394	2.00E4	0
194	468441	4205394	470108	4204359	481787	4224492	473829	4215579	2.00E4	0
195	450889	4167283	457000	4164100	476293	4199583	470108	4204359	2.00E4	0
196	485965	4231759	493280	4233811	500364	4247658	494158	4246224	2.00E4	0
197	493280	4233811	485965	4231759	470108	4204359	476293	4199583	2.00E4	0
198	494158	4246224	500364	4247658	502308	4268832	495693	4267759	2.00E4	0
199	491815	4294130	498442	4296478	480663	4316491	474924	4312862	5.00E1	0
200	450889	4167283	457000	4164100	440525	4137775	434714	4140019	5.00E4	0

PolyID	utm-x_1	y_1	x_2	y_2	x_3	y_3	x_4	y_4	resist.	head
201	434714	4140019	440525	4137775	429710	4098933	419107	4102497	5.00E4	0
202	429710	4098933	447060	4090786	457704	4129326	440525	4137775	1.00E5	0
203	440525	4137775	457704	4129326	465468	4157473	457000	4164100	1.00E5	0
204	457000	4164100	465468	4157473	491976	4200649	479510	4206078	1.00E5	0
205	479510	4206078	491976	4200649	506082	4232252	494989	4236965	1.00E5	0
206	494989	4236965	506082	4232252	512928	4247443	500364	4247658	5.00E4	0
207	500364	4247658	512928	4247443	512928	4269879	502308	4268832	5.00E4	0
208	502308	4268832	512928	4269879	519738	4306994	498442	4296478	1.00E5	0
209	519738	4306994	558322	4313030	536933	4261353	512928	4269879	1.00E5	0
210	512928	4269879	536933	4261353	529455	4242059	512928	4247443	2.00E5	0
211	512928	4247443	529455	4242059	506398	4195296	491975	4200754	2.00E5	0
212	491975	4200754	506398	4195296	491528	4147773	465468	4157473	2.00E5	0
213	465468	4157473	491528	4147773	474431	4084078	447060	4090786	2.00E5	0
214	474431	4084078	523720	4085044	529495	4141445	491528	4147773	5.00E5	0
215	491528	4147773	529495	4141445	546581	4187639	506398	4195296	5.00E5	0
216	506398	4195296	546581	4187639	567906	4232252	529455	4242059	5.00E5	0
217	529455	4242059	558322	4313030	618599	4301341	567906	4232252	5.00E5	0
218	567906	4232252	618599	4301341	659471	4287246	612425	4221629	1.00E6	0
219	612425	4221629	567906	4232252	546581	4187639	589800	4172334	1.00E6	0
220	589800	4172334	546581	4187639	529495	4141445	573296	4131674	1.00E6	0
221	573296	4131674	529495	4141445	523720	4085044	557010	4083364	1.00E6	0
222	467777	4326581	469955	4328638	480663	4316491	477342	4314349	5.00E1	0
223	465310	4342844	469380	4342566	469955	4328638	465952	4324945	5.00E1	0
224	469380	4342566	474613	4342649	474613	4332216	469955	4328638	5.00E1	0
225	469955	4328638	474613	4332216	489638	4316792	485914	4310536	5.00E1	0
226	485914	4310536	489638	4316792	506680	4301080	498442	4296478	5.00E3	0
227	489638	4316792	494830	4333521	474613	4342649	474613	4332216	1.00E5	0
228	489638	4316792	506680	4301080	528231	4314682	494830	4333521	1.00E6	10
229	393307	4193969	388705	4167413	404122	4164744	413418	4185822	1.00E4	0
230	413418	4185822	404122	4164744	416317	4159357	425522	4177353	2.00E4	0
231	416317	4159357	408114	4140901	397587	4143113	404122	4164744	2.00E4	0
232	404122	4164744	397587	4143113	383458	4145046	388705	4167413	1.00E4	0
233	383458	4145046	379270	4119457	395009	4119457	397587	4143113	1.00E4	0
234	397587	4143113	408010	4141058	405363	4121334	395009	4119457	2.00E4	0
235	395009	4119457	379270	4119457	379224	4099276	395757	4099111	1.00E4	0
236	395757	4099111	395009	4119457	405363	4121334	406509	4107141	2.00E4	0
237	406509	4107141	395757	4099111	412878	4089071	419107	4102497	5.00E4	0
238	419107	4102497	412878	4088811	423784	4072586	429710	4098933	5.00E4	0
239	429710	4098933	423784	4072586	439432	4064416	447060	4090786	1.00E5	0
240	439432	4064416	447060	4090786	474431	4084078	467044	4054705	1.00E5	0
241	474431	4084078	523720	4085044	523720	4043626	467044	4054705	5.00E5	0
242	460740	4311384	458976	4308865	463741	4299428	467098	4304398	10	8
243	467098	4304398	463741	4299428	466853	4293872	471457	4299376	10	9
244	471457	4299376	466853	4293872	471637	4287288	476781	4292792	10	6
245	476781	4292792	483498	4284490	477907	4279908	471637	4287288	10	9
246	455090	4303334	458976	4308865	463741	4299428	456743	4290675	10	15
247	456743	4290675	457437	4285020	466853	4293872	463741	4299428	10	16
248	466853	4293872	457437	4285020	460398	4276664	471637	4287288	10	17
249	471637	4287288	477907	4279908	463972	4266612	460398	4276664	10	15
250	460398	4276664	452230	4268919	443040	4271006	457437	4285020	10	15

PolyID	utm-x_1	y_1	x_2	y_2	x_3	y_3	x_4	y_4	resist.	head
251	452230	4268919	460398	4276664	463972	4266612	457183	4268048	10	16
252	457771	4314661	460740	4311384	468742	4321427	467974	4322469	10	4
253	480984	4287644	483498	4284490	492440	4290407	491815	4294130	5.00E2	3
254	492440	4290407	483498	4284490	487736	4277542	493426	4282994	1.00E3	0
255	491815	4294130	492440	4290407	498625	4295111	498442	4296478	1.00E3	0
256	498625	4295111	500282	4283393	493426	4282994	492440	4290407	1.00E4	0
257	493426	4282994	500282	4283393	502308	4268832	495693	4267759	2.00E4	0
258	460740	4311384	468742	4321427	474924	4312862	470175	4300987	10	2
259	456101	4184726	459354	4183642	465437	4195349	462629	4196653	2.00E4	0

Appendix B

The FORTRAN code of the variable density module is included in this appendix. The variable density module consists of two files: vardens.cmn, which contains the common block of data used in the variable density module, and vardens.for, which contains the functions and subroutines for the computation of variable density flow. Input of density data makes use of the package Match, developed and written by P.A. Cundall, which is explained in detail in Strack (1989). The `cdir$` commands are vectorization directives for the CrayC916.

Vardens.cmn

```
c  NVDMX: Maximum number of density points
c  NVDPTS: Number of density points
c  DVDNU0: Additive constant nu0
c  DVDBE: Scale factor beta
c  DVDBSQ: Scale factor beta squared
c  DVDX: Array with x-values of data points
c  DVDY: Array with y-values of data points
c  DVDZ: Array with z-values of data points
c  DVDAL: Array with alpha values
c  DVDDEL: Array with delta values
c  DVDDELSQ: Array with delta square values
c  DVDNUG: Array with given nu-values
c  DVDLU: Matrix stored after LU decomposition
c  INDX: Integer array used for LU decompostion
c  DUM1,2,3: Dummy arrays for summation

      PARAMETER (NVDMX=200)
      PARAMETER (DZERO=0.D0,DONE=1.D0,DTWO=2.D0,DTHREE=3.D0)
      PARAMETER (D1D6=1.D0/6.D0,DHALF=0.5D0,D1D3=1.D0/3.D0)
      COMMON /CBVD/ NVDPTS,DVDNU0,DVDBE,DVDBSQ,
     .DVDX(NVDMX),DVDY(NVDMX),DVDZ(NVDMX),
     .DVDAL(NVDMX+1),DVDDEL(NVDMX),DVDDELSQ(NVDMX),DVDNUG(NVDMX),
     .DVDLU(NVDMX+1,NVDMX+1),INDX(NVDMX+1),
     .DUM(NVDMX),DUM1(NVDMX),DUM2(NVDMX),DUM3(NVDMX)
```

Vardens.for

```
      BLOCK DATA BDVD
      IMPLICIT REAL*8 (D)
      INCLUDE 'vardens.cmn'
      DATA NVDPTS,DVDBE /0,1/
      END

      SUBROUTINE VDINPUT
      IMPLICIT REAL*8 (D)
      IMPLICIT CHARACTER*1 (A), LOGICAL (L)
      SAVE
      CHARACTER*32 AFILE
      INCLUDE 'vardens.cmn'
      INCLUDE 'MATCH.CMN'
      DIMENSION AWORD(30)
      DATA AWORD  /'B','E','T','A',' ','S','O','L','V',' ',
     .             'C','O','N','T',' ','C','O','I','N',' ',
```

```
     .            'T','E','S','T',' ','Q','U','I','T','!'/
      LERROR=.FALSE.
      LMISS=.FALSE.
10    IF(LMISS.OR.LERROR) WRITE(9,9001)
      LERROR=.FALSE.
      LMISS=.FALSE.
      WRITE(9,9005)
      READ(8,9000) ALINE
      CALL TIDY
      IF(LMISS.OR.LERROR.OR.ILPNT(2).EQ.0) GOTO 10
      IF (ILPNT(4).EQ.0) THEN
        CALL MATCH(AWORD,1,JUMP)
        IF (LERROR) GOTO 10
        GOTO (100,200,300,400,500,600),JUMP
 100      DVDBE=DVAR(2)
          DVDBSQ=DVDBE**2
          GOTO 10
 200      CALL VDSOLVE
          GOTO 10
 300      CALL VDCONTROL
          GOTO 10
 400      DCOIN=DVAR(2)
          CALL VDCOIN(DCOIN)
          GOTO 10
 500      GOTO 10
 600      RETURN
      ENDIF
      NVDPTS=NVDPTS+1
      DVDX(NVDPTS)=DVAR(1)
      DVDY(NVDPTS)=DVAR(2)
      DVDZ(NVDPTS)=DVAR(3)
      DVDNUG(NVDPTS)=DVAR(4)
      DVDDEL(NVDPTS)=DVAR(5)
      DVDDELSQ(NVDPTS)=DVDDEL(NVDPTS)**2
      IF(LMISS.OR.LERROR) NVDPTS=NVDPTS-1
      GOTO 10
9000  FORMAT(80A1)
9001  FORMAT(' ERROR: ILLEGAL COMMAND OR MISSING PARAMETERS')
9005  FORMAT
     .(' (x,y,z,nu,delta)..<BETA>(b)..<SOLVE>..<CONTROL>..'
     . '<COIN>(tol)..<QUIT>',/)
      RETURN
      END

      SUBROUTINE VDCOIN(DCOIN)
      IMPLICIT REAL*8 (D)
      SAVE
      INCLUDE 'vardens.cmn'
      DTOL=DCOIN*DCOIN
      DO I=1,NVDPTS-1
        DO J=I+1,NVDPTS
          DIST=(DVDX(I)-DVDX(J))**2+
     .         (DVDY(I)-DVDY(J))**2+
     .         (DVDZ(I)-DVDZ(J))**2
          IF (DIST.LT.DTOL) WRITE(7,9000)I,J,DSQRT(DIST)
        ENDDO
```

```
      ENDDO
 9000 FORMAT(' POINTS ',I4,' AND ',I4,' ARE A DISTANCE ',
     .       1E13.5,' FROM EACH OTHER')
      RETURN
      END

      SUBROUTINE VDCHECK
      IMPLICIT REAL*8 (D)
      SAVE
      INCLUDE 'vardens.cmn'
      WRITE(7,9000)DVDBE
      WRITE(7,9001)
      DO I=1,NVDPTS
        WRITE(7,9002)I,DVDX(I),DVDY(I),DVDZ(I),DVDNUG(I),DVDDEL(I)
      ENDDO
 9000 FORMAT(' BETA: ',1P,E13.5)
 9001 FORMAT(
     .' I    X            Y            Z            NU           DELTA')
 9002 FORMAT(I5,1P,5E13.5)
      RETURN
      END

      REAL*8 FUNCTION DFVDNUM(DX,DY,DZ,M)
      IMPLICIT REAL*8 (D)
      SAVE
      INCLUDE 'vardens.cmn'
      DNUM=DVDBSQ*((DX-DVDX(M))**2+(DY-DVDY(M))**2)+
     .     (DZ-DVDZ(M))**2+DVDDELSQ(M)
      DFVDNUM=DSQRT(DNUM)
      RETURN
      END

      REAL*8 FUNCTION DFVDNU(DX,DY,DZ)
      IMPLICIT REAL*8 (D)
      SAVE
      INCLUDE 'vardens.cmn'
      DO M=1,NVDPTS
        DNUM=DSQRT( DVDBSQ*((DX-DVDX(M))**2+(DY-DVDY(M))**2)+
     .       (DZ-DVDZ(M))**2+DVDDELSQ(M) )
        DUM(M)=DVDAL(M)*DNUM
      ENDDO
      DVDNU=0.D0
CDIR$ NOVECTOR
      DO M=1,NVDPTS
         DVDNU=DVDNU+DUM(M)
      ENDDO
CDIR$ VECTOR
      DFVDNU=DVDNU+DVDNU0
      RETURN
      END

      SUBROUTINE VDCONTROL
      IMPLICIT REAL*8 (D)
      SAVE
      INCLUDE 'vardens.cmn'
      DALTOT=DZERO
```

```
      DO I=1,NVDPTS
        DALTOT=DALTOT+DVDAL(I)
        DNU=DFVDNU(DVDX(I),DVDY(I),DVDZ(I))
        WRITE(7,9000)I,DVDAL(I),DNU,DVDNUG(I)
      ENDDO
      WRITE(7,9001)DVDNU0,DALTOT
 9000 FORMAT(' I,ALPHA,NUCOMPUTED,NUGIVEN ',I4,1P,3E13.5)
 9001 FORMAT(' NU0,SUM OF ALPHA-S ',1P,2E13.5)
      RETURN
      END

      REAL FUNCTION RFNUGRID(CZ)
      IMPLICIT COMPLEX (C), REAL*8 (D)
      SAVE
      DX=REAL(CZ)
      DY=AIMAG(CZ)
      DZ=DFELEV()
      RFNUGRID=DFVDNU(DX,DY,DZ)
      RETURN
      END

      SUBROUTINE VDSOLVE
      IMPLICIT REAL*8 (D)
      SAVE
      INCLUDE 'vardens.cmn'

      NEQ=NVDPTS+1
      DO I=1,NVDPTS
        DO J=1,NVDPTS
          DVDLU(I,J)=DFVDNUM(DVDX(I),DVDY(I),DVDZ(I),J)
        ENDDO
        DVDLU(I,NEQ)=DONE
      ENDDO
      DO J=1,NVDPTS
        DVDLU(NEQ,J)=DONE
      ENDDO
      DVDLU(NEQ,NEQ)=DZERO

      CALL LUDCMP(DVDLU,NEQ,NVDMX+1,INDX,DUM)

      DO I=1,NVDPTS
        DVDAL(I)=DVDNUG(I)
      ENDDO
      DVDAL(NEQ)=DZERO
      CALL LUBKSB(DVDLU,NEQ,NVDMX+1,INDX,DVDAL)
      DVDNU0=DVDAL(NEQ)
      RETURN
      END

      SUBROUTINE VDSPECDIS2(DX,DY,DZ,DQX,DQY,DQZ)
      IMPLICIT REAL*8 (D)
      SAVE
      INCLUDE 'vardens.cmn'
      DK=DFAQK()
      DH=DFAQH()
      DZB=DFAQZB()
```

```
      DZT=DFAQZT()
      DTOL=1.d-8
      DO M=1,NVDPTS
        DXMSQ=DVDBSQ*(DX-DVDX(M))**2
        DYMSQ=DVDBSQ*(DY-DVDY(M))**2
        DZM=DVDZ(M)
        DZMSQ=(DZ-DZM)**2
        DZTMSQ=(DZT-DZM)**2
        DZBMSQ=(DZB-DZM)**2
        DELSQM=DVDDELSQ(M)
        DRM=DSQRT(DXMSQ+DYMSQ+DZMSQ+DELSQM)
        DRMT=DSQRT(DXMSQ+DYMSQ+DZTMSQ+DELSQM)
        DRMB=DSQRT(DXMSQ+DYMSQ+DZBMSQ+DELSQM)
        DTESTSQ=DXMSQ+DYMSQ+DELSQM
        IF (DTESTSQ.LT.DTOL*DZMSQ .AND. DZ.LT.DZM) THEN
          DP1=0.5D0*DTESTSQ/(DZM-DZ)
        ELSE
          DP1=DZ-DZM+DRM
        ENDIF
        IF (DTESTSQ.LT.DTOL*DZBMSQ .AND. DZB.LT.DZM) THEN
          DP2=0.5D0*DTESTSQ/(DZM-DZB)
        ELSE
          DP2=DZB-DZM+DRMB
        ENDIF
        IF (DTESTSQ.LT.DTOL*DZTMSQ .AND. DZT.LT.DZM) THEN
          DP3=0.5D0*DTESTSQ/(DZM-DZT)
        ELSE
          DP3=DZT-DZM+DRMT
        endif
        DLOG1=DLOG(dp1/dp3)
        DLOG2=DLOG(dp2/dp3)
        DDIS=DLOG1+((DZB-DZM)*DLOG2+(DRMT-DRMB))/DH
        DUM1(M)=DVDAL(M)*(DX-DVDX(M))*DDIS
        DUM2(M)=DVDAL(M)*(DY-DVDY(M))*DDIS

        DPART1=DTHREE*( (DZT-DZ)/DH*(DRMT-DRMB)+DRM-DRMT )
        DPART2=-DTWO*(DZ-DZM)*DLOG1+DTWO*(DZB-DZM)*(DZT-DZ)/DH*DLOG2
        DPART3=DELSQM/DH*( -DH/dp1+(DZ-DZB)/dp3-(DZ-DZT)/dp2 )
        DUM3(M)=DVDAL(M)*(DPART1+DPART2+DPART3)
      ENDDO
      DQX=0.D0
      DQY=0.D0
      DQZ=0.D0
CDIR$ NOVECTOR
      DO M=1,NVDPTS
        DQX=DQX+DUM1(M)
        DQY=DQY+DUM2(M)
        DQZ=DQZ+DUM3(M)
      ENDDO
CDIR$ VECTOR
      DQX=DK*DVDBSQ*DQX
      DQY=DK*DVDBSQ*DQY
      DQZ=DK*DVDBSQ*DQZ
      RETURN
      END
```

```
      REAL*8 FUNCTION DFPOT2HEAD(DPOT,DX,DY,DZ)
      IMPLICIT REAL*8 (D)
      SAVE
      INCLUDE 'vardens.cmn'
      WRITE(*,*)'DPOT,DX,DY,DZ ',DPOT,DX,DY,DZ
      DK=DFAQK()
      DH=DFAQH()
      DZB=DFAQZB()
      DZT=DFAQZT()
      DTOL=1.d-8
      DO M=1,NVDPTS
        DXMSQ=DVDBSQ*(DX-DVDX(M))**2
        DYMSQ=DVDBSQ*(DY-DVDY(M))**2
        DZM=DVDZ(M)
        DZMZM=DZ-DZM
        DZMSQ=(DZ-DZM)**2
        DZTMSQ=(DZT-DZM)**2
        DZBMSQ=(DZB-DZM)**2
        DELSQM=DVDDELSQ(M)
        DRMSQ=(DXMSQ+DYMSQ+DZMSQ+DELSQM)
        DRMTSQ=(DXMSQ+DYMSQ+DZTMSQ+DELSQM)
        DRMBSQ=(DXMSQ+DYMSQ+DZBMSQ+DELSQM)
        DRM=DSQRT(DRMSQ)
        DRMT=DSQRT(DRMTSQ)
        DRMB=DSQRT(DRMBSQ)
        DPART1=DHALF*(DRMSQ-DZMSQ)*DLOG(DZMZM+DRM)+DHALF*DZMZM*DRM
        DPART2=DHALF*(DZT-DZM)*(DRMTSQ-DZTMSQ)*DLOG(DZT-DZM+DRMT)+
     .         dhalf*DRMT*DZTMSQ-d1d3*DRMTSQ*DRMT
        DPART3=DHALF*(DZB-DZM)*(DRMBSQ-DZBMSQ)*DLOG(DZB-DZM+DRMB)+
     .         dhalf*DRMB*DZBMSQ-d1d3*DRMBSQ*DRMB
        DUM1(M)=-DPART1+(DPART2-DPART3)/DH
      ENDDO
      DHEAD=DPOT/(DK*DH)-DVDNU0*(DZ-(DZT**2-DZB**2)/(2.D0*DH))
CDIR$ NOVECTOR
      DO M=1,NVDPTS
        DHEAD=DHEAD+DVDAL(M)*DUM1(M)
      ENDDO
CDIR$ VECTOR
      DFPOT2HEAD=DHEAD
      RETURN
      END

      REAL*8 FUNCTION DFHEAD2POT(DHEAD,DX,DY,DZ)
      IMPLICIT REAL*8 (D)
      SAVE
      INCLUDE 'vardens.cmn'
      DK=DFAQK()
      DH=DFAQH()
      DZB=DFAQZB()
      DZT=DFAQZT()
      DTOL=1.d-8
      DO M=1,NVDPTS
        DXMSQ=DVDBSQ*(DX-DVDX(M))**2
        DYMSQ=DVDBSQ*(DY-DVDY(M))**2
        DZM=DVDZ(M)
        DZMZM=DZ-DZM
```

```
          DZMSQ=(DZ-DZM)**2
          DZTMSQ=(DZT-DZM)**2
          DZBMSQ=(DZB-DZM)**2
          DELSQM=DVDDELSQ(M)
          DRMSQ=(DXMSQ+DYMSQ+DZMSQ+DELSQM)
          DRMTSQ=(DXMSQ+DYMSQ+DZTMSQ+DELSQM)
          DRMBSQ=(DXMSQ+DYMSQ+DZBMSQ+DELSQM)
          DRM=DSQRT(DRMSQ)
          DRMT=DSQRT(DRMTSQ)
          DRMB=DSQRT(DRMBSQ)
          DPART1=DHALF*(DRMSQ-DZMSQ)*DLOG(DZMZM+DRM)+DHALF*DZMZM*DRM
          DPART2=DHALF*(DZT-DZM)*(DRMTSQ-DZTMSQ)*DLOG(DZT-DZM+DRMT)+
     .           dhalf*DRMT*DZTMSQ-d1d3*DRMTSQ*DRMT
          DPART3=DHALF*(DZB-DZM)*(DRMBSQ-DZBMSQ)*DLOG(DZB-DZM+DRMB)+
     .           dhalf*DRMB*DZBMSQ-d1d3*DRMBSQ*DRMB
          DUM1(M)=-DPART1+(DPART2-DPART3)/DH
        ENDDO
        DPOT=DHEAD*DK*DH+DK*DH*DVDNU0*(DZ-(DZT**2-DZB**2)/(2.D0*DH))
CDIR$ NOVECTOR
        DO M=1,NVDPTS
          DPOT=DPOT-DK*DH*DVDAL(M)*DUM1(M)
        ENDDO
CDIR$ VECTOR
        DFHEAD2POT=DPOT
        RETURN
        END
```